Monitoring seagrass: An investigation with multi-temporal satellite imagery in Boullanger Bay, Tasmania

by

Kan Otera

UTAS

School of Geography and Environmental Studies,

University of Tasmania

A thesis submitted in partial fulfilment of the requirements for a Master Degree at the School of Geography and Environmental Studies, University of Tasmania

October 2009

Declaration

This thesis contains no material which has been accepted for the award of any other degree or diploma in any tertiary institution, and to the best of my knowledge and belief, contains no material previously published or written by another person, except where due reference is made in the text of the thesis.

Signed

Kan Otera

31/ October/ 2009

Abstract

Seagrass plant communities play an ecologically important role in Australian and Tasmanian coastal regions. They provide key ecological functions such as: organic matter provision; assimilation of energy into ecosystems; nutrient trapping and cycling; shore line protection and formation; substrate sediment stabilization; enhanced biodiversity; and trophic transfers to adjacent habitats in tropical and temperate regions. The temperate Tasmanian seagrass communities, however, have experienced a period of decline in their abundance due to various disturbances as have other coastal areas in the world. Seagrasses are subject to rapid environmental changes arising from not only natural causes but also human-induced pressures, such as sea level rise, coastal development, sewage discharges and sediment run-off. In spite of the value of these aquatic plant communities, virtually no monitoring of the abundance and distribution of seagrasses habitats, in particular at a large geographic scale has been conducted in Tasmania, such as Boullanger Bay. Information on the extent and status of submerged aquatic vegetation (SAV), here largely seagrass meadows, at multi-spatial and multi-temporal scales are needed to support effective conservation and management. Due to resourcing challenges for boat or diver based monitoring, production of such information on the natural dynamics of SAV can only feasibly be tackled by the application of remote sensing techniques. However, a lack of knowledge about the efficacy of remote sensing techniques for seagrass mapping and monitoring persists.

In the response to this need, this thesis summarises the development of an appropriate image processing scheme that produced viable data for interdisciplinary purposes in this particular location. Methods for mapping and monitoring SAV habitats distribution in Boullanger Bay at multiple spatial and temporal scales are trialled. Three case studies were conducted, including: (1) comparison between two hybrid image classification approaches for the investigation of method effectiveness; (2) change detection analysis of land cover classes in Boullanger Bay at two different spatial scales to determine the contribution of the moderate spatial resolution of Landsat and Advanced Land Observing Satellite (ALOS); and (3) change detection analysis to determine the efficacy of the moderate spatial resolution and annual temporal resolution of Landsat in both intertidal or subtidal seagrass dominated environments.

Multi-temporal thematic map series of change detection results were produced over 18 years, from 1990 to 2008. The spatial and temporal changes in the occurrence of SAV meadows in Boullanger Bay were identified and presented that show the extent and distribution of SAV habitats and their rate of change.

Case Study 1 investigated the efficacy of the remote sensing technique performed in the case studies was investigated. Two hybrid approaches: Independent Component Analysis (ICA) based Maximum Likelihood Classifier (MLC) approach and Principal Component Analysis (PCA) based ISODATA approach were compared to assess their ability to classify land cover objects. '*Error Matrix*', image classification accuracy assessment technique demonstrated the better image classification accuracy of ICA based MLC approach (Overall accuracy: 88.4%, Kappa coefficient: 0.86) than PCA based ISODATA approach (Overall accuracy: 82.7%, Kappa coefficient: 0.79).

Case Study 2 provided '*from – to*' change between the classified land covers produced from Case Study 1. Write Function Memory Insertion (WFMI) change detection approach is used to effectively visualise the '*from – to*' change between the land cover types. The study

indicated that the saltmarsh/seagrass boundary was relatively stable over the study period. Conclusions about the relative change of habitats across the whole Boullanger Bay study site are limited due to image processing issues related to cloud and deeper water confounding the results. For SAV, it appears that there has been a decadal scale decline between 1990 and 2000 and then the areas remain stable through to 2008.

In Case Study 3, firstly, an ICA based Multiple-date Composite Image (MCI) change detection analysis was performed to identify the spatial and temporal changes in the intertidal habitats, especially the *Zostera muelleri* seagrass, in the Welcome Inlet area. A relatively stable overall coverage was identified with fluctuating losses and gains in SAV meadows in many areas throughout the monitoring period at rates ranging from annual to decadal. Secondly, a WFMI approach was used for change detection analysis in the open subtidal area of the Boullanger Bay to identify the stability of subtidal SAV meadows from 1990 to 2008. The method revealed the very high stability of sand patches (i.e. uncolonised areas) within the dense *Posidonia australis* seagrass meadows over the 18 year period.

Issues of the accuracy of thematic maps derived from Landsat and ALOS imagery were identified, including misclassification of land cover types in deep water areas i.e. > circa 7 m. However, the overall efficacy of the satellite sensors for mapping and monitoring SAV meadows in Boullanger Bay was supported.

Acknowledgments

The production of this research project has been attributed to the material support by U.S. Geological Survey; Australian Centre for Remote Sensing, Geoscience Australia; TASMAP library aerial photo, the Department of Primary Industries, Parks, Water and Environment; the LIST., (Land Information System Tasmania), the Department of Primary Industries, Parks, Water and Environment; SEAMAP Tasmania, the Tasmanian Aquaculture and Fisheries Institute, University of Tasmania.

The accomplishment of the project has been made by the contributions from a number of individuals and organisations. In particular, I would like to acknowledge the Centre for Spatial Information Science, University of Tasmania for the provision of a workplace to use ENVI and ArcGIS. Special thank is to be given to my supervisor Dr. Richard Mount, School of Geography and Environmental Studies, University of Tasmania for the quality of his support to and supervision of my work.

My acknowledgements are also extended to the staff and students of the School of Geography and Environmental Studies, University of Tasmania. Finally, I wish to thank my family for all their support.

Table of Contents

List of Tables and Figures

Chapter 1 Introduction

1.1 Chapter overview

Satellite remote sensing technologies have become increasingly useful for numerous environmental management applications. This research project utilises recent developments in satellite remote sensing technologies to map and monitor submerged aquatic vegetation (SAV), encompassing; seagrass and macro algae communities, in Boullanger Bay in the north west of Tasmania. Chapter 1 provides an introduction to the science of satellite remote sensing in the context of its application to the mapping and monitoring of SAV meadows. The aim of this project, which is to satisfy the need for information about the distribution of SAV meadows at multi-temporal and spatial scales, is also outlined and the key research questions are introduced. Additionally, the requirements for the investigation into the appropriate remote sensing techniques for mapping and monitoring SAV meadows are also described. An outline of the thesis structure and some of the limitations, associated mainly with the lack of ancillary data, that frame this project are also described.

1.2 Satellite remote sensing

Remote sensing refers to a suite of scientific techniques that facilitate the detection of objects, features, and phenomena without being directly in contact with the entities being surveyed or observed (Lillesand and Kiefer, 2008). Remote sensing includes such applications as magnetic resonance imaging (MRI) of the internal structure of living bodies and photographs taken in the visible and near-infrared wavelengths. However, the term is commonly used to refer to the analysis of images to map and monitor phenomena on the Earth, especially images taken from satellites.

Geostationary and sun-synchronous satellites provide platforms that carry specialised sensors to detect information on objects, areas, or phenomena at a distance from the Earth. Satellite remote sensing employs sensors to detect electromagnetic radiation, reflected or emitted from the target objects, area, or phenomenon on the Earth (Lillesand and Kiefer, 2008). The recorded electromagnetic radiation data provides information about the proposed resources under investigation through the acquired data analysis (Lillesand and Kiefer, 2008). Digitally extracted information can be used for various study area or industries.

1.3 What is SAV mapping and monitoring via satellite remote sensing?

The general function of a map is to represent objects or phenomena on the surface of the Earth (McKenzie *et al.* 2001a). Mapping by remote sensing technologies is a method for locating objects and measuring their extent and orientation. Through the addition of ancillary information, maps can represent not just simple geographical data, but also a variety of other attributes. The use of maps to spatially represent a variety of different types of information facilitates their use across interdisciplinary studies (McKenzie *et al.* 2001a). There are a variety of methods for mapping seagrass meadows from *in situ* observation to remote sensing (Kirkman 1997; McKenzie *et al.* 2001a; McKenzie *et al.* 2001b). For example, Kelly *et al.* (2001) used a method of predictive mapping consisting of multiple logistic regression models and a Boolean logic model to produce maps of seagrass cover probability, the susceptibility of seagrasses to storms, and area suitable for seagrass restoration. Spruzen *et al.* (2008) used mathematical calculations to estimate the extent of seagrass coverage over large geographical areas in north-west Tasmania. However, the distribution mapping of submerged plant beds over large areas is generally produced by mapping from aerial photography. While aerial photography has been available for some time, satellite imagery has become a popular remote sensing platform for surveying marine habitats, such as seagrass and kelp beds (Kirkman 1996; Edyvane 2003). For instance, SEAMAP Tasmania, a coastal benthic habitat mapping project, uses both aerial photographs and satellite imagery to produce digital information of benthic habitats around Tasmania's coastline (Kirkman 1997). There are several points that should be taken into account when mapping SAV by satellite remote sensing. The capability of sensors to locate underwater objects, such as seagrass, relies heavily on the level of spatial resolution and contrast that can be achieved (Dekker *et al.* 2007). Atmospheric condition, such as weather conditions, principally the amount of cloud cover, and other variables, such as tidal level, are also critical factors to be taken into account when using satellite remote sensing to map seagrass meadows (Klemas 2001). Cloud coverage in satellite imagery often prevents researchers from successfully classifying the area under the cloud (Ozesmi and Bauer 2002). Ideally, satellite images should be cloud-free. For marine coastal environments, tidal levels are also another concern when using satellite remote sensing data. Most seagrass species exist in shallow off-shore and intertidal coastal zones (Short *et al.* 2001). Unless water column turbidity is acceptable for satellite sensors to detect underwater objects, periods of high tide should be avoided in order to acquire the sufficient reflectance of electromagnetic radiation. These factors are to ensure that atmospheric effects that might impact on the ability of the sensor to detect objects are minimised. This is especially important when mapping seagrass by satellite remote sensing because inaccuracies associated with atmospheric effects can have a large impact on the image processing of a digitally thematic map and accuracy of output results (Dobson *et al.* 1995; Klemas 2001).

Monitoring by satellite remote sensing technology is referred to as a method of detecting changes in an object's location, extent and spectral features through time. Satellite remote sensing has several advantages for monitoring objects. These include; precision, periodic repetition of observation and the ability to offer a synoptic view covering large areas of ground (Kirkman 1996; Ozesmi and Bauer 2002). Additionally, satellite imagery is generally available during different seasons allowing for coverage throughout the year (Butler and Jernakoff 1999; Klemas 2001; Ozesmi and Bauer 2002; Navalgund *et al.* 2007). On the other hand, there are also limitations in the ability of satellite remote sensing technologies to detect, underwater objects in aquatic environments due to light attenuation. Yet, with ongoing technical developments in satellites and sensors, the potential areas within which remote sensing technologies can be utilised have been expanding (Ferwerda *et al.* 2007). Critically, objects, such as SAV which were previously not suitable for satellite remote sensing have now become accessible due to the availability of high resolution sensors (Ferwerda *et al.* 2007; Silva 2008). Today, the scale of monitoring by satellite remote sensing can be varied from global to national to local, depending upon the types of sensors used and project priorities (Paine and Kiser 2003). High accuracy remote sensing techniques are now available that can monitor changes in the distribution of SAV from shallow water environments over large geographical areas (Ferwerda *et al.* 2007). Selection of the satellite sensor and platform still relies on the research objective, available financial resources and the geographic scale of the object in practice (Kirkman 1996; Butler and Jernakoff 1999; Klemas 2001). Recent developments in remote sensing techniques have focussed on the ability to detect smaller changes in target resources through time (Ferwerda *et al.* 2007). Previously, it was difficult to detect seagrass decline of less than 10% in its early stages by remote sensing (Duarte 2002).

This recent technical development in image analysis has high potential for detecting such small changes in coverage of objects over large extents, such as seagrass meadows.

1.4 Is satellite remote sensing effective for this project?

Satellite remote sensing is a important tool for projects dedicated to the mapping and monitoring of seagrass beds. It offers many advantages over traditional modes of imaging in projects that require the collection of data over a large geographical areas (Ozesmi and Bauer 2002; Ferwerda *et al.* 2007). The primary advantages of satellite remote sensing for mapping and monitoring seagrass meadows over extensive areas are adapted from Ferwerda *et al.* (2007). These include: the ease of accessibility that remote sensing techniques provide; ability to undertake synoptic observation of large areas taken from one precise location; and the possibility of regular and precise monitoring over long time frames. Further advantages are the production of digital archived images for national and international standardisation, and cost effectiveness compared to traditional aerial photography. Also, due to the vulnerability and inaccessibility of some coastal regions, remote sensing survey is a valuable technique (Silva 2008). In particular, boat or diver based monitoring in Boullanger Bay (the study area of this research project) is a challenge. There are three types of survey methods for seagrass meadows observation, including: direct field mapping; mapping by aerial photography, and mapping by satellite remote sensing (Kirkman 1997). For remote sensing techniques, each sensor and sensor platform is designed for the specific purpose of image acquisition. Among those remote sensing techniques, aerial photography has been the preferred technique for seagrass mapping (Dobson *et al.* 1995; Kendrick *et al.* 2000; Ozesmi and Bauer 2002; Ferwerda *et al.* 2007). The value of using aerial photography depends on the size and extent of the objects to be surveyed and the flight height and speed from which observation is conducted. Valta-Hulkkonen et al. (2004) argue that aerial photography has the advantage of providing high accuracy when measuring submerged objects. They also argue that additional advantages of using aerial photography for aquatic vegetation mapping include: providing high spatial resolution with high spatial accuracy; the ability to record images from sufficient spectral length of the visible wavelength; and the possibility of achieving high temporal resolution.

The high spatial resolution of aerial photography, [For instance, aerial photographs can have a spatial resolution of 0.1 m at a 1:20,000 scale (Dobson *et al.* 1995)] enables an observer to detect small objects, such as seagrass patches of around 10 metres in area. Another advantage of aerial photography is the ability to provide a high temporal resolution that generally facilitates the avoidance of high atmospheric effects, such as cloud coverage, in acquired images.

Although satellite remote sensing has different capabilities compared to aerial photography, such as lower spatial resolutions and low temporal resolutions that might also be limited by atmospheric effects (Ferguson and Korfmacher 1997), it is regarded as an appropriate method for this project. For mapping and monitoring coastal regions, satellite remote sensing has many advantages (Butler and Jernakoff 1999; Ozesmi and Bauer 2002). Satellite imagery is effective at providing images of objects over large geographic areas (Dobson *et al.* 1995; Butler and Jernakoff 1999; Ozesmi and Bauer 2002). Additionally, the ability of satellite images to provide simultaneous information on areas adjacent to those being surveyed facilitates the extension of the research to questions such as the correlation between surrounding environments and seagrass meadows (Ozesmi and Bauer 2002). Basically, higher spatial resolutions are preferable in order to map detailed seagrass habitat for optical identification. However, since seagrasses are located over extensive areas, low spatial resolution with high spectral resolution associated with satellite remote sensing are potentially more appropriate than high spatial resolution and low spectral resolution associated with aerial photography. Satellite sensors that have multiple spectral bands, including not only visible and near-infrared but also other wavelengths, usually provide a better spectral resolution than conventional color photographs (Ferguson and Korfmacher 1997). Further spectral bands allow the extraction of additional information from images through subsequent spectral analysis.

Archived satellite data is a base for the ongoing analysis of the characteristics, attributes and condition of phenomena or objects (Coppin *et al.* 2004). Additionally, the anticipated long sensor life associated with satellite platforms allows regular coastal resource monitoring at seasonal or annual periods over long time frames (Ozesmi and Bauer 2002). A significant consideration for monitoring vegetation is the frequency and timing of image acquisition. While repeat acquisition of aerial photographs in order to cover large areas is possible, such approaches are considered too expensive for the majority of monitoring projects (Ferguson and Korfmacher 1997) and often logistically impossible to arrange within the project timeframe. Consideration of phenological variation is essential, since each type of vegetation has different seasonal and annual phenological scales (Klemas 2001). Objects may also experience rapid transformation in response to rapid environmental change. An appropriate monitoring schedule is crucial to discriminate such natural changes from changes in objects caused by extrinsic effects resulting from human-induced disturbances. The cycling period of satellite remote sensing images is capable of meeting such a monitoring standard. Another advantage of satellite images derives from their digital format. This allows them to be organised into Geographical Information System (GIS) databases that, in turn, facilitates the synthesis and compilation of diverse data sources and types (Ferguson and Korfmacher 1997; Kirkman 1997; Ozesmi and Bauer 2002). Digitally archived data derived from satellite imagery can then be used as baseline data for future research at nationally and internationally standardised scales (Kirkman 1997). This project requires the mapping of seagrass meadows over a broad and extensive range and the monitoring of those seagrass meadows though time. Thus satellite images have been identified as the most useful remote sensing method for this project.

1.5 Value of this project

Submerged aquatic vegetation plays an important role in Australia's marine and freshwater ecosystems. Tasmanian seagrass communities also provide unique food chains and habitats for numerous marine species and shorebirds, and support shoreline formation processes (Bryant 2002; DPIPWE 2009). Recently, large seagrass beds were found in the north-west of Tasmania, including Boullanger Bay, the study area for this project (Rees 1993; Kirkman 1997). Like other areas throughout Australia and the world, Tasmanian seagrass communities have period of decline and have suffered degradation. Seagrass meadows in the Tasmania have already been destroyed by eutrophication from sewage and fertiliser discharge (Rees 1993; Sprod *et al.* 2003; CCNRM 2005). The loss of aquatic plant communities causes serious damage to marine biological diversity and their associated ecosystems (Sprod *et al.* 2003). With ongoing seagrass decline, a number of studies have demonstrated that aquatic plants, such as seagrass and macroalgae species, play critical ecological roles in providing habitats for other aquatic organisms (Kelly 2005; Pasqualini *et al.* 2005; Oliveira *et al.* 2006; Thorhaug *et al.* 2006). Information on the extent and status of seagrass meadows at multi-spatial and temporal scales is a crucial factor for seagrass conservation and management

(Kirkman 1990; Kirkman 1996; Kirkman 1997; Butler and Jernakoff 1999; Kemp 2000). However, digitally archived information on the abundance and distribution of SAV habitats in Boullanger Bay and how these distribution changes through time, especially at a large-scale are limited. As people are increasingly recognising the ecological importance of such aquatic plant communities, need for knowledge about their natural dynamics, condition and distribution is increasing throughout the world. In Tasmania, accurate spatial and temporal information on such aquatic plants community is also crucial not only for coastal ecosystem conservation or management but also for commercial (e.g. aquaculture) and recreational activities. Mapping SAV meadows in Boullanger Bay is also important for interdisciplinary research and various industrial purposes due to the limited areal information on SAV meadows. Additionally, limited temporal information on the distribution of SAV beds has prevented the incorporation of SAV distributions into environmental studies and conservation or management. There is thus a need for updating information on seagrass condition and distribution in Boullanger Bay observed in previous research (Rees 1993).

In Australia, a few papers dealing with the characterisation of seagrass meadows based on landscape ecology concepts have been published (Butler and Jernakoff 1999). These previous researches at large geographic scale of several hectares defined predominant habitats of different seagrass species (Butler and Jernakoff 1999). Ample opportunity still remains for a mapping and monitoring project to investigate seagrass natural dynamics in terms of multiple spatial and temporal variations, such as habitat ratio, patch size and three-dimensional structure (Butler and Jernakoff 1999). No integrated standard approach for mapping and monitoring seagrass has been established due to the differences in monitoring objective and resource availability (Butler and Jernakoff 1999). This is also the case in the remote sensing technology field. A number of remote sensing techniques for image classification and change detection procedures have been developed for mapping and monitoring purposes. However, lack of knowledge about what kind of classification approach is effective for particular features of interests in a particular study area, still remains (Lu and Weng 2007). A standard method of image classification and change detection for mapping and monitoring the coastal environment, including SAV meadows, has not been established yet. Different methods have different merit dependent upon the given object, study area, and research purpose. No single optimal method can be applied for all cases due to diverse environmental, technical, economic, and historical conditions (Coppin *et al.* 2004; Lu *et al.* 2004; Meehan *et al.* 2005). Thus, the development of an appropriate method for mapping and monitoring SAV meadows in Boullanger Bay, while being drawn from existing methods, will necessarily be established. An assessment of the advantages and disadvantages of multiple methods is required to find out what combination of which different methods will be the most appropriate approach for this research project. A key determinant here will be both the characteristics of the research site itself and the requirement that the method developed is able to produce data that can be used for a range of purposes.

1.6 Research purpose, aims and objectives

This research is intended to support the development of an appropriate image processing scheme that will produce valuable data for interdisciplinary purposes in this particular location. Ideally, it will also provide insights through the comparison of methodologies useful for other SAV projects.

The overall aim of this thesis is to determine the extent to which remote sensing techniques can detect changes through time in the coverage of intertidal and subtidal habitats in shallow, temperate, sheltered embayments such as Boullanger Bay, in north west Tasmania. These habitats include saltmarsh, sand and, especially, submerged aquatic vegetation (SAV), such as seagrass.

The research objectives are:

1) To identify and select satellite image data and methods related to the study needs including taking into account spatial, temporal and spectral resolutions (Methods);

2) To test innovative candidate remote sensing methods suitable for the study area and study aims (Case Study1);

3) To perform change detection on habitats at two different spatial scales to determine whether the moderate spatial resolution of Landsat and ALOS is effective (Case Study 2); and

4) To perform change detection on habitats to determine whether the moderate spatial resolution and annual temporal resolution of Landsat is effective (Case Study 3) in:
    a) Intertidal seagrass-dominated environments, and
    b) Subtidal seagrass-dominated environments

1.7 Outline of research report

A brief outline of this report is as follows:

Chapter 1 describes the need for this research in the context of satellite remote sensing and the application of satellite remote sensing techniques for mapping and monitoring the distribution of seagrass.

Chapter 2 comprises a literature review. This literature review describes the background of this report, encompassing: a description of the study area; the ecology of seagrass; and the history of remote sensing techniques for mapping and monitoring seagrass.

Chapter 3 describes the methodologies that were applied in this research. In summary, the methods used include procedures for image selection, image pre-processing, image transformation, image classification, change detection, and an assessment of the accuracy of geometry and image classification results.

Chapter 4 describes Case Study 1: the comparison between two image classification approaches to investigate method effectiveness.

Chapter 5 describes Case Study 2: change detection using the classification result generated from the Case Study 1 for detecting changes in the distribution of the classified land covers.

Chapter 6 describes Case Study 3: change detection for two areas, the intertidal flats across the Welcome Inlet and the subtidal open water area of the Boullanger Bay, in order to detect the change of habitats in the distribution of SAV meadows, especially intertidal seagrass for the Welcome Inlet and subtidal seagrass for the subtidal area of the bay.

Chapter 7 presents the results of each case study

Chapter 8 discusses the results of this research in order to identify the critical points in this research.

Chapter 9 summarises the results of this research in terms of the significance for seagrass mapping and monitoring and discuss some final conclusions.

Chapter 2 Back ground of Boullanger Bay, Tasmania

2.1 *Chapter overview*

Rapid environmental change due to natural and human-induced disturbances can lead to the rapid decline and loss of natural resources. One response to this situation is the development of technologies for mitigating the occurrence of environmental change so as to minimise resulting decline or loss of environmental services, values and habitats. This research project seeks to identify environmental changes associated with submerged aquatic vegetation meadows and ability of remote sensing technologies designed to map and monitor those changes. The decline and loss of seagrass has been identified as a significant environmental problem throughout the world, potentially including Tasmania (CCNRM 2005). Recently developed remote sensing methods, together with key technical developments with satellites and sensors, have been applied in the distribution mapping and monitoring of seagrass habitats (Phinn *et al.* 2006b; Anstee *et al.* 2009). This chapter details the significance of SAV, especially seagrass habitat to the ecology of the Boullanger Bay environment and the importance of utilising and applying recent advances in remote sensing techniques and methods for mapping and monitoring such seagrass habitats.

Information on the general characteristics, ecological function and status of seagrasses presented and reviewed in this chapter were collected from previous studies from both Australian and international environments. The methodological rationale for setting up Case study areas within Boullanger Bay is introduced. A description of the general biology and the extent of information as to the current distribution and status of seagrass are outlined to establish the ecological significance of this project. The relevance of a scheme for mapping and monitoring seagrass habitats is related to requirements associated with their conservation and management, in addition, those stemming from fisheries management. Finally, a review of previous research utilising satellite remote sensing techniques for seagrass and wetland mapping and monitoring are described. Key technical and methodological advances associated with these studies are assessed in terms of their applicability to the requirements of the research study undertaken here.

2.2 *Why multi-spatial scale study locations are required?*

There are two central reasons for selecting Case Study locations with different spatial scales in this project: (1) the need for further information on ecological dynamics analysis at different scales, and (2) the need for further information on the effectiveness of remote sensing techniques at different scales.

Mapping at multiple spatial scales is crucial to acquire sufficient information to monitor the health status of seagrass (McKenzie *et al.* 2001a). Butler and Jernakoff (1999) have identified the need for multi-scale information on the natural dynamics of seagrass species and their environmental variability in time and space. Such information is vital for successful conservation and management of seagrass meadows as it facilitates decision-making on the location of reserves and the temporal scale of conservation projects (Butler and Jernakoff 1999; McKenzie *et al.* 2001a). In order to provide information on the objects of interest from different points of view, mapping and monitoring projects can be conducted at multi-temporal and multi-spatial, in particular, two basic spatial scales: regional and local (Butler and Jernakoff 1999). Regional scale research produces information that is useful in ascertaining synoptic-level patterns in the landscape; commonly changes are evident at hectare scales and the information tends to be used as a qualitative indication of broad scale changes. Local scale research produces more detailed information associated with quantitative measures of seagrass abundance or other attributes (Butler and Jernakoff 1999). As for a project that needs qualitative rather than quantitative information, larger scale research is typically conducted, and quantitative management does not use broad scale mapping and monitoring due to the low precision of maps and a lack of detailed information on object features (Butler and Jernakoff 1999). When using satellite sensors of low spatial resolution, for instance, large scale mapping and monitoring allows for the detection of broad changes in seagrass distribution and abundance. On the other hand, it is difficult to detect small changes due to the large extent of the pixels. Duarte (2002) has argued that it is critical to obtain information at small areal scales because the seagrass meadow monitoring with low spatial resolution tends to detect only decline that is already substantial. Early knowledge of any possible decline can allow for intervention so as to mitigate or stop the decline from reaching the stage at which it accelerates rapidly. Such information on the early stages of decline is now regarded as significant for the development of early warning systems (Duarte 2002). In this regard, mapping and monitoring current extents of seagrass distribution at small geographic scales facilitates later comparisons with areas of potential recolonisation (Short *et al.* 2001). This is especially important for species which have high recolonisation capabilities, while also being vulnerable to numerous threats to their ability to recolonise an area. Potential areas of seagrass habitat are areas where seagrass species used to exist, at some time in the past, yet do not exist at present (Short *et al.* 2001). Potential area mapping and monitoring is particularly crucial for the seagrass species of fast recoloniser, such as, *Zostera muelleri* and macroalgae but may not be useful for the seagrass species of slow recoloniser, such as *Posidonia australis* (Clarke and Kirkman 1989). Two case study areas in this project focus on not only individual seagrass species in different tidal areas but also on potential areas of seagrass habitat where seagrass recolonisation could occur in the future. Investigation of the recolonisation speed or ratio of slow and fast recolonisers can be attempted through two different spatial scales and multi-temporal scales. Information on different temporal patterns in the abundance and distribution of seagrass meadows at diverse spatial scales is also crucial to identify changes in secondary productivity associated with seagrass habitats (Butler and Jernakoff 1999).

For this project, the recently developed computational method, known as Independent Component Analysis (ICA) was used for Welcome Inlet area to analyse satellite images. Investigation of the effectiveness of this technique, in accordance with the purposes of the research project, is crucial for future mapping and monitoring research into seagrass meadows in the Boullanger Bay area. The spatial scale of the study area is a significant factor in the application of ICA for image analysis. Conducting this study at multiple spatial scales is thus considered as one useful way to identify and evaluate the effectiveness of ICA technique for seagrass mapping and monitoring procedure.

2.3 *Ecology of seagrass: general biology and present status in Boullanger Bay*

Seagrasses are regarded as an important marine habitat of nearshore coastal environments throughout the world (Kirkman 1996). Sixty seagrass species, which are categorised into 13 genera and 5 families are identified globally (Short *et al.* 2001). Seagrasses are submerged marine flowering plants generally adapted to soft sediment ocean floor with their rhizome in nearshore areas (Short and Wyllie-Echeverria 1996; Kirkman 1997; DEHAA 1998; Butler and Jernakoff 1999; Short *et al.* 2001). They have a greater requirement for light than most macroalgae (Kirkman 1997; Duarte 1991). Majority of seagrass species are living in subtidal marine environment, although some species, such as *Zostera* spp. and *Halophila* spp., need to emerge from the water surface at low tidal stage or to live in area containing fresh water inflow for their reproduction, (Short *et al.* 2001). Additionally, several species can live only in particular environments, such as fresh water, estuarine, marine, or hypersaline conditions (Short *et al.* 2001).

Seagrass meadows are strongly controlled by ambient coastal environments in terms of geographical configuration, water flow, water nutrient component, and biological relationship with other species (Short and Wyllie-Echeverria 1996; Butler and Jernakoff 1999; Kemp 2000; Orth *et al.* 2006). In such a complex relationship, seagrasses participate in numerous important ecological services, including: organic matter provision; assimilation energy into ecosystem; nutrient trap and cycling; shore line protection; substrate sediment stabilization; enhanced biodiversity; and trophic transfers to adjacent ecosystems (Kirkman 1997; Butler and Jernakoff 1999; Kemp 2000; Duarte 2002; Orth *et al.*, 2006). Among these services, water current flow, water nutrient trap and cycle, and coastal marine food web structure are strongly associated with the geometry, condition and species of seagrasses (Short and Wyllie-Echeverria 1996; Hemminga and Duarte 2000; Kemp 2000). In this regard, seagrass is known as a marine ecosystem engineer (Kemp 2000; Bos *et al.* 2007). Rhizomes of seagrass provide substrate and shoreline stability and uptake of nutrients (Short and Wyllie-Echeverria 1996; Kirkman 1997; DEHAA 1998; Butler and Jernakoff 1999; Kemp 2000). Stabilised substrate sediments together with seagrass plants attenuate water current flows and protect the coastline from water energy (DEHAA 1998; Orth *et al.* 2006). Another role of seagrass is to provide organic carbon and oxygen through its photosynthesis (Orth *et al.* 2006). Seagrass provides not only nursery habitat for many marine species of fishes, invertebrates and crustacean but also seagrasses can be primary producer for some marine herbivores as a food source (Short and Wyllie-Echeverria 1996; Kirkman 1997; DEHAA 1998; Butler and Jernakoff 1999; Beck *et al.* 2001). Seagrass contributes to nutrient trap and cycling in surrounding ecosystem through its detritus food chain[1] (DEHAA 1998) and grazing food chain[2]. Consequently, they are a biological indicator of natural or human induced disturbances in coastal marine ecosystem through their loss and degradation (Ciraolo *et al.* 2006; Orth *et al.*, 2006).

2.3.1 Australian and Tasmanian seagrasses

Australian seagrass communities are a prominent part of coastal ecosystem function in both temperate (44° S) and tropical (10° S) areas of the coastline (Kirkman 1997; Butler and Jernakoff 1999; Sprod *et al.* 2003). Seagrass meadows are regarded as one of the most vulnerable environments in nearshore or estuarine areas of Australia (Kirkman 1996). Australian coasts sustain the broadest assemblage of seagrass habitats with about 51,000 square km and the highest taxonomical diversity of seagrass throughout the world (Kirkman 1997; Butler and Jernakoff 1999). South-western Australia possesses the highest biomass and

---

[1] Food chain associated with the consumption of non-living particulate organic biomass
[2] Food chain associated with the consumption of living plant biomass

diversity of seagrass in temperate region in Australia (Rees 1993; Short *et al.* 2001). Along the protected area of the Great Australian Bight and across South Australia and Tasmania, large areas of seagrass meadows occur (Butler and Jernakoff 1999; Kendrick *et al.* 2000). There are six marine and two estuarine species of seagrass identified in Tasmania: *Posidonia australis, Amphibolis antarctica*, *Halophila australis*, *Heterozostera tasmanica* and *Zostera muelleri* (Rees 1993; Short *et al.* 2001; CCNRM 2005) (Figure 2.1, 2.2, 2.3 and 2.4). Tasmanian seagrass communities also provide unique food chains and habitats for numerous marine species and shorebirds, and support shoreline formation processes (Bryant 2002; DPIPWE 2009). In the far north-west Tasmania, extensive seagrass beds of over 8,000 ha are supported by flat landscape ranging over tidal flats (Sprod *et al.* 2003; CCNRM 2005). Large seagrass beds of which are mainly composed of *P. australis* were identified in the coast of north-west Tasmania (Kirkman 1997). *P. australis*, a dominant specie in Boullanger Bay, is a subtidal seagrass widely occurs in 1– 15 m of water of sheltered estuarine, marine embayments and near shore areas with more or less continuous distribution along the temperate coast line of Australia from the southern half of mainland coast to the northern coast of Tasmania (Kirkman 1997; Waycott and Sampson 1997; Trautman, & Borowitzka 1999). In addition to *P. australis*, Mount et al. (unpub) recently observed several intertidal and subtidal seagrass species, including; *A. antarctica*, *H. australis*, *H. tasmanica* and *Z. muelleri* in Boullanger Bay area. As with other seagrass community in other area in the world, these Tasmanian seagrass species provides valuable resources for natural environment and human society in this area.

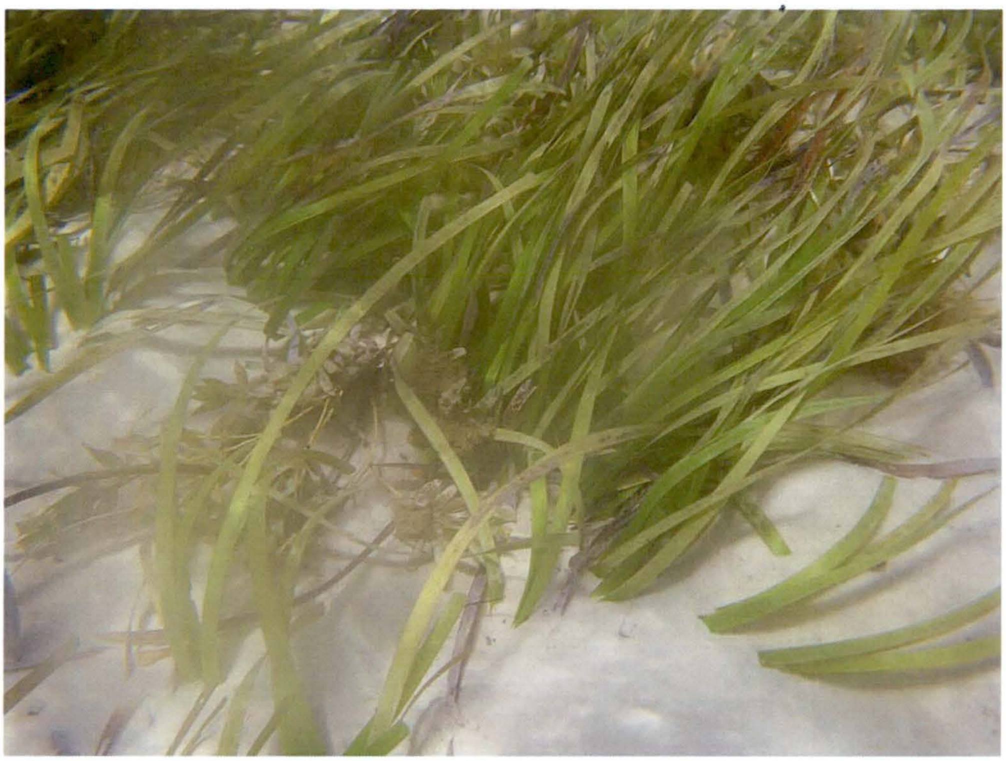

Figure 2.1 *Posidonia australis* (Subtidal specie)

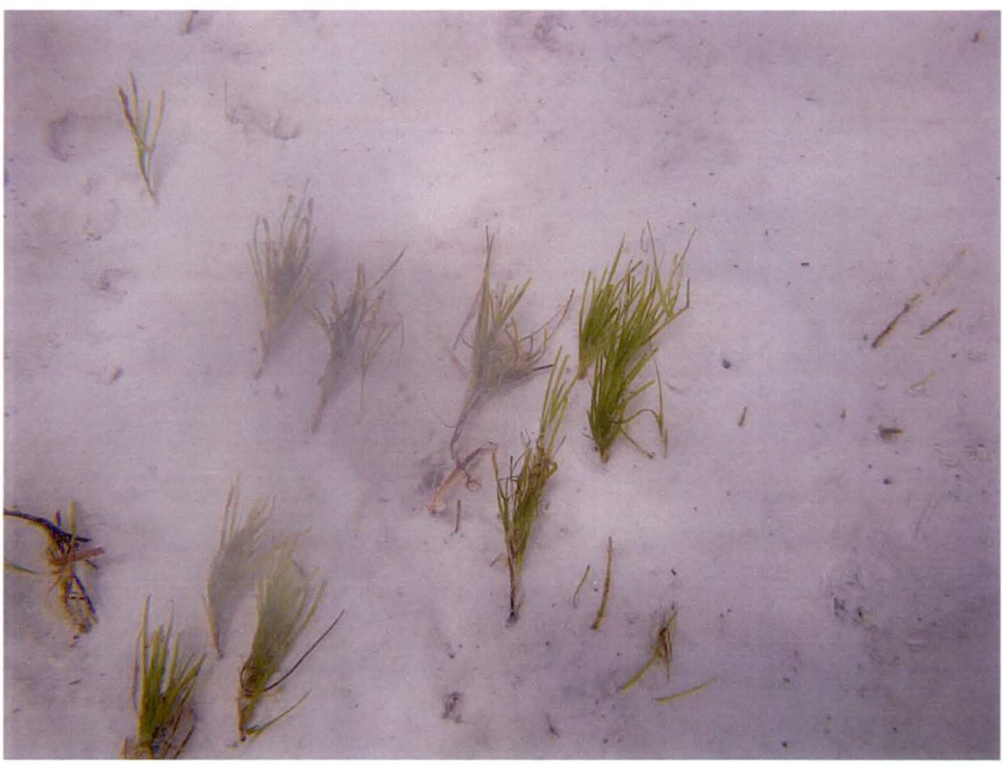

Figure 2.2 *Heterozostera tasmanica* (Subtidal specie)

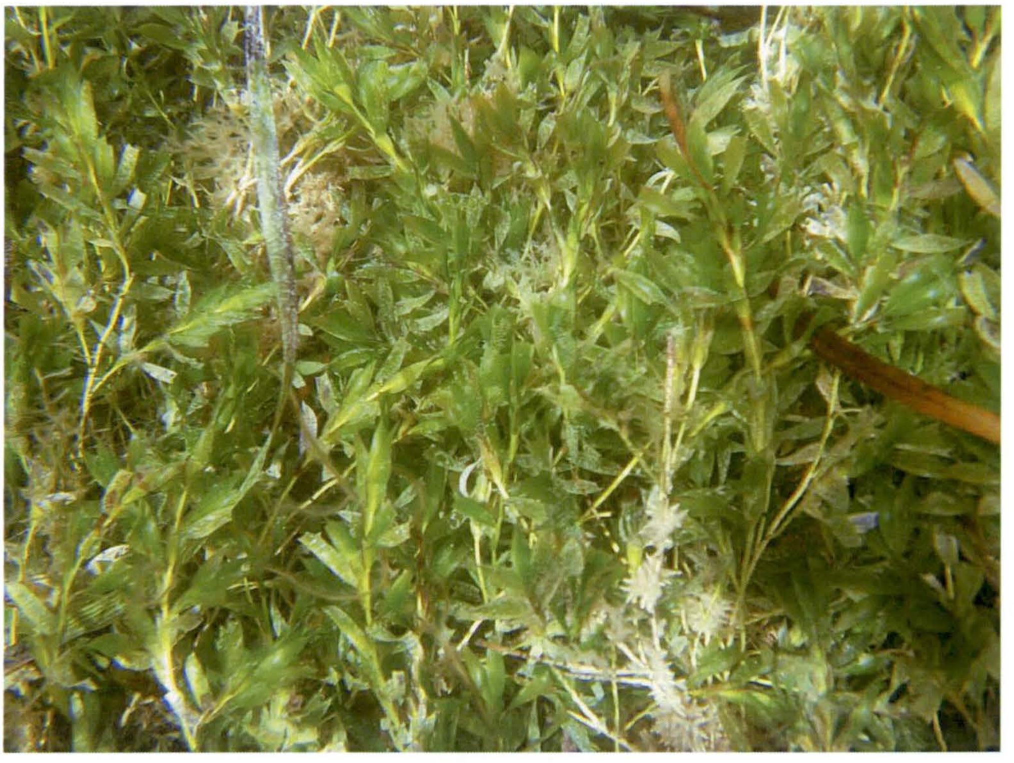

Figure 2.3 *Amphibolis Antarctica* (Subtidal specie)

Figure 2.4 *Zostera muelleri* (Intertidal specie)

2.3.2 Seagrass status

Worldwide decline or demise of seagrass has occurred in last 40 to 50 years with increasing rates of its population decline (Short and Wyllie-Echeverria 1996; Butler and Jernakoff 1999; Kemp 2000; Short *et al.* 2001; Orth *et al.*, 2006). Seagrass communities are affected by environmental change, especially water and sediment quality because of the special requirements for light and sediment conditions (Duarte 2002). Environmental changes arisen from not only natural causes, such as disease, hurricanes and grazing by herbivores but also coastal human-induced pressures, encompassing: coastal development, sewage discharges, heavy metal accumulation, sediment run-off, eutrophication and invasive species, are in the context of the seagrass decline (Short and Wyllie-Echeverria 1996; DEHAA 1998; Butler and Jernakoff 1999; Kemp 2000; Short *et al.* 2001; Duarte 2002; Orth *et al.* 2006). While the amount of actual seagrass loss might be larger, 90,000 ha of seagrass loss at over 40 locations throughout the world have been reported by previous researches (Short and Wyllie-Echeverria 1996; Hemminga and Duarte 2000). Seagrass decline is also ongoing in Australia like other areas in the world (Kirkman 1997). Numerous natural and anthropogenic disturbances are attributed to the seagrass decline in Australia (Kirkman 1997). Although the scale of seagrass loss due to natural disturbances, such as cyclones and floods, is larger with over 1,000 km² than the scale of human-induced losses with 450 km², mostly, the seagrasses destroyed through human-induced disturbances have been species like *P. australis,* which is unlikely to recover quickly (Kirkman 1997). The largest decline and loss of seagrass meadows have been attributed to the eutrophication of water columns caused by human activity in Australia (Kirkman 1996). Tasmanian seagrass communities have been faced with the situation of population decline (CCNRM 2005). They have been also destroyed and disjoined by coastal development and poor catchment management together with threats, encompassing; dredging, land clearing, sediment run off, and sewage and stormwater discharges (Sprod *et al.* 2003; CCNRM 2005). Additionally, multiple threats derived from natural or human-induced, or cumulative impacts associated with these threats cause serious seagrass loss and decline at geographic scales from square metres to hundreds square kilometres (Butler and Jernakoff 1999; Kemp 2000; Orth *et al.*, 2006). According to the common remark as to the resilience of temperate Australian seagrasses, such as *Posidonia spp.* and *Amphibolis spp.* once they were destroyed, a recovery of these species in same area are unlikely happened (Clarke and Kirkman, 1989). Therefore the degradation and loss of these species is important not only to present but also future marine coastal environments.

2.4 The value of mapping and monitoring seagrass meadows

With ongoing seagrass loss worldwide including Australia, concern over seagrass conservation and management is of major interest due to the important role of seagrass in the coastal environment at local, regional and national scales (Butler and Jernakoff 1999; Orth *et al.*, 2006). However, the quality and quantity of information on the distribution, environment and functional significance of seagrass are fragmented and varied between species (Butler and Jernakoff 1999). General models of seagrass ecophysiology, ecology and ecological correlation have yet to be formulated due to the limited information on Australian seagrasses (Butler and Jernakoff 1999). In Tasmania, limited research into seagrass habitat distribution and population change rate has been conducted (Rees 1993; Kirkman 1997). Lack of comparative studies at comparable temporal and spatial scale limits synthesised and integrated approaches for seagrass conservation and management program. Together with the growing awareness of seagrass values and vulnerability, proper conservation and management activity is regarded as a vital task to support sustainable seagrass communities (Kirkman 1996). Information on natural change in seagrass habitat distribution at multiple spatial and temporal scales is regarded as key information for developing management plans (Butler and Jernakoff 1999; Orth *et al.*, 2006). In order to support successful programmes, baseline information on the extent and status of seagrass meadows via mapping process are required as a first step (Kirkman 1990; Kirkman 1996; Kirkman 1997; Kemp 2000; Mount 2007). Next, regular monitoring of the seagrass meadows at multi-temporal scales (e.g. annual or seasonal) on a longer term basis produces the information on seagrass meadows compared to the baseline (Kirkman 1990; Kirkman 1996; Ferguson and Korfmacher 1997). Seagrass mapping and monitoring processes are thus central to meeting high standards for conservation and management project (Dobson *et al.* 1995; Thomas 1995). In particular, information on the following is useful: rate of seagrass population change in response to natural and human-induced disturbances; how seagrass changes distribution and composition at seasonal and annual differences; and whether seagrass can recolonise or not (Kirkman 1997).

2.4.1 Administrative perspective

There are also reasons for seagrass community mapping and monitoring from administrative and ecological perspectives. From the administrative perspective, sound scientific decisions that underpin time management, cost management, and project site selection are crucial to effective projects and programmes, not only conservation and management but also other coastal activities, such as, coastal development or aquaculture (Kirkman 1996; Butler and Jernakoff 1999; Kemp 2000; Orth *et al.*, 2006). The quantitative and qualitative information on seagrass distribution through long term-periodic data will support decision makers to make those critical decisions (McKenzie *et al.* 2001a; Orth *et al.*, 2006). Mapping and monitoring processes are then core components of the coastal zone programs as they produce information on the change in seagrass distribution, abundance and diversity (Kirkman 1997; Kemp 2000). For instance, geographic information on seagrass distribution over large areas assists the site selection of Marine and Estuarine Protected Areas (MEPAs) or vulnerable sites to natural and human-induced disturbances (Butler and Jernakoff 1999; McKenzie *et al.* 2001a). Information on ecologically important seagrass beds assists managers to select the location of marine parks and reserves (Kirkman 1997). Finer geographic scale information assists identifying an appropriate scheme of coastal development that mitigates the impact on seagrass meadows (McKenzie *et al.* 2001a). Additionally, the susceptible area of seagrass meadows to natural or human-induced disturbances, such as hurricane, oil spills or other pollution events can be analysed by finer scale geographic information (Kirkman 1997). However, the paucity of appropriate mapping and monitoring programmes makes it difficult to conduct comprehensive assessments of actual seagrass loss in the first place of the conservation and management projects (Short and Wyllie-Echeverria 1996). Paucity of seagrass loss and change rate derived from monitoring programmes is also obstructing the formulation of global conservation policy (Duarte 2002).

2.4.2 Ecological perspective

From an ecological perspective, mapping and monitoring seagrass meadows are crucial for identifying the natural population dynamics of seagrass community and correlation between seagrass habitats and natural or human-induced disturbances, such as sediment run-off derived from coastal development, decreased light intensity arising from sea level rise, and eutrophication (Butler and Jernakoff 1999; Duarte 2002; Ferwerda *et al.* 2007). In particular, the effect of rapid environmental change on seagrass community habitats is not been well known (Orth *et al.*, 2006). Uncertainties as to the present loss rate and expected loss of seagrass meadows are due to the lack of regular monitoring (Duarte 2002). The responses of seagrasses to such an unprecedented environmental change in quantity and quality of their habitats could be identified through monitoring programmes. (Orth *et al.*, 2006). In accordance with the information on the seagrass response, the specific requirements for seagrass habitat sustainability, the seagrass's resilience to damage, required duration for recovery, and required conditions for seagrass restoration could be estimated (Meehan and West 2000). For instance, transplantation of seagrass, one potential method of conservation and management for the mitigation or restoration of seagrass decline due to human-induced disturbances in the coastal environment needs such information on the response of seagrass to improve the transplantation scheme (Cambridge and Kendrick 2009). Continuous monitoring of the seagrass meadows at multiple temporal scales is then essential to detect positive or negative response of seagrass distribution. Moreover, seagrasses can be used as a biological indicator to measure the health of adjacent coastal and estuarine ecosystems whether tropical and temperate regions, because of their sensitivity (Bortone 2000; Orth *et al.*, 2006). Degradation and extent loss of seagrass meadows represents that the degradation and loss of adjacent ecosystem functions that seagrass supports (Abal and Dennison 1996; Orth *et al.*, 2006). Widespread seagrass distribution across tropic and temperate regions often enables better evaluation of coastal ecosystem trends at large geographic scale than the assessment based on other coastal habitats, such as coral reefs, mangroves, or salt marsh as their distributions are mainly restricted to only tropical or temperate region (Orth *et al.*, 2006). Another feature of seagrass meadows is that they are effective indicator and their degradation and recovery rates can be measured with a defined temporal scale via a monitoring process and used to assess environmental impacts or coastal environment recovery program (Longstaff and Dennison 1999; Orth *et al.* 2002).

2.4.3 Seagrass monitoring

Nineteen seagrass conservation programs are currently carried out globally, with monitoring of 30 seagrass species over 44 countries (Orth *et al.*, 2006). Information from these monitoring programs can be used not only for their individual conservation program at regional or local scale but also can be integrated to develop global seagrass conservation and management program and environmental impact assessment program (Orth *et al.*, 2006). Seagrass population dynamics of species and regions are mostly unknown globally (Kenworthy 2000). In Australia, despite their seagrass communities are extremely important habitats supporting coastal ecosystems, very little of the Australian coastlines is systematically monitored, which in turn, means information on seagrass distribution and temporal dynamic also still remains poor (Kirkman 1997). Lack of synthesized data from mapping and monitoring processes prevents seagrass management programmes from further understanding global processes, threats, and changes and limits improvement in the programmes (Orth *et al.*, 2006). While it may have the least representation of seagrass diversity and abundance in Australia, Tasmanian seagrass communities have not been well explored because of the limited survey of benthic biota (Kirkman 1997; Sprod *et al.* 2003). Although the distribution of Tasmanian seagrass species have been identified through prior researches (Rees 1993; Kirkman 1997) and the SEAMAP Tasmania programme has mapped the majority of the seagrass beds around the coast, a comprehensive survey of the whole Tasmanian coast has not yet taken place. While extensive seagrass beds have been identified in the far north-western Tasmania, the digitally archived map series of Boullanger Bay at large geographic scale, recording change through time is still limited. If there have been changes in seagrass distribution in this area, it is hard to measure the extent of change due to a lack of time series data (Kirkman 1997). Thus, if seagrass distribution in the Boullanger Bay, study area for this project was systematically mapped and monitored at multiple spatial and temporal scales, it would to produce valuable information for conservation and management (Kirkman 1997).

2.5 Satellite remote sensing techniques for image classification and change detection

Recent satellite remote sensing image analysis techniques are numerous. Effectiveness of an individual technique varies with the target object, area, and environmental condition of the study area when the imagery was acquired. Investigation into the remote sensing technique of choice is important to identify the effectiveness of the techniques so that appropriate application of remote sensing techniques is performed for meaningful research activity afterwards.

Extensive seagrass loss and degradation has led to an increase in the seagrass research effort together with the establishment of marine protected areas and conservation projects during the last decade throughout the world (Orth *et al.* 2006). The number of research projects into the mapping and monitoring of seagrass distribution has also been increasing. There are several primary research methods in remote sensing for seagrass mapping and monitoring, including: aerial photography, acoustic methods, videography, and satellite imagery (Kirkman 1990; Butler and Jernakoff 1999). Each method has advantages and disadvantages for seagrass mapping and monitoring application. With ongoing technical development, remote sensing methods have received attention for underwater object observation, and numerous techniques have been developed so far (Rogan and Chen 2004). In particular, satellite remote sensing is one of the major methods for seagrass mapping and monitoring. However, the literature evaluating research methods into coastal area, including seagrass observation, still remains insufficient (Butler and Jernakoff 1999), especially in the area of satellite remote sensing. In response to the need for satellite remote sensing method assessment of coastal area, Ozesmi and Bauer (2002) evaluated the satellite remote sensing techniques for wetland application. Ferwerda et al. (2007) also examined remote sensing techniques of seagrass monitoring application, yet it was not emphasised on spectral image analysis techniques like the research of Ozesmi and Bauer (2002). While these method evaluation research papers are valuable (Butler and Jernakoff 1999), difficulty in application of the methods examined in these papers still remain. That is there is no single technique of satellite remote sensing that can be applied for all conditions of areas and objects in marine coastal region (Lu *et al.* 2004). As other types of remote sensing methods, satellite remote sensing techniques selection highly relies on whether those techniques meet the regulations of particular object, the scale and status of study area and the purpose of observation (Butler and Jernakoff 1999). In addition, the same technique does not necessary ensure the equivalent effectiveness to similar objects because the status of the object is often influenced by numerous environmental variables. As a result, numerous satellite remote sensing techniques have been developed for different applications, and therefore, an appropriate technique should be identified for each observation project (Phinn *et al.* 1999).

Image classification and change detection techniques are central procedures of image analysis for satellite remote sensing (Dobson *et al.* 1995; Ozesmi and Bauer 2002; Lu *et al.* 2004;

Coppin *et al.* 2004). Phinn et al. (1999), Ozesmi and Bauer (2002) and Lu and Weng (2007) addressed satellite image classification techniques. Dobson et al. (1995) summarised major change detection techniques of satellite remote sensing and aerial photography for coastal analysis. Although the coastal region was not main theme, Lu et al. (2004) and Coppin et al. (2004) also summarised change detection techniques for satellite based monitoring. According to these review articles, the remote sensing techniques identified as useful techniques for coastal environment are: unsupervised classifier; maximum likelihood classifier; principal component analysis (PCA) and independent component analysis (ICA) for image classification; and PCA, ICA, Image Algebra, Write Function Memory Insertion (WFMI), and Multi-date Composite Image (MCI) analysis for change detection.

2.5.1 Image classification

Image classification is divided into two main types: unsupervised classification and supervised classification. The main difference is to label classes prior to or after computational classification processing using ground truth data or ancillary information or expert knowledge of study area. Unsupervised classification is executed by computer processing without any prior information related to class categories in observed image, yet supervised classification uses ancillary information to label class categories before computer processing defines each category. Ozesmi and Bauer (2002) indicated unsupervised classification is very common method for the classification of wetland habitats, including submerged aquatic vegetation based on the review of previous research. In particular, when a large number of class categories are required, unsupervised classification is most effectively used (Ozesmi and Bauer 2002).

For supervised classification, a number of techniques have also been used for coastal area mapping (Ozesmi and Bauer 2002). Among others, the Maximum Likelihood classifier is the most common supervised classification techniques for wetlands or coast area mapping (Macleod and Congalton 1998; Everitt *et al.* 2009). Everitt et al. (2009) also employed Maximum Likelihood classifier to map black mangrove on the Texas Gulf Coast in their research. They sampled 5 classes in QuickBird images for each site to classify images. Although few errors were identified due to mixed vegetation, highly accurate results of overall accuracy (90.0% for site 1 and 90.7% for site 2) and kappa coefficient (0.866 for site 1 and 0.861 for site 2) were obtained (Everitt *et al.* 2009). Additionally, some researchers also employed minimum distance to mean classifier for seagrass mapping with QuickBird-2, Landsat 5, and CASI-2 (Phinn *et al.* 2006b). Minimum distance classifier produced high accuracy for QuickBird-2 and CASI-2, yet not for Landsat 5 (Phinn *et al.* 2006b). According to this result, type of satellite imagery highly influences the accuracy of resultant thematic map. Both unsupervised and supervised classification techniques are very common for coast area mapping. Yet, a simple determination of which classification technique, unsupervised or supervised classifier is more feasible and suitable to detect specific object for coastal area mapping is not possible. In the image classification results of Macleod and Congalton (1998), the ISODATA showed higher accuracy than maximum likelihood classifier. On the other hand, research by Everitt et al. (2009) showed that the maximum likelihood classifier produced higher accuracy than ISODATA. Therefore, the type of image classification technique is also highly associated with the study area condition and proposed object (Butler and Jernakoff 1999), and the choice of image classification technique influences the resultant map. Thus, both unsupervised and supervised classification methods are attempted to investigate utility into SAV mapping in Boullanger Bay area for this project.

2.5.2 *Change detection*

Numerous change detection algorithms have been also developed so far. In particular, Write Function Memory Insertion (WFMI), Multi-date Composite Image (MCI), Image Algebra (e.g. image differencing, image regression, image ratio and change vector analysis), Image Transformation (e.g. PCA and ICA) and Post-Classification Comparison are major change detection techniques (Dobson *et al.* 1995; Lu *et al.* 2004; Coppin *et al.* 2004). For the detection of change in vegetation community, vegetation index image differencing, notably, using Normalised Difference Vegetation Index (NDVI) is a common technique at present. However, the constraint of this technique for this project is that since NDVI employs near-infrared radiation, which is strongly attenuated by the water column. Instead, MCI can be employed for under water object delineation. Coppin et al. (2004) indicates the highest utility for MCI in natural environment. While natural change in natural resources is often subtle, MCI is capable of detecting the subtle change. Additionally, MCI and Post-classification are the only techniques that can obtain "*from – to*" change in objects from image time series (Macleod and Congalton 1998). However, they also indicate the difficulty of MCI in the process of image interpretation for change detection. According to the summary of recent change detection techniques by Lu et al. (2004), most common methods are image differencing, PCA, and Post classification comparison. Macleod and Congalton (1998) attempted these three techniques for monitoring eelgrass in Great Bay, New Hampshire based on Landsat TM image. They concluded that image differencing was better technique than PCA and Post-classification comparison. While many scientists have used Post-classification technique (Munyati 2000; Xia *et al.* 2007; Alphan *et al.* 2009), Post-classification is a technique highly influenced by the accuracy of classified images. This technique is straightforward to detect "*from – to*" change, yet unless, high quality classified images are obtained, potential for the least accuracy of change detection remains (Macleod and Congalton 1998). In this regard, image differencing avoids misclassification inherent in the Post-classification because full image classification is not required for image differencing (Macleod and Congalton 1998). For PCA, inadequacy of change detection for eelgrass meadows was indicated due to low accuracy in error matrix and Khat accuracy by Macleod and Congalton (1998). Jensen et al. (1993) used image algebra for change detection of waterlilies and cattails at seasonal differences in a fresh water reservoir on the Savannah River Site in South Carolina. They also managed to obtain sufficient change detection result of waterlilies and cattails based on Image algebra technique. However, Mas (1999) found Post-classification technique is the most effective over the six methods he examined including: (1) image differencing; (2) vegetation index differencing; (3) direct multi-temporal unsupervised classification; (4) post-classification; (5) a combination between image enhancement and post-classification; and (6) PCA. WFMI is also a straightforward technique that can delineate change or unchanged area between different temporal images (Dobson *et al.* 1995; Jensen 2005). Individual band from multi-temporal satellite images are inserted into specific write function memory banks (red, green, and/or blue) in computer software for digital image processing to delineate change and unchanged area through specific color combinations derived from correlation of write function memory banks (Dobson *et al.* 1995; Jensen 2005). Since this technique cannot produce "*from – to*" change, WFMI is often employed with other digital image processing techniques to attempt change detection analysis. Different change detection techniques have their own advantages and disadvantages, thus, no single approach can be applied for all cases of change detection (Lu *et al.* 2004). Several approaches of combination between several change detection techniques, encompassing; MCI and WFMI are thus attempted to detect change in SAV distribution in Boullanger Bay in this project.

2.5.3 PCA and ICA

There is a need for monitoring programme via satellite remote sensing technique that ensures the detection of small decline in seagrass distribution at early stage of the decline over large geographic areas (Kirkman 1997; Duarte 2002). Unsupervised image feature extraction techniques such as PCA, and especially ICA, are regarded as effective change detection techniques to extract features of small changes.

PCA is powerful statistical technique to decorrelate the original interband correlation of observed satellite imagery (Fung and LeDrew 1987). PCA can be used for a range of image analysis purposes, encompassing; image transformation technique in pre-processing stage, image classification stage as an unsupervised classifier, and change detection technique (Fung and LeDrew 1987; Du *et al.* 2002; Ozesmi and Bauer 2002; Munyati 2004; Paolini *et al.* 2006; Deng *et al.* 2008). PCA is often used in combination with other techniques for change detection purposes whereas single usage of PCA can play a role as an image transformation technique or unsupervised classification (Lu *et al.* 2004). PCA based change detection is widely used at present (Li and Yeh 1998; Munyati 2004; Zhong and Wang 2006; Deng *et al.* 2008; Song *et al.* 2009). In particular, PCA is regarded as a good utility method for land use change detection (Li and Yeh 1998; Deng *et al.* 2008; Song *et al.* 2009). Li and Yeh (1998) concluded that PCA has the ability to reduce errors in change detection analysis using multi temporal satellite images. Song et al. (2009) indicated the utility and feasibility of PCA based change detection for rapid land use in the urban area. Deng et al. (2008) also used PCA based change detection, yet not only with unsupervised but also supervised classification. Moreover, their approach resulted in better accuracy than using post-classification method in terms of overall, producer's, user's and kappa coefficient index. Despite the good results, little research into PCA based change detection for coastal environment has been conducted (Munyati 2004). While PCA has been often used either individually or with other techniques, in most cases, PCA applications often include artificial object in the imagery, and do not consist of only natural objects. This is particularly because of large spectral feature differences between natural and artificial objects. Even though there is a difference of spectral feature between nature objects, artificial object typically have unique spectral feature. Therefore, change detection of a natural area would be difficult to interpret, especially if it was vegetation change detection, since all objects in the image have a similar spectral response. Munyati (2004) found better effectiveness for PCA than post-classification approach for coastal wetland change detection in Zambia, yet also found the difficulty of image interpretation when insufficient ancillary data or knowledge is prepared, as it is difficult to understand the meaning of the principal components. Although it depends on the components of image, PCA application for land use development is therefore regarded as quite effective, yet for change detection in natural environments, it might have difficulty in image interpretation.

Independent Component Analysis (ICA) is a recently developed statistical and computational technique (Robila *et al.* 2000), which is an extension of PCA (Gilmore *et al.* 2004). It is also spectrally dependent like PCA (Shah *et al.* 2007) and it has high potentiality for seagrass mapping and monitoring in this project. Elements of ICA and PCA application overlap: either individually usable or hybrid usage for feature extraction; or image classification; or change detection because ICA was developed based on PCA. However, there is a clear difference between ICA and PCA. ICA uses higher-order statistics than 2nd order statistics of PCA (Zhong and Wang 2006). Higher-order statistics can be exploited to separate a mixture of signals into different components, called independent components, without prior knowledge about the statistics of the source (Hyvärinen and Oja 2000; Du *et al.* 2004). ICA derived independent components are assumed to have a non-Gaussian distribution and mutually independent in the image (Gilmore *et al.* 2004). Although PCA enables the reduction of band dimension to produce inter-bands decorrelation (Robila *et al.* 2000), extracted features, called principal components are not mutually independent unlike the independent components derived from ICA. Additionally, principal components are assumed Gaussian in distribution, which is a bell shaped distribution in histogram. Most satellite remote sensing imagery do not have a Gaussian distribution (Zhong and Wang 2006; Shah *et al.* 2007). Generally, latent variables in observed images consist of features with non-Gaussian distribution, especially, in rich nature areas. ICA produces either uncorrelated bands or the reduction of higher-order dependencies at once (Zhong and Wang 2006). ICA technique is therefore considered to have more utility than PCA in the empirical application of satellite remote sensing for mapping and monitoring projects, especially if the spectral distribution of acquired image is non-Gaussian (Zhong and Wang 2006). Thus, ICA can be subject to applications for image feature extraction, classification and change detection based on spectral analysis. Yet, ICA application for change detection procedure has not been summarised in major review articles in practice (Dobson *et al.* 1995; Lu *et al.* 2004; Coppin *et al.* 2004). On the other hand, while ICA was developed recently, many experts have already found its utility for various kinds of objectives (Du *et al.* 2004; Gilmore *et al.* 2004; Zhong and Wang 2006; Shah *et al.* 2007). For instance, Du et al. (2004) used ICA as a classification technique via multi-spectral satellite imagery for urban and suburban areas. They concluded that ICA is a kind of spectral analysis based unsupervised classification and a more powerful technique than the single usage of unsupervised classification, such as ISODATA. In the research by Zhong and Wang (2006), ICA was performed for the detection of change in land cover due to land salinisation based on multi-spectral and temporal images. They firstly produced independent components that are different land cover features based on spectral characteristics in the image, through ICA. Supervised classifier, Maximum Likelihood was then applied for the analysis of the independent components shown images. They concluded the better effectiveness of ICA than PCA in this method, and also indicated that ICA based Maximum Likelihood classifier managed to identify not only the change area but also the '*from – to*' change feature in the image through time series. In this regard, ICA can be performed either individually or combination with other classification technique or change detection technique like PCA can be applied. Particularly, when ICA is employed with other spectral analysis techniques, such as image classification approaches and anomaly detection, the accuracy of resultant classified images can be improved by independent components derived from ICA (Zhong and Wang 2006; Shah *et al.* 2007). Scientists are increasingly recognised ICA as a better technique than PCA in many cases of satellite remote sensing application on account for these empirical advantages, although the effectiveness of PCA and ICA still highly depends on the proposed object and condition of study location. However, despite the growing recognition of ICA utility, most applications of ICA have been for land use classification or change detection like PCA application (Du *et al.* 2004; Zhong and Wang 2006; Shah *et al.* 2007; Benlin *et al.* 2008). While previous research performed ICA technique focusing on the land use area mapping and monitoring, feasibility and utility of ICA revealed by many researchers would be reliable for coastal area mapping and monitoring. In accordance with the high utility, ICA is attempted for mapping and monitoring SAV in this project instead of other techniques like PCA. It is assumed that each coastal feature is extracted as statistically independent features. Additionally, small change in seagrass areal extent may potentially be extracted by ICA technique with an appropriate extent of study location.

The techniques mentioned in this section can be used individually or in combination with each other to improve either image classification or change detection accuracy. Further, there has been no attempt of satellite remote sensing based image classification and change detection of SAV meadows in Boullanger Bay, and, there is no previous application of change detection techniques. Therefore, several techniques of image classification and change detection via satellite remote sensing were attempted to investigate the utility and feasibility of those techniques for SAV mapping and monitoring in Boullanger Bay.

Chapter 3 Methodology

3.1 Chapter overview

Remote sensing image analysis procedures are sometimes complex due to numerous factors that should be taken into account for successful analysis. Several elements, such as user's requirement, study area scale, research budget, and competence and knowledge of analyst are highly attributed to the image analysis scheme and influences on the quality of the result (Lu and Weng 2007). This chapter aims to make sense of the nature of satellite remote sensing procedures performed in this project before describing the empirical procedures in three case studies of this project. A description of the study area of Boullanger Bay, including two Case study areas, is provided so as to detail the specific local attributes of the research location. The basic processes of remote sensing image analysis is followed by; selection of suitable satellite imagery, image pre-processing, image transformation, image classification, change detection, and the accuracy assessment of resultant data.

3.2 Study area: Boullanger Bay in northwest Tasmania

Boullanger Bay, including subtidal and intertidal open water areas, and several river catchment areas, is located in the Cradle Coast region, in the far northwest of Tasmania (40.6°S, 144.6°E) (Figure 3.1). Boullanger Bay is about 15km × 10km and approximately 15,000 hectares in area. It is situated between the north-western tip of the main island of Tasmania to the west and Robbins Island to the east, while to the north the bay eventually opens out to Hunter Island and Three Hummock Island in far western Bass Strait. Boullanger Bay is connected by Robbins Passage to Big Bay and the entire complex is composed of large and shallow intertidal embayments. The area is one of the most important in Australia for migratory birds, including the eastern curlew and ruddy turnstone, and for Tasmanian resident shore birds, such as the sooty and pied oystercatchers and the hooded plover (Bryant 2002; Sprod *et al.* 2003; CCNRM 2005; Spruzen *et al.* 2008). As noted by Crawford and White (2007), areas of coastal open water and estuaries, such as Boullanger Bay, provide numerous environmental, social and economical benefits and values for the Cradle Coast region. In particular, wetlands in this area are one of the most outstanding sites of environmental significance in the Cradle Coast region, and although not formally recognised under the Ramsar Convention, it is argued that it would meet critical criteria for inclusion (Bryant 2002; Crawford and White 2007). Seagrass meadows and saltmarshes that compose the wetlands provide food webs and habitats for marine ecosystems and feeding habitats for shorebirds, which are common in this area (Crawford and White 2007). Diverse species of native birds, for instance, from the threatened wedge-tailed eagle to the superb fairly-wren, are also found living in this area (Sprod *et al.* 2003). Intertidal and subtidal open water areas in this region contain some of the most prominent and significant seagrass beds in Tasmania, being covered by approximately 8,000 ha of seagrass beds (Rees 1993; Sprod *et al.* 2003). Most seagrass beds in the bay are located in soft sediment basin, shallow (less than 10m), clear and low wave energy water areas (Figure 3.2, 3.3). This study area is contained in the marine bioregion 'Boags', in which the dominant seagrass is *P. australis* (Figure 3.4) (Rees 1993; Sprod *et al.* 2003). Previous research conducted by Rees (1993) identified the presence of several seagrass species, encompassing; *A. Antarctica* and *Z. muelleri*. Recent fieldwork in January 2010 conducted by Mount *et al.* (unpub) identified that there were extensive subtidal and intertidal seagrass habitat beds, including not only the former three species but also *H.*

australis and *H. tasmanica*. The climate at a regional scale is temperate, with high rainfall (Figure 3.5) (Sprod *et al.* 2003) and high cloud coverage. However, as the air in this area is known as being the 'cleanest' in the world – in that the air contains very little particulate matter – it provides one of the clearest places in the world to conduct remote sensing activities (Sprod *et al.* 2003). Consequently, Boullanger Bay is regarded as an appropriate study area for the evaluation of satellite imagery application and the observation of seagrass meadows distribution by satellite remote sensing technology. In order to detect small scale changes in the distribution of SAV, including seagrass community and to identify the effectiveness of remote sensing computational techniques, the study region was further subdivided into two smaller case study areas: (1) the Welcome River inlet; and (2) a subtidal open-water area of Boullanger Bay.

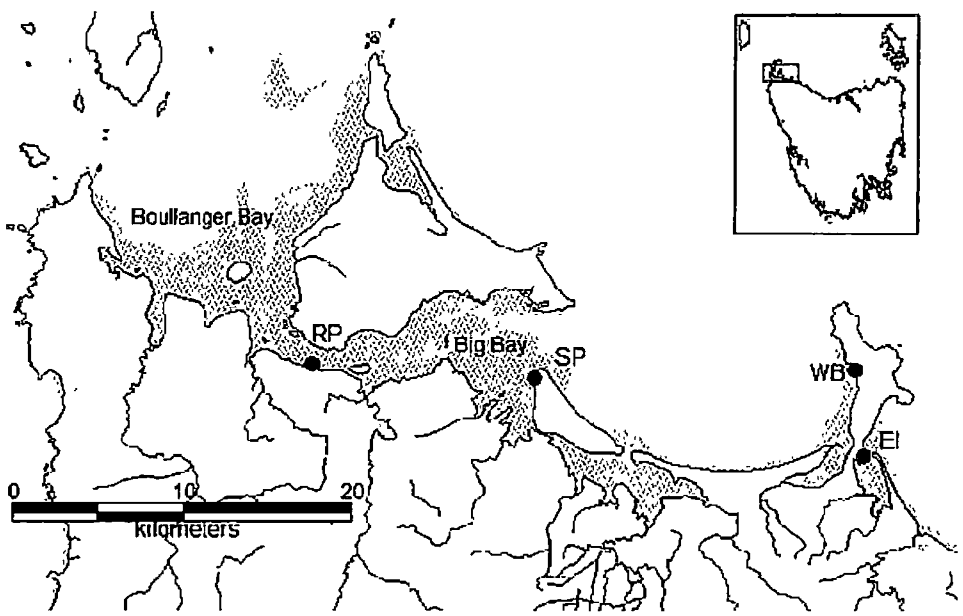

Figure 3.1 Boullanger Bay, Source: (Dunn 2000).

Figure 3.2 Shallow soft sediment basin, Boullanger Bay

Figure 3.3 Intertidal seagrass meadows

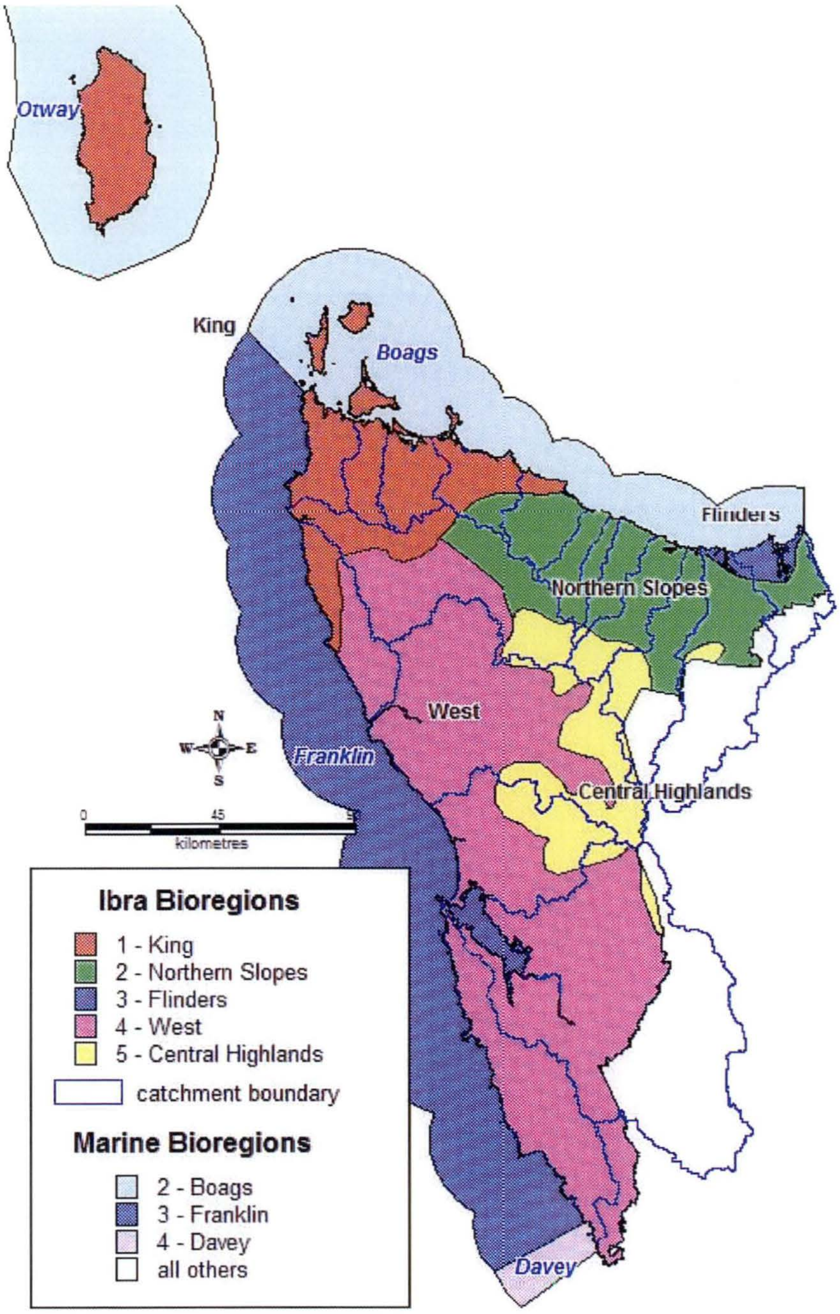

Figure 3.4 Bioregions in the northwest Tasmania, Source: (Sprod *et al*. 2003).

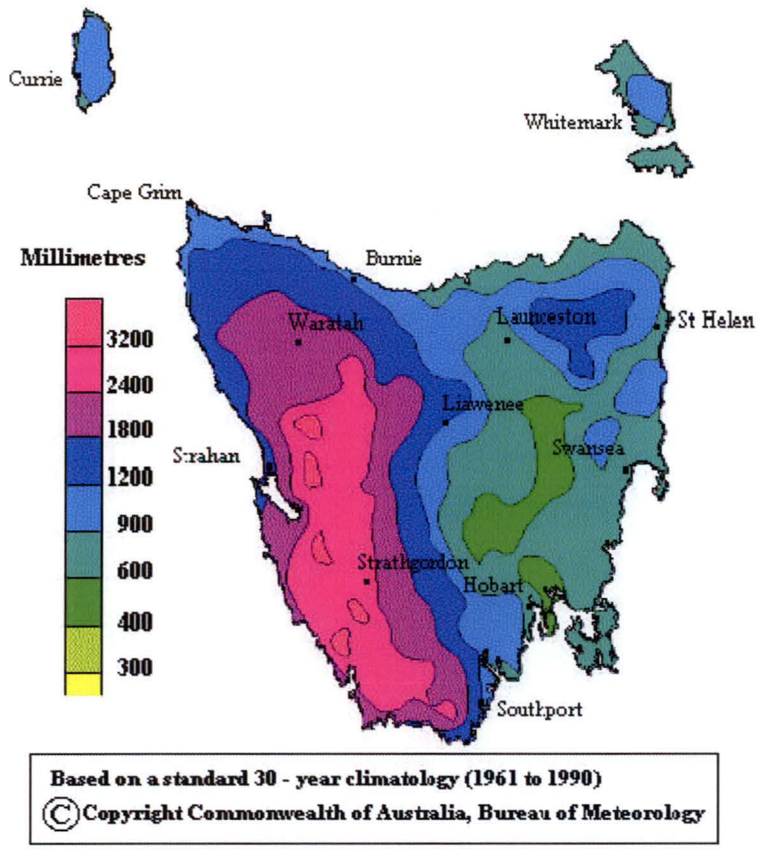

Figure 3.5 Annual rainfall in Tasmania, Source: (Sprod *et al.* 2003).

3.2.1 Case Study area 1: Intertidal SAV change detection analysis, Welcome Inlet

The Welcome River inlet was selected to identify the change in the distribution of intertidal SAV community (Figure 3.6). Investigation of remote sensing image analysis techniques to map and changes in the distribution of intertidal seagrass meadows was the co-objective of this case study. The Welcome River inlet is characterised by having an open marine inlet with a strong fresh water influence (Crawford and White 2007).The total area of the Welcome River catchment is 67,400 ha (CCNRM 2005), while the Welcome Inlet has an area of approximately 500 ha. A large area of salt marsh is located in the Welcome River inlet. According to Crawford and White (2007), this plant community is the one of the most threatened in Tasmania. The most abundant seagrass species at this area is *Z. muelleri* (Rees 1993). The Welcome River inlet is regarded as estuarine, and the Welcome River Reserve located in the lower Welcome Inlet supports nationally significant swamp forest communities in Tasmania (Crawford and White 2007). Additionally, the benthic macro invertebrate fauna species richness of Welcome Inlet is the highest compared to any other estuaries in the Cradle Coast Region (Edgar *et al.* 1999). The Welcome River catchment consists of many river tributaries that support ecosystems and biological diversity. Historically, tributaries of the Welcome River flowed through extensive and low-lying swamp forests. However, these forests have been cleaned and the river has been subjected to major alterations in water flow due to drainage channels constructed in order to expand adjacent upland farming (DPIWE 2003).

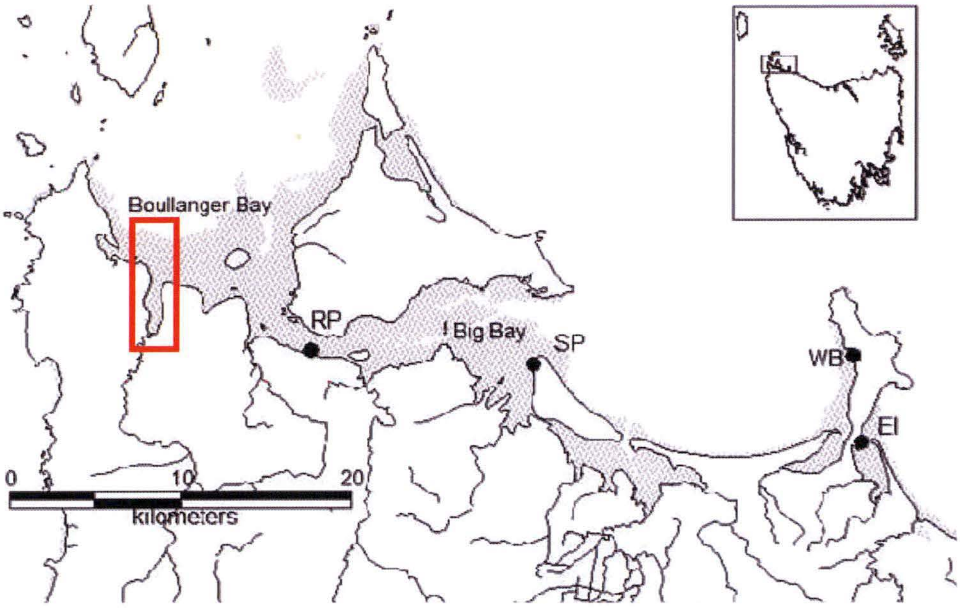

Figure 3.6 Map of the Welcome area. The red square depicts the case study site. Source: (Dunn 2000).

3.2.2 Case Study area 2: Subtidal patchy SAV habitats change detection analysis, Boullanger Bay

Boullanger Bay, Case Study area 2, is an open water near-shore area located west of Robbins Island, east of the north-western tip of the main island of Tasmania, and south of Hunter Island (Figure 3.7). The area contains outstanding coastal and marine biological diversity (Sprod *et al.* 2003; CCNRM 2005). Extensive, but patchy seagrass meadows range over the sea floor in the subtidal open water area of Boullanger Bay. The landscape of far northwest Tasmania is mainly composed of depositional sediments, largely derived from Tertiary and Quaternary age materials (Sprod *et al.* 2003). The bottom of Boullanger Bay is made up from this sort of soft sediment, which produces extensive flat landscapes (Sprod *et al.* 2003). As the result of ecological succession, extensive and stable seagrass meadows of over 8,000 ha in area exist as a critical primary producer for the wider ecosystem of Boullanger Bay (Rees 1993; Sprod *et al.* 2003). *P. australis* is the dominant species in the subtidal area of Boullanger Bay (Rees 1993; Kirkman 1997; Sprod *et al.* 2003; CCNRM 2005). *P. australis* prefers sheltered embayments, and forms large continuous meadows in waters from 1 to 15m deep (Trautman and Borowitzka 1999). Unlike some other species of intertidal seagrasses, *P. australis* is a particularly slow recoloniser of areas from which it has been displaced (Kirkman 1997; DEHAA 1998; Meehan and West 2000). Within Boullanger Bay, there are patchy uncolonised areas (Figure 3.8), of about 25m radius, in the beds of *P. australis* in Boullanger Bay (Mount pers. comm.). These uncolonised areas, and their surrounding seagrass meadows, are interesting ecological features and effective sites to investigate the stability of established seagrass meadows over time like the survey conducted by (Meehan and West 2000).

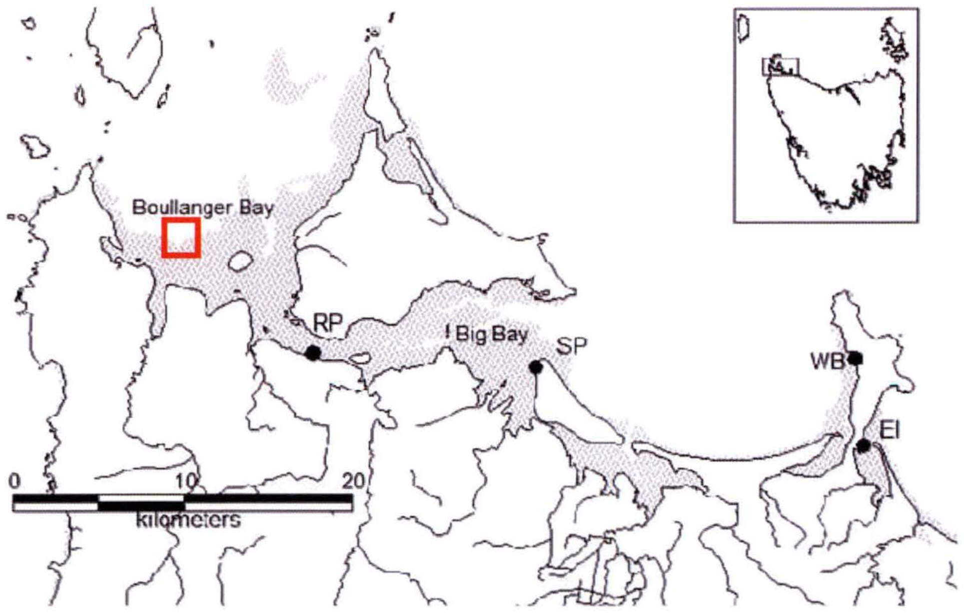

Figure 3.7 Map of the subtidal open water area. The red square depicts the case study site. Source: (Dunn 2000).

Figure 3.8 Patchy uncolonised areas of seagrass meadows. Bright areas represent mostly sand, and dark areas represent submerged aquatic vegetations

3.3 Image data

Appropriate image selection is a first important process of the remote sensing image analysis for a specific research purpose (Phinn 1998). Satellite and its loaded sensors are designed for specific purposes. Factors, including; research purpose and objects of interests, geographic scale of the study location, satellite image resolution size, availability of different temporal data, budget and time limitation for research, and the competence of analyst for the candidate image, are significantly involved in the image selection (Lu and Weng 2007). Each satellite data has each strength and weakness in terms of spatial, spectral, temporal and radiometric resolution according to the designed purposes. These components influence on the quality of the resultant data, such as thematic map and the result of change detection analysis. Identical resolutions of those four factors are preferable for better quality of change detection image analysis (Jensen 2005). Appropriate temporal correlation based on similar anniversary date and time in a day of image acquisition between multi-temporal images is crucial, especially when change detection analysis takes place (Jensen 2005; Deng *et al.* 2008). In practice, it is however; often difficult to obtain such an ideal status of multi-temporal or multi-sensor satellite imagery due to the limitation of research, especially budget limitation. Comparison of the strength and weakness of these four factors between different satellite sensors is prerequisite for appropriate satellite image selection so that the better effectiveness of the subsequent image analysis is derived (Dobson *et al.* 1995; Lu and Weng 2007). Another consideration over the image selection is atmospheric condition of the acquired imagery. Satellite imagery holding corresponding temporal information is better for change detection to constrain different atmospheric impacts, such as sun angle and phenology of plant community on the image (Jensen *et al.* 1993; Jensen 2005; Deng *et al.* 2008). In particular, cloud coverage and tide condition are critical factors for this project. Since less cloud coverage provides more original spectral response of the features in the image without regard to atmospheric distortion (described later section in this chapter), as less cloud coverage as possible is ideal for subsequent analysis. Additionally, tide condition is also very important for classification and change detection analysis of coastal area, especially of submerged aquatic vegetation (Macleod and Congalton 1998; Ozesmi and Bauer 2002). Tidal stage between multi-temporal images is ideally better as much identical as possible for change detection (Jensen 2005). Generally, the ability to 'see underwater' is a weakness of satellite remote sensing. Specifically, the greater the distance between the water surface and a submerged object the more restricted is the observation of that submerged object. This is due to the rapid absorption of electronic magnetic radiation by water and reflection by constituents within the water column such as plankton and suspended sediments (Phinn *et al.* 2006a). Although high tide level might not be suitable for mapping submerged vegetation in this regard, an image acquired after low tide might not be suitable as well. In part because, after the low tide, there is likely to be turbulence that performs like a dust storm, preventing satellite sensor, especially Landsat TM, from detecting sufficient reflectance from the submerged vegetation (Macleod and Congalton 1998). Consideration about water clarity should be taken into account as well as identical tide level between multi-temporal images. Thus, variability of tide stage and water clarity over the multi-temporal data should be cared to make the spectral response of submerged object as mush equal as possible for subsequent change detection analysis. In this research project, three satellite sensor (ALOS, Landsat TM and ETM+) and aerial photography were available for image analysis.

3.3.1 Landsat 5 Thematic Mapper and7 Enhanced Thematic Mapper plus

Imagery of Landsat 5 Thematic Mapper (TM) and 7 Enhanced Thematic Mapper plus (ETM+), distributed from the U. S. Geological Survey (USGS) were used for image analysis in this project. Only the image of Landsat acquired in February 2000 was brought from Australian Centre for Remote Sensing (ACRES). Critical requirement for remote sensing change detection analysis is the availability of at least two dates of satellite imagery (Deng *et al.* 2008). Data availability derived from satellite and its sensor life expectancy is the most important consideration over change detection research. Among the conventional satellite imagery, Landsat series are prominent for change detection analysis in terms of historically archived data that has the ability for data comparison associated with various dates combination, with same sensor (Paine and Kiser 2003; NASA 2009). Landsat series are natural resource survey satellites first launched in 1972 (Verbyla 1995). The series of Landsat is ranging from 1 to 7, and Landsat 5 Thematic mapper (TM) has been operating for 25 years since 1984 and 10 years for Landsat 7 ETM+ (Figure 3.9) (NASA 2009). Landsat TM and ETM+ are satellite consists of cross-track scanner with instantaneous field of view (IFOV) of 30 by 30m in ground resolution cell (Sabins 1997). 185 km swath consists of 5667 scan lines in the scan direction and 30m width in the orbit direction compose each scene (Sabins 1997). Either Landsat TM or ETM+ has seven spectral bands, ranging from 0.45 μm to 12.5 μm except for panchromatic band of ETM+ (Table 3.1) (NASA 2009). In fact, these multispectral bands containing the visible wavelength of radiation are important for mapping underwater object by remote sensing as only shorter wave radiations can penetrate perceptibly into the water column (Brivio *et al.*, 2001). In addition, these multispectral bands support large potential for proposed image analysis of '*independent component analysis*' in this project (described in later section). Temporal and radiometric resolutions are 16-days orbit cycle and 8-bits respectively (Markham *et al.* 2004). In practice, general spatial resolution of 25 m (except thermal wavelength) can define large object, and these are the most frequently employed satellites for regional scale mapping (Lu and Weng 2007). Yet, these sensors are generally not suitable for detecting small individual object (NASA 2009), such as small patches of seagrass (Mumby *et al.* 1999). While aerial photography is better for detecting such a small seagrass patch, moderate spatial resolution of Landsat is adequate for detecting seagrass meadows at local area and high potential for change detection. Further, because of time and cost limitation, aerial photography was not practical for this research. Application of Landsat TM and ETM+ for this project was then determined in accordance with the synoptic perspective over the ability of these satellite sensors.

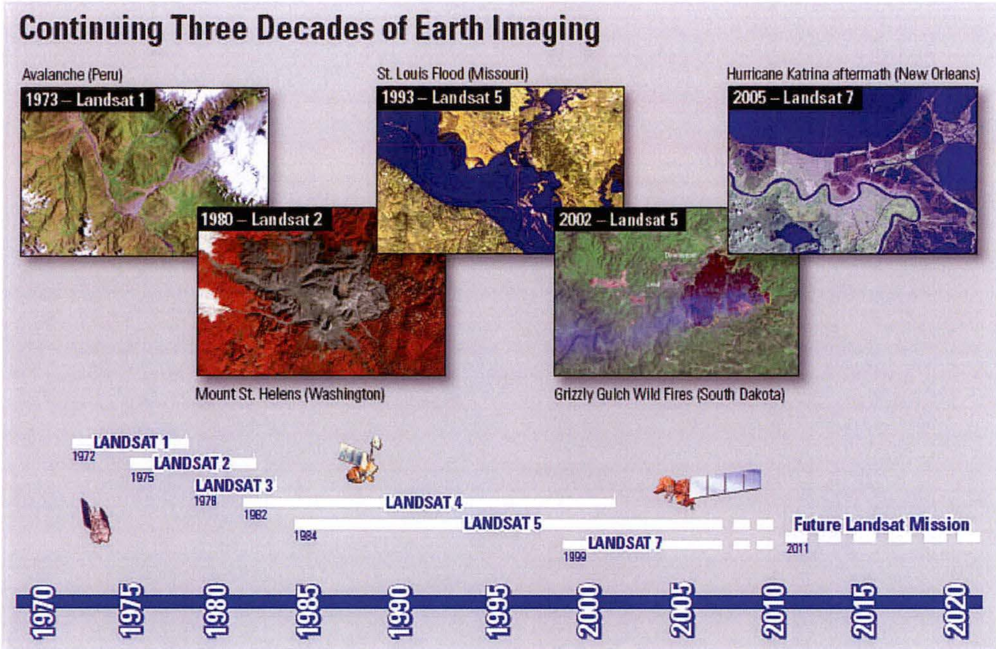

Figure 3.9 The history of Landsat series, Source: (USGS 2005).

Table 3.1 Sensor characteristics of Landsat 7 Enhanced Thematic Mapper

Orbit	Near polar sun synchronous
Altitude	705 km
Spectral resolution	
Panchromatic	0.45 ~ 2.35 μm
From visible to middle infrared	0.45 ~ 2.35 μm
Thermal IR	10.5 ~ 12.5 μm
Number of spectral bands	7
Spatial coverage	
Cross track coverage	183 km
Temporal resolution	Every 16 days
Spatial resolution cell	
Panchromatic	15 by 15 m
From visible to reflected IR	30 by 30 m
Thermal IR	120 by 120 m
Radiometric resolution	8 bits

3.3.2 *Advanced Land Observing Satellite (ALOS)*

An image acquired in 2006 by the Advanced Land Observing Satellite (ALOS) was one of multi-temporal satellite images used for change detection analysis. This image was brought from Australian Centre for Remote Sensing (ACRES), Geoscience Australia. The main purpose of ALOS is a land observation at local area, such as identifying land objects, features and phenomena on the surface of the Earth (JAXA 2007). ALOS is equipped with three sensors, including; Advanced Visible and Near Infrared Radiometer type-2 (AVNIR-2), Panchromatic Remote Sensing Instrument for Stereo Mapping (PRISM), and Phased Array type L-band Synthetic Aperture Radar (Palsar) (JAXA 2007). AVNIR-2, consists of along track scanner in ALOS, is effective for land and coastal area observation (GA 2009). Aims of this sensor is to provide land coverage maps with high spatial accuracy and land-use classification maps for monitoring regional environments (GA 2009). Multispectral combination of wavelengths ranges between region of visible and near infrared (Blue: 0.42-0.5 μm, Green: 0.52-0.6 μm, Red: 0.61-0.69 μm, Near Infra Red: 0.76-0.89 μm) (EORC 1997; JAXA 2007) (Table 3.2). In this regard, AVNIR-2 has also the ability to detect SAV meadows in terms of its spectral resolution, which is corresponding to Landsat TM and ETM+. Although it was basically designed for land cover classification, high spatial resolution of 10m and radiometric resolution of 8 bits are assumed to be applicable to delineate SAV meadows clearly. Therefore, change detection analysis in this project subjected the ALOS image, 2006 for identifying change in SAV meadows.

Table 3.2 Sensor characteristics of AVNIR – 2

Orbit	Sun-Synchronous, Sub-Recurrent
Altitude	Altitude: 691.65 km (at Equator)
Spectral resolution	
Visible:	Band 1 : 0.42 to 0.50 μm
	Band 2 : 0.52 to 0.60 μm
	Band 3 : 0.61 to 0.69 μm
Near infrared:	Band 4 : 0.76 to 0.89 μm
Number of spectral bands	4
Spatial coverage	70 km (at Nadir)
Temporal resolution	Every 46 days, Sub Cycle: 2 days
Spatial resolution cell	
From visible to near infrared	10 by 10 m (at Nadir)
Radiometric resolution	8 bits

3.3.3 Orthorectified Aerial Photography

All data of orthorectified aerial photography was acquired from TASMAP library aerial photo, the Department of Primary Industries, Parks, Water and Environment (DPIPWE) for this research. Orthorectified aerial photography was used for accuracy assessment in this project, yet not using them for mapping and monitoring SAV meadows. The aerial photography used to compare with the Landsat TM and ETM+ as reference data were acquired in 1996. There are some reasons for this, encompassing; better accuracy of orthorectified aerial photography, data availability and areal scale of mapping. In practice, aerial photography has a proven ability to measure the extent of submerged objects with higher spatial accuracy than satellite remote sensing sensors while it is dependent upon the extent and size of object (Valta-Hulkkonen *et al.* 2004). Such a high accuracy together with high spatial resolution allows the application of aerial photography for accuracy assessment of image classification generated from the satellite imagery. Data availability of aerial photography was another reason. Aerial photography has also outstanding in terms of historical imagery. However, time and budget limitation to this research restricted to use aerial photography for change detection analysis. Aerial photography is obviously major method to detect seagrass meadows. Yet, simply, the cost of the aerial photography flights and post processing is significant, and time consuming of data processing did not match up this time limited research unlike using satellite imagery (Ozesmi and Bauer 2002). Further, satellite imagery is more effective for synoptic SAV meadows mapping at large geographic area than aerial photography (Ozesmi and Bauer 2002).

3.4 Is multi-temporal satellite imagery suitable for SAV mapping and monitoring?

"The distribution of Australian seagrass communities should be mapped at appropriate spatial scales and, in key areas, monitored at appropriate temporal scales" (Kirkman 1997, pp. 25). Multi-temporal satellite imagery has great potential for monitoring scheme of this project. Multi-temporal satellite imagery ensures not only for the production of initial baseline information but also the continual production of subsequent information on habitat change at large scale over long period (Kirkman 1996). SAV meadows monitoring between 1990 to 2008 is one of research purposes in this project. In particular, short interval monitoring (basically annual basis) was attempted through multi-temporal satellite image acquired from 2000 to 2008. Multi-temporal satellite imagery of Landsat 5 was then available to meet such a standard of this monitoring scheme. Additionally, systematically integrated format of satellite data facilitates the continual analysis of monitored information between different remote sensing platforms for time series comparison (Butler and Jernakoff 1999). In this regard, application of multi-sensor and temporal satellite imagery has potential for long term monitoring programme.

3.4.1 Values for this temporal difference (monitoring interval)

Limited information on suitable monitoring period to identify the natural population dynamics of individual seagrass specie is available (Campbell and McKenzie 2004; Boese *et al.* 2009). Change detection between 1990 and 2008, including annual interval monitoring between 2000 and 2008, was attempted to determine change in SAV distributions. Temporal information on the fluctuation in seagrass meadows distribution used to be neglected

(Kirkman 1997), yet it is now regarded as important information to obtain the variability of seagrass natural dynamics. Kirkman (1997) indicated that large geographic scale seagrass monitoring needs to be conducted for one to five year cycle basis since the fluctuation at large geographic scale is likely to occur. Kendrick et al. (2000) conducted 30 years change detection to indentify spatial and temporal seagrass change in distribution on Success and Parmelia Banks, Western Australia. Changes of dense canopy species: *Amphibolis antarctica*; *Amphibolis griffithii*; *Posidonia australis*; *Posidonia sinuosa* and *Posidonia coriacea*, were detected through aerial photography in their research, for four irregular years 1965, 1972, 1982 and 1995. Although, these seagrass species are regarded as stable habitat species that is often subject to long term monitoring, this research does not have description about the reason for the irregular monitoring over long period and effectiveness of these irregular time series availability. Provided if there is no concern of limitation over the research budget or another reason, the biology and ecology of species should be taken into account for the arrangement of seagrass monitoring temporal cycle. Natural dynamics of seagrass colonisation is varied dependent upon species and their habitat location and condition. *Posidonia* spp., for example, is subtidal seagrasses that have high stability in their habitat distribution and low recolonisation ability, especially after the destruction of their habitats. Yet the other seagrasses in intertidal areas, such as *Zostera* spp. have the instability of their habitat and high recolonisation ability that they can recolonise even after the destruction of their habitat. Additionally, most seagrass communities in the tropical region generally have high recolonisation ability compared to temperate region. Intertidal seagrasses in tropical region can recolonise over tens of kilometres within three years (Campbell and McKenzie 2004). Additionally, the recolonisation of subtidal seagrass meadows (> 5m) in the tropics can occur within two years from initial loss (Preen et al., 1995). Boese et al. (2009) also reported *Zostera marina* has quick recovery that was completed within 24 months. Both researches monitored such intertidal species every three and two months respectively for three years. Although the study locations of both researches were in the tropics, it provides a good model of intertidal seagrass monitoring cycle for this project as the both of them showing the capability of three years monitoring for intertidal seagrasses. Study location for this project was temperate region that contains either subtidal or intertidal species. 18 years were set up as long term monitoring of either inter-tidal or subtidal seagrass meadows to obtain the sufficient response of the natural dynamics of those seagrass species. Such a long term monitoring is then expected to be a baseline model of monitoring time-frames for seagrass recolonisation in the same location (Butler and Jernakoff 1999). Short periodic monitoring cycle (from six month to 12 month) with annual year basis was also conducted between 2000 and 2008. Because of limitation of available free satellite data from data distributer (U.S. Geological Survey), annual cycle monitoring between 1990 and 2000, and annual cycle monitoring with common date between adjacent years could not be performed. However, the short periodic monitoring was assumed to not only detect the natural dynamics but also discriminate the natural change of seagrass distribution from changes due to other factors.

3.5 Image pre-processing

There are errors inherent in satellite imagery associated with the geometry of objects and the brightness values of the pixels (Navalgund *et al.* 2007; Hong and Zhang 2008). Image pre-processing usually implements the correction of numerous distortions in acquired image and calibration of data, encompassing; geometric rectification or image registration for geometric distortion, radiometric correction and calibration for systematic distortion and atmospheric distortion (Lu and Weng 2007). Certain types of satellite imagery brought by data distributer are usually not ready for immediate use due to several issues, such as geometric, spectral and radiometric distortions (Lillesand and Kiefer 2008), especially when they were provided by data distributer as free sources. In short, further image pre-processing is required to correct distortions inherent in raw satellite imagery. The Landsat 5 TM and 7 ETM+ data provided from U.S. Geological Survey (USGS) for this project were composed of L1G and L1T class data. L1T class data already addressed geometric, radiometric and precision correction by the National Land Archive Production System (NLAPS) (GLCF 2009). While L1G class data is also radiometrically and geometrically corrected, the pixels in the image are not georeferenced. The assumption of L1G data is the accuracy of Landsat data is less than 3 – 4 pixels (GLCF 2009). To turn things around, image pre-processing of distorted images is thus required to develop them more decent and ready for subsequent image analysis by applying appropriate mathematical models, which are both definite and statistical models (Navalgund *et al.* 2007).

3.5.1 Geometric distortion and correction processes

Geometric distortion is a source of imprecise image that contains different shape, size and place of a pixel from that is meant to be. Geometric distortion usually produces more severe errors in images than radiometric distortion. Moreover, geometric distortion can result from further factors than radiometric distortions (Richards and Jia 2006). For instance, potential sources are: the rotation and curvature of the Earth; the finite scan rate of some sensors; the wide field of view of some sensors; the variation in platform altitude, attitude, and velocity; the sensor limitations; and the panoramic effects related to the imaging geometry (Richards and Jia 2006; Lillesand and Kiefer, 2008). In particular, this project use Landsat TM, equipped with a cross-track scanner. In the context of this scanner, peculiar systematic distortions, encompassing; scan skew and cross-track distortion, are assumed to attribute geometric distortion inherent in the acquired images of Landsat series (Sabins 1997). Thus, care in addressing geometric distortion is crucial.

Geometric correction or georeferencing method used for this project was implemented via ENVI 4.6 digital image processing software (RSI 2009). '*Georeferencing*' is a spatial information data processing technique that establishes a conformation between geographical locations and images (e.g., satellite imagery and aerial photography) through geographical reference data (Hill 2006). '*Image to image*' registration approach was performed in this project to ensure that each corresponding pixel represent the same location over the different scenes (Anstee *et al.* 2009). The method is based on mathematical relationships between the positions of each pixel in acquired data image and the points on the ground that has same coordinates that is called Ground Control Point (GCP) (Richards and Jia 2006). In accordance with practical utility that it does not rely on the prior knowledge of distortion sources to model and then correct the geometric distortion (Richards and Jia 2006), this approach was employed for this project. As for reference data, geometrically collected image that is corresponding in the area of ground to the acquired imagery is essential for geometric correction processing in this approach. L1T data, which is geometrically well corrected, was then used as a reference data for the image to image registration for L1G data of Landsat and ALOS image. Through corresponding GCPs, based on common landmark objects in both the reference data and acquired satellite imagery, coefficient values required for mapping polynomials are estimated by calculation of ENVI (Richards and Jia 2006). For first-order polynomial transformation, the minimum number of four GCPs are required (GCPs > $(\text{degree} + 1)^2$) (RSI 2009; Verbyla 1995). However, in order to avoid undue effects of any GCPs that have significant root mean square (RMS) errors on the polynomial coefficients, further GCPs were selected for the first order mapping in this project. Additionally, the distribution of GCPs is another consideration for the effectiveness of mapping polynomials. For example, well distributed GCPs in images, located close to the each corner edge of the image and in dense around the objects or features of research purpose ensure the quality of the affine transformation over the image (Verbyla 1995). '*Nearest neighbour resampling*' was required for the integration of pixel size over different satellite data. Original pixel brightness values are rearranged to the nearest corresponding grid position for the correct geometry of the image (Lillesand and Kiefer, 2008). Sincc thc '*nearest neighbour resampling*' ensures quick computer calculation and the maintenance of the original pixel brightness value (Lillesand and Kiefer, 2008; Verbyla 1995), this resampling approach was employed in this project for subsequent spectral image analysis.

3.5.2 Radiometric distortion and correction

Radiometric distortion causes the error of brightness values of pixels (Richards and Jia 2006). Radiometric correction is applied to eliminate or compensate radiometric distortion except for actual fluctuation in image (Paolini *et al.* 2006). The radiometric distortions are derived from the influence of atmosphere, from the differences between sensors and from the wavelength reliance of electromagnetic radiation from the sun (Richards and Jia 2006). Above all, the atmospheric distortion is the most significant and results in an obscured image due to the scattering of solar radiation. High cloud coverage, sun glitter on sea surface, and water column scattering and attenuation are major atmospheric distortion sources, especially when the remote sensing imagery of seagrass distribution is acquired. The radiometric correction is thus crucial to change the sensor output digital number (DN) to the output values independent of atmospheric conditions (Bajjouk *et al.* 1996). Additionally, difference of grey scale value between satellite remote sensing data for earth observation image analysis is a common difficulty inherent in multi-temporal and multisensory data application (Hong and Zhang 2008). Several factors for the different responses of sensor are encompassing: differences in relative radiometric response between sensors; changes in satellite sensor calibration over time (i.e. aging); differences in illumination and observation angles; variation in atmospheric effects; reflectance anisotropy (i.e. BRDF effects); topography (i.e. slope-aspect effects); and actual changes in target reflectance (Paolini *et al.* 2006 p.686).

Comparison of multi-temporal images using same color metric system is prevented due to such differences (Hong and Zhang 2008). Additionally, change detection between the data of Landsat TM and ETM+ involves the context of the radiometric discrepancy (Paolini *et al.* 2006). When the multi-temporal and multi-sensor satellite images are processed for change detection, radiometric normalisation between adjacent year images is crucial for improving the spectral validation of resultant images. Radiometric correction were therefore, applied for acquired satellite imagery for this project. However, water depth collection for water column scattering and attenuation was not managed to implement in this project due to the time limitation of research.

3.5.2.1 Cloud and other land cover class removal

Existence of cloud in satellite imagery has an effect on the spectral reflectance from other objects or phenomena (Hoan and Tateishi 2008). Provided if cloud was removed from the image, it would be possible to enhance spectral reflectance from other objects or phenomena. It is therefore crucial to filter out cloud pixels for subsequent image analysis that is highly affected by cloud coverage (Ackerman *et al.* 1997; Chang *et al.* 2001). This theory is also applied other objects or phenomena that is not relevant to feature class of interest in the research. Simple and effective way of cloud removal is to mask out cloud in acquired image. Using ENVI software (RSI 2009), the cloud or land cover mask of the satellite imagery can be attempted by the function of '*mask*'. Identification of appropriate digital number values between visible bands is important to define threshold of cloud pixel value for cloud detection (Ackerman *et al.* 1997). Different, though similar, band minimum and maximum values for each visible band are used between acquired images for this approach due to the different cloud coverage and the particle size of cloud. In practice, however, large spectral variability of cloud and the presence of objects, such as beach, contain similar brightness values, often prevents this approach from designating the appropriate digital number values. For the mask of coastal upland area, the application of either decision tree classification method or Normalised Difference Vegetation Index (NDVI) for image acquired at high tide condition can be attempted.

3.5.2.2 Radiometric normalisation

Image matching or radiometric calibration method is essential for change detection research to discriminate between actual changes and extrinsic changes (Coppin *et al.* 2004). When change detection analysis is performed with multi-temporal or multi-sensor data, radiometric calibration is essential to remove or compensate atmospheric distortion effects over the images (Eckhardt *et al.* 1990; Lu and Weng 2007). Radiometric normalisation is one of the relative radiometric correction (Image matching) techniques often used for change detection analysis to get rid of radiometric inconsistency derived from different radiometric response between sensors, changes in sensor calibration, sun elevation difference, and difference of atmospheric effects, between images (Munyati 2000; Ju *et al.* 2006; Paolini *et al.* 2006). As the result, radiometric normalisation ensures that differences of brightness values between multi-temporal images eventually express actual changes on the object or phenomena in the image (Paolini *et al.* 2006; Hong and Zhang 2008). For change detection in this project, this approach is thus very important not only to remove atmospheric effect over multi-temporal satellite images but also to normalise radiometric discrepancy between Landsat TM and ETM sensors (Janzen *et al.* 2006; Paolini *et al.* 2006). Particularly, for subtle spectral analysis for change detection in satellite remote sensing, radiometric normalisation between adjacent year images plays an important role (Janzen *et al.* 2006). In order to implement radiometric correction, ancillary data, such as climate data and illumination geometry, or *Pseudo Invariant Feature* (PIF) are required (Janzen *et al.* 2006). PIF is a statistically invariant target that has consistent reflectance values over time through images (Janzen *et al.* 2006; Hong and Zhang 2008). PIF is often involved with radiometric normalisation approach, especially as a linear regression technique (Hong and Zhang 2008). Radiometric normalisation approach highly relies on the local knowledge and ability of analyst for manual selection of PIFs (Janzen *et al.* 2006). Eckhardt et al. (1990) defined five criteria for PIFs, encompassing: (1) the targets should be approximately the same elevation so that the thickness of the atmosphere over each target is approximately the same; (2) the targets should contain only minimal amounts of vegetation because vegetation spectral reflectance is subject to change over time; (3) the targets must be in relatively flat areas so that changes in sun angle between images will produce the same proportional increases or decreases in insolation to all normalization targets; (4) the spatial pattern of the normalization target should not change over time; (5) and a set of targets must have a wide range of brightness values for the regression model to be reliable.

Generally, artificial objects are ideal for PIF targets. Yet, when the study location is remotely natural environment area like this project, it is often hard to find the suitable ground targets of constant spectral reflectance that can be used as PIF for radiometric correction since selection of PIF is conducted subjectively by analyst knowledge with image interpretation (Janzen *et al.* 2006). Non-subjective method for PIF selection based on principal component analysis was also developed by Du et al. (2002). PCA was employed to extract PIF between multi-temporal satellite images (Du *et al.* 2002; Janzen *et al.* 2006; Ju *et al.* 2006). However, Paolini et al. (2006) indicated this approach cannot be applied for extracting PIFs common to all images, especially when the case of the combination of Landsat TM and ETM+ images. Hence, subjectively manual selection of PIF together with the visual assist of aerial photography was performed for each pair of adjacent year images to extract PIFs.

3.5.3 Band dimensional expansion

One critical regulation of Independent Component Analysis (ICA) application for feature detection is that the number of desired independent components cannot over the data dimensionality, i.e. the number of original spectral bands (Du *et al.* 2004; Shah *et al.* 2007). Although this may not be a large concern over the case of hyperspectral satellite imagery, it is, for the case of multi-spectral satellite imagery since the number of features in acquired image generally exceeds the number of the multi-spectral bands (Shah *et al.* 2007). All the individual features in the images are impossible to be extracted by ICA approach when using multi-spectral imagery (Du *et al.* 2004; Zhong and Wang 2006). Since this project also uses multi-spectral satellite imagery, i.e. Landsat and ALOS, this limitation has to be overcome. Data dimensional expansion of multi-spectral imagery is then required to meet the regulation of ICA for extraction of the desired number of independent components. In other words, the production of artificial spectral bands is required for ICA (Du *et al.* 2004; Shah *et al.* 2007). The concerns over this band expansion are the number of additional bands and the spectral discrepancy of additional bands. As mentioned above, the less number of total independent components than proposed features in the image does not extract all proposed features properly. Further, the larger number of additional independent components does not necessary mean that all proposed features of interest can be extracted as well (Du *et al.* 2004). Provided if spectral discrepancy between two feature classes are subtle or nothing, the two classes are not separated no matter how many nonlinear independent components are generated (Du *et al.* 2004). Since ICA is about to be computed based on spectral features in the image, linear combination of original bands from multi-spectral imagery does not generate additional hidden information (Shah *et al.* 2007). Non-linear combination of original bands, however, can generate additional independent components with additional hidden information (Shah *et al.* 2007). Highlight the spectral discrepancy between features in acquired image is generated by this approach to provide more information underlying in the image for additional feature detection (Du *et al.* 2004). Multiplication is for example, a simple and effective way of the data expansion (Du *et al.* 2004). Artificial band, for instance, X_iX_j, can be generated by the simple multiplication based on two original bands, X_i and X_j, and when same band are multiplied, i.e. X_i^2, the generated band highlights spectral difference from other spectral measurements within same pixel (Du *et al.* 2004). Therefore, non-linear operations, such as, X_i^2, $X_i \cdot X_j$, X_i / X_j, (Where X_i is a band of multi-spectral imagery, and $i \neq j$) improve ICA ability to extract desired and sufficient features from image (Shah *et al.* 2007).

3.6 Image transformation

Satellite imagery consists of numerous features, which in turn, all kind of images can be decomposed into several features that have corresponding spectral characteristics in an image (Richards and Jia 2006). Image transformation for feature extraction in the application of satellite remote sensing aims to improve image feature distinguishability based on spectral characteristics (Shah *et al.* 2007). Spectrally transformed image features or bands derived from multi or hyperspectral data allows obtaining some other hidden features or preserving principal features in the acquired image (Navalgund *et al.* 2007). In brief, feature extraction for satellite remote sensing is to identify these features in satellite imagery mainly through statistical and computational techniques (Shah *et al.* 2007). Performance of subsequent image analysis, such as image classification, anomaly detection and spectral mixing can then be improved by the extracted features (Shah *et al.* 2007). Selection of appropriate image transformation technique is crucial for successful image classification (Lu and Weng 2007). Yet, only the technique that are the most effective to extract features in the image of multi or hyperspectral data should be selected to avoid miss classification due to the application of several techniques at once in classification procedure (Lu and Weng 2007). Among the feature extraction techniques, principal component analysis is one of the most popular techniques (Robila *et al.* 2000), with independent component analysis has been drawing attention for feature extraction application in recent years. Visually and spectrally well represented data set for each feature category plays important role for image classification procedure, notably for supervised classification (Lu and Weng 2007).

3.6.1 Principal component analysis (PCA)

Numerous techniques have been developed and employed to investigate spectral, spatial and temporal variability for multi-temporal satellite imagery (Lotsch *et al.* 2003). Principal Component Analysis (PCA) is a statistical, non-parametric technique that extracts relevant patterns or information from high dimensional data sets (Robila *et al.* 2000; Smith 2002; Shlens 2005). High interband correlation is contained in most remotely sensed multi or hyper-spectral data (Fung and LeDrew 1987). Satellite imagery also contains interband correlation, for example, Landsat TM has high interband correlation between the first three visible bands (Fung and LeDrew 1987). In other words, the redundancy of data involves in satellite image processing of all spectral bands (Fung and LeDrew 1987). With increasing redundancy of data, image processing cost is also increasing as the result, especially for change detection analysis that requires at least two or more satellite imagery (Fung and LeDrew 1987). Since redundancy of multi or hyper-spectral data, especially between adjacent bands (interband correlation), exists in acquired imagery, PCA was developed to attempt to get rid of such redundancy of data set (second-order dependencies) by transforming observed spectral axes to orthogonal on a new coordinate system (Behrens 1998; Robila *et al.* 2000; Shensi 2005). This enables PCA to extract hidden or underlying features in image scene based on analytical solutions using linear algebra (Shlens 2005).

PCA is relies on the spectral and spatial features of observed images (Fung and LeDrew 1987; Behrens 1998). PCA produces uncorrelated or orthogonal components, called '*principal component*' based on eigenvectors of correlation or covariance matrices, for satellite remote sensing image analysis (Fung and LeDrew 1987; Robila *et al.* 2000; Lotsch *et al.* 2003). According to given scenes, land features vary in their spectrum and space, which in turn, given several principal components also vary in the variance of data but several not

(Behrens 1998). Correlation or covariance matrices can be derived from subsets or total study area of observed images in accordance with the proposed research objects and purpose (Fung and LeDrew 1987). Uncorrelated components, produced from correlation matrices are called '*standardised principal components*' and from covariance matrices '*non-standardised principal components*'. Principal components are varied dependent upon also whether subset or whole image and standardised or non-standardised data since eigenvectors differ considerably based on these factors (Fung and LeDrew 1987). Subset of principal component analysis should be taken into account. Principal components extracted from the subset of entire study area are subject to miss image analysis for change detection due to variability and uncertainty of unextracted area (Fung and LeDrew 1987). Only extracted features from subset area could be referred to as principal components, yet these components cannot be applied for entire study area (Fung and LeDrew 1987). While this project has several sub-case study areas, these are sets of individual study areas, contained in the main study area, Boullanger Bay; thus application of principal component analysis is possible to detect features in these subsets area. Standardised principal components have equal variance between each principal component band (Fung and LeDrew 1987; Behrens 1998). Correlation matrix for standardised principal component analysis is transformed through the normalisation process of the covariance matrix at first (Behrens 1998). On the other hands, non-standardised principal components contains unequal weight of variance that is information on scene, notably higher in the first couple of principal component bands (e.g. PC1 and PC2) and lower minor components (e.g. PC3 and PC4) (Fung and LeDrew 1987; Robila *et al.* 2000). Yet, that high variance in the first several principal components does not necessary ensures containing the scene information on interest for the research purpose (Behrens 1998). If the covariance approach is used for imagery that shows unchanged area dominant in the study area, changed area could be extracted by minor principal components (PC3 or later) (Fung and LeDrew 1987). This is because unchanged area should be highly correlated area, yet changed area is attributed to small portion of entire image that is low correlated area. Thus, when addressing change detection using a covariance approach, changed area is likely to come up in minor principal components. According to the comparison between the standardised and non-standardised components by Fung and LeDrew (1987), standardise principal components are more suitable for change detection. While non-standardised principal components are generally a sort of summary of all spectral bands, standardised principal components can extract the underlying features within satellite data (Fung and LeDrew 1987). In another respect, standardised principal components can produce visually more accurate and enhanced information for change detection purpose as compared with non-standardised principal components (Fung and LeDrew 1987).

3.6.2 Independent component analysis (ICA)

Independent Component Analysis (ICA) is a recently developed statistical and computational technique for linear transformation (Hyvärinen 1999; Hyvärinen and Oja 2000). ICA is attempted to detect a linear representation of non-Gaussian data for producing original signals, which is statistically independent or as independent as possible from each other (Hyvärinen and Oja 2000; Robila *et al.* 2000). Such a linear representation delineates specific pattern underlying in the data, then ICA plays a role for feature extraction from the data (Hyvärinen and Oja 2000). In other words, ICA performs blind source separation technique that finds original signal or latent variables, called independent components (Hyvärinen and Oja 2000). ICA is extension or variant of PCA and factor analysis in which producing not only decorrelated data like PCA but also original signals, mutually and statistically independent components (Lathauwer *et al.* 2000; Robila *et al.* 2000; Gilmore 2004). ICA is regarded as more powerful technique than classic techniques like PCA in extracting the hidden factors or sources (Gilmore 2004; Shah *et al.* 2007). Based on vector matrix notation, ICA mixing model is written as;

$$x = As$$

Where x is the observation, the random vector with elements of the mixtures x_1 to x_n, A is the matrix, and s is the independent components, the random vector with elements of the mixtures s_1 to s_n (Hyvärinen and Oja 2000; Gilmore 2004).

For satellite remote sensing, ICA is employed for image feature extraction based on spectral characteristics of multi or hyper-spectral images (Robila *et al.* 2000). For coastal wetland areas like this project, image classification is difficult due to spectral confusion with adjacent land cover classes (Ozesmi and Bauer 2002). Yet, ICA is assumed to distinguish such spectral similarity as statistically independent as possible. Those extracted independent components can be employed as training samples for supervised classification procedure. Additionally, ICA is also used as unsupervised classification on account for its ability that can classify underlying objects in image without knowledge of spectral characteristics in an unknown image (Du *et al.* 2004). Multi or hyper-spectral image analysis is in the context of interband correlation, then, optimal subset of bands through data dimensional reduction by feature extraction is essential (Shah *et al.* 2007). A thing should be taken into account for ICA application for satellite remote sensing is the number of bands and features proposed for extraction. Larger number of bands than the number of feature proposed for extraction is desirable in order to extract each specific feature as independent components (Shah *et al.* 2007). Weight matrix of ICA is a square matrix (Du *et al.* 2004). As the result, the number of independent components is assumed to be equal to the data dimensionality which is the number of spectral bands (Du *et al.* 2004). Smaller number of spectral bands is unable to extract all specific features supposed to be detected as independent components (Du *et al.* 2004). In addition to this, noise of the image is likely to be extracted as one of independent components instead of specific land features. The other consideration is what wavelength is contained in each band of satellite's sensor acquired the image used for ICA. As ICA is based on spectral characteristics, features delineated by independent components are varied along with its spectral response. Then, multi or hyper-spectral satellite imagery that has large number of bands with wide range of wavelength is ideal for ICA feature extraction to detect diverse features. In another respect, the control of feature's number in the image is also crucial to match up its number to the number of satellite bands. For this project, data dimensional expansion for producing additional bands to make the sufficient number of spectral bands and masking out suppress features in image to extract small features, and controlling the spatial subset of study area are important factors for enhancing ICA ability.

3.7 Image classification

The purpose of satellite image classification is to automatically classify pixels in an acquired image into the category of earth land cover object or phenomena (Navalgund *et al.* 2007). Conventional image classification defines feature classes based on the spectral characteristics of individual pixels although there are other types of image classification technique. Spectral characteristic is defined by spectral reflectance over bandwidth in different wavelength (Navalgund *et al.* 2007). Multi-spectral image classification is a process of analysing those multi-spectral features and categorising pixels into classes based on approximate value of spectral reflectance to produce thematic land cover information (Navalgund *et al.* 2007). Two major multi-spectral image classifications are unsupervised and supervised classification (Navalgund *et al.* 2007). For the image classification of coastal area, especially wetlands, the most popular classification approach is unsupervised classification or clustering to produce a thematic map (Ozesmi and Bauer 2002). Additionally, supervised classification is also common classification technique for coastal regions (Ozesmi and Bauer 2002). Since the approach of image classification can influence on class differentiation the prudent selection of classification technique is prerequisite for coastal region image classification standard (Lu and Weng 2007).

3.7.1 Training stage

The quantity and quality of training pixels involves in the context of the image classification quality (Lillesand and Kiefer, 2008). Appropriate number and position of training pixels allows classification algorithm to calculate reasonable estimation of feature classes (Richards and Jia 2006). This project employed seed pixel approach for training stage instead of using ground truth data of each feature class from study location. This approach digitises polygons called Region of Interest (ROI) that is on behalf of each class in the acquired image. Generally, the minimum pixel number of 10 N is ideally for training pixels of each specified class when N dimensional multispectral data is addressed (Swain and Davis 1978; Jensen 2005). In the case of multispectral satellite, for instance, Landsat TM and ETM, which contains 7 bands, needs approximately 70 pixels per class. In practice, more than such a minimum number of training pixels is ideal to assure the spatial independence of pixels (Richards and Jia 2006). Additionally, randomly dispersed ROI for each class is more useful for better accuracy of classification results than the single ROI of each class with the large number of training pixels to avoid biased result of classification (Lillesand and Kiefer, 2008).

3.7.2 Supervised classification

Supervised classification is a pixel based classifier that generates a signature through merging the spectra derived from all training-set pixels from a given feature class (Lu and Weng 2007). In short, each pixel is categorised into each land cover class that is mutually exclusive. Supervised classification uses training samples of known signature classes based on ancillary data, such as maps, aerial photography and local information, to classify pixels of unknown signature (Navalgund *et al.* 2007). Resultant signature class consists of contributions of all spectral information from the training data-set pixels (Lu and Weng 2007). Generated signatures are then employed to categorise the spectral data into a thematic map as the result of image classification (Lu and Weng 2007). Supervised classification is particularly useful when relatively few land cover classes are proposed, when there is a ground truth data with verified training sites, and when land cover of study area is homogeneous that each proposed class is perceivable (Deng *et al.* 2008). On the other hand, there is however, a mixed pixels limitation remaining in the thematic map generated by supervised classifier, especially when using low or moderate spatial resolution imagery (Lu and Weng 2007) like Landsat imagery. Numerous supervised classifications have been developed until now. Among the classifiers, '*maximum likelihood*' classifier is assumed to have a potential for coastal area classification.

3.7.2.1 Maximum likelihood classifier

Maximum likelihood classifier (MLC) is one of popular parametric classifiers that uses the means and variances of spectral information from training samples (Ozesmi and Bauer 2002; Richards and Jia 2006; Lu and Weng 2007). MLC assumes that the statistics for each class in each band from the training samples are multivariate-normal (Gaussian) in their distribution (Navalgund *et al.* 2007). Statistical probability of a given pixel assigned into a specific class is then calculated (RSI 2009). All pixels are classified when the threshold value of the probability is not designated. Each unknown pixel is then placed in the class in accordance with the given highest probability of membership, which is the maximum likelihood (Ozesmi and Bauer 2002; RSI 2009). Generally, MLC produces better accuracy than the other supervised classifier, including '*minimum distance to means*' or '*parallel piped*' classifiers since the covariance of the data is addressed (Ozesmi and Bauer 2002). Discriminant function is calculated by ENVI for MLC based on the assumption of normal statistics, written as:

$$g_i(x) - \ln p(\omega_i) - \tfrac{1}{2} \ln |\Sigma_i| - \tfrac{1}{2}(x - m_i)^t\, \Sigma_i^{-1}\, (x - m_i)$$

Where: i = class

x = n-dimensional data (where n is the number of bands)

$p(\omega_i)$ = probability that class ω_i occurs in the image and is assumed the same for all classes

$|\Sigma_i|$ = determinant of the covariance matrix of the data in class ω_i

Σ_i^{-1} = its inverse matrix

m_i = mean vector

(Richards and Jia 2006, cited from p. 196; RSI 2009).

MLC is the most common supervised classifier applied for mapping coastal and wetland areas (Ozesmi and Bauer 2002; Wabnitz *et al.* 2008; Everitt *et al.* 2009). There are however, several difficulties inherent in this classifier. One of them is potential large error arisen from mixed pixels. MLC is a hard classification that definitive decision is applied for each feature class with each pixel assigned to a single class (Lu and Weng 2007). In this regard, when using medium spatial resolution imagery, large errors might be occurred by the hard classification principle associated with the mixed pixel problem attributed to large pixel size and heterogeneity landscape (Lu and Weng 2007). Another difficulty is a noisy classification (Lu and Weng 2007). Noisy resultant data of classification is likely to be generated due to the high dispersion of the same class pixels (Lu and Weng 2007). Although this is technically not error, it might be a difficulty dependent upon the subsequent use of the resultant data. Noisy map, for instance might not allow easy image interpretation for several of change detection techniques, such as multiple-date composite image insertion. Further, MLC assumes that the Gaussian spectral distribution of both dataset and parameters generated from the training samples, yet this assumption is often prevented on account of complex landscape, which contains non-gaussian spectral distribution (Lu and Weng 2007). Thus, these are the challenges inherent in MLC. Simple application of MLC might have these challenges associated with the landscape variability of study area and medium spatial resolution.

3.7.3 Unsupervised classification

Unsupervised classification is also a per-pixel or pixel based classifier that brings pixels together based on spectral value's similarity (Ozesmi and Bauer 2002). It identifies natural groups or structures, within multi or hyperspectral satellite data through clustering-based algorithm to produce a thematic map (Lu and Weng 2007; Navalgund *et al.* 2007). Clustering-based algorithm plays a role of dividing the acquired image into a designated number of spectrally different clusters in accordance with the statistical information derived from the image (Lu and Weng 2007). Unsupervised classification is thus ideal approach if feature classes are determined only based on spectral distinctions (Deng *et al.* 2008), since unlike supervised classification, no prior knowledge for feature classes is required. Only the requirement for unsupervised classification approach is to label each cluster after satisfying number of cluster is generated through the integration of spectral classes into meaningful classes (Lu and Weng 2007). Analyst produces the label of feature class to each cluster based on ancillary information (Ozesmi and Bauer 2002). Advantages of unsupervised classification are the resultant class attributes distinct units and less processing time than supervised classifier (Ozesmi and Bauer 2002). Disadvantage is the resultant clusters does not necessary match up with desired features classes (Ozesmi and Bauer 2002). Unsupervised classification is most successful approach when there is a need of a large number of clusters (Deng *et al.* 2008). This characteristic of unsupervised classification approach often meets the standard of coastal area mapping because coastal area environment has numerous features. Application of unsupervised classification technique is therefore, popular for coastal region classification to distinguish a large number of classes (Macleod and Congalton 1998; Ozesmi and Bauer 2002; Gullström *et al.* 2006; Shanmugam *et al.* 2006; Deng *et al.* 2008).

3.7.3.1 ISODATA

Iterative self-organizing data analysis (ISODATA) unsupervised classification is popular classifier for coastal area classification (Ozesmi and Bauer 2002). It is implemented in accordance with specified iterations and recalculates statistics with respect to each iteration (Everitt *et al.* 2009). Class means distributed evenly in the image data is calculated at the beginning by this classifier, and then remaining pixels are clustered iteratively using minimal spectral distance to mean principle to allocate a cluster for each selected pixel (Everitt *et al.* 2009; RSI 2009). With respect to each iteration of clustering, new means are calculated and shifted to new place of feature space, and pixels based on the newly calculated means are then reclassified (RSI 2009). Number of iteration is dependent upon user's requirement. When the designated number of iteration is reached or the number of pixels in each class changes by less than the designated pixel change threshold, recalculation process is about to finish (RSI 2009). This technique is useful, especially when there is a time limitation for image processing, distinct class units are required, no prior knowledge of study area is available, and the landscape of study area is complicated (Ozesmi and Bauer 2002).

3.8 Change detection

Change detection in satellite remote sensing is a process to identify non-change and actual change in the geometry or status of proposed object or phenomena in terms of the differences between spatial and spectral information by observation through multi-temporal images. As increasing demand for change detection of natural features together with increasing natural environment hazard, numerous technique of change detection via satellite remote sensing has been developed (Lu *et al.* 2004). However, analysts have often reached different conclusions about the ability and effectiveness of change detection methods (Lu *et al.* 2004). This may be because of the influence of complicated factors derived from qualitative and quantitative differences of various research requirements and objectives. In practice, the change detection of a proposed object is sometimes difficult to mcct the high standard of successful monitoring project with specific objective and study location, especially without using the appropriate selection of change detection method associated together with suitable algorithm (Lu *et al.* 2004). Application of multi-temporal satellite imagery is common method for large areal change detection (Morisette 1997). For satellite imagery change detection, generally, individual pixels in acquired image are addressed. Changes in the geometry or status of proposed object are identified based on the different brightness value of each pixel corresponding position in between compared images (Morisette 1997). Methods include: Write Function Memory Insertion (WFMI); Multi-date Composite Image (MCI); Image Algebra; Post-classification Comparison; Principal Component Analysis (PCA); are major change detection approaches using satellite imagery (Dobson *et al.* 1995; Coppin *et al.* 2004; Lu *et al.* 2004). In recent practice, Image Algebra, Post-classification Comparison and Principal Component Analysis are the most commonly employed single use techniques (Lu *et al.* 2004). On the other hand, hybrid approach combined with several techniques is also applicable for change detection method. Yet, unless careful structure of change detection method is organised, considerable error might be remained in the result (Fung and LeDrew 1987). For instance, MCI change detection approach using PCA technique has been popular for previous researches (Munyati 2004; Deng *et al.* 2008). For this project, MCI approach was implemented with application of ICA. WFMI approach employed either one of the two methods; PCA based ISODATA classifier or ICA based MLC classifier.

3.8.1 Multiple-date Composite Image (MCI) approach

Multiple-date Composite Image (MCI) approach is a process that allows extracting change and unchanged information through single integrated dataset generated from two different temporal images (Jensen 2005). The single composite data set can then be processed in numerous ways for change detection analysis (Jensen 2005). One of ways is to apply unsupervised classification for the composite data set. All *N* bands of the composite data set is analysed by unsupervised classification so that clusters of change and unchanged is produced (Jensen 2005). Another popular way of MCI approach is application of image transformation techniques, such as PCA for the composite data set. Either standardised (based on correlation matrices) or non-standardised (based on variance-covariance matrices) PCA can be used for the composite data set to extract change information (Jensen 2005). Yet, in practice, application of standardised PCA technique, which is based on correlation matrix, has been major approach in the MCI method rather than using non-standardised PCA (Fung and LeDrew 1987; Macleod and Congalton 1998). While PCA based MCI approach is popular, this project attempted to use ICA technique for MCI instead of unsupervised classifier and PCA. Reason for that is the better ability of ICA to extract subtle changes in objects of interests than the application of unsupervised classifier and PCA. Additionally, most satellite data is assumed non-Gaussian distribution of features in the image. ICA can attempt to detect such distribution of features but PCA has low potential due to its assumption of application for data with a multivariate Gaussian distribution (Shah *et al.* 2007). Advantage of MCI approach is the requirement of only single classification technique (i.e. unsupervised classification or ICA or PCA) (Jensen 2005). Yet the resultant data of MCI approach is often subject to the difficulty of image interpretation. In particular, the subtle changes of natural environment like the study area of this project are likely to be involved in such a difficulty.

3.8.1.1 ICA based approach

ICA can play a role of classification or feature extraction for MCI change detection approach in order to detect change and non-change area in a composite image. Numerous researches have commonly employed PCA for MCI approach so far (Fung and LeDrew 1987; Dobson *et al.* 1995; Munyati 2004; Deng *et al.* 2008; Deng *et al.* 2009). In practice, however, some researchers concluded another approach, such as image differencing was better accuracy than PCA for change detection (Macleod and Congalton 1998), while some researches indicated the effectiveness of PCA based MCI approach (Fung and LeDrew 1987; Munyati 2004; Deng *et al.* 2008). In this regard, image transformation technique basis MCI approach highly relies on research purpose and study area. In other words, the distribution pattern of proposed research objects in study area is involved in the effectiveness of the approach. Few previous researches into ICA basis MCI approach have been conducted until now (Zhong and Wang 2006; Benlin *et al.* 2008). Yet, ICA capability for MCI change detection approach was indicated by those studies since ICA is based on the assumption of application for non-Gaussian data. Zhong and Wang (2006) found the capability of ICA basis MCI change detection approach for detecting land cover changes due to land salinisation in Daqing, Heilongjiang province, China using multi-temporal remote sensing analysis. Band dimensionality expansion was also carried out in this research to match the number of desired features up to the number of the features in the image. Land cover change was successfully delineated through independent components. Further, according to the comparison between PCA application and ICA application for MCI, ICA produced higher accuracy than PCA in MCI change detection approach (Zhong and Wang 2006). Benlin et al. (2008) used composite image, consists of the two of first principal component generated from two different time images, for ICA processing. ICA revealed feasibility and effectiveness for image classification and change detection (Benlin *et al.* 2008). According to them, this method was attributed to extract most mainly changed areas. However, it was assumed subtle changes between two images might have not been able to be extracted by this method. It is because this method employed the composite image composed of the two principal components, which contain only principal information of original images. While this method is effective, there is no need to use principal component when subtle change detection is required. Additionally, ICA has been often used in image classification procedure, especially for land cover classification in practice. Although, it was not change detection method, many researches indicated the effectiveness of ICA as a classification technique (Robila *et al.* 2000; Du *et al.* 2004; Gilmore *et al.* 2004; Shah *et al.* 2007). Some of them concluded that ICA has better classification ability than PCA or ISODATA, and also importance of band generation to improve the ability of ICA (Du *et al.* 2004; Shah *et al.* 2007). From these perspectives of previous researches, ICA basis MCI change detection approach is assumed to have sufficient ability for change detection in seagrass distribution in this project.

3.8.2 Write Function Memory Insertion (WFMI) approach

Write Function Memory Insertion (WFMI) approach basically provides visual assistance for change detection, using any sort of geometrically corrected multi-temporal data (Jensen

2005). WFMI is a simple yet powerful method. Qualitative ability of WFMI to delineate the change area is visually the most helpful among other methods (Jensen 2005). Individual spectral bands from different temporal data or derivative data, such as principal components or independent components can be assigned into each red, green and blue of write function memory banks to identify changes through the output imagery (Jensen 2005). The spectral and geometrical changes between different temporal images can be highlighted by specific colors on the generated image. For instance, when time 1 (T1) image is assigned into the blue memory plane and time 2 (T2) image is assigned into the green and red memory planes, differences will be generated through cyan and red in ENVI application (RSI 2009). Cyan represents the change of brightness values that original value of T1 increased between T1 and T2, and red represents the decrease of original values between T1 and T2. Additionally, the capability of change detection analysis between the maximum of three imageries at single process is another advantage of WFMI (Jensen 2005). The single application of WFMI is not quantitative change detection approach that provides the amounts of change information between two date images. Yet, WFMI can be applied for post-classification approach together with another function of image analysis software. In other words, '*from – to*' change can be extracted by WFMI approach through combination with '*Mask*' function of ENVI software. Since specified data values are set out for each land cover class in a thematic map, class by class '*from – to*' change can be extracted by the '*Mask*' function. This project thus employed this modified WFMI approach to detect the class by class '*from – to*' change. Two types of results generated from the different image classification methods (PCA based ISODATA and ICA based MLC) were prepared for the modified WFMI approach. One of the two results with better accuracy than the other result was then subject to the approach in case study 5 of this project.

3.8.2.1 PCA based ISODATA

As described previous section, PCA can play a role of feature extraction from image. This function of PCA can be applied for image classification procedure as one component of pre-processing steps. The application of principal components derived from PCA for image classification technique is one of important steps in WFMI approach to obtain '*from – to*' change information (Deng *et al.* 2008). By using PCA for feature extraction, the accuracy of image classification is enhanced. For instance, Gluck et al. (1996) employed PCA in ISODATA unsupervised classification for wetland mapping. They subjected first three principal components to ISODATA classification with selected 250 clusters. In this research, eleven classes with overall accuracy of 72% were eventually obtained to separate the wetlands from uplands. Increase of classification accuracy ensures the precision of change detection as this is an extension process to classification. Since classification accuracy directly influences on the accuracy of WFMI change detection approach (Deng *et al.* 2008), PCA application for this method is attributed to the success of subsequent change detection analysis. The disadvantages of PCA, such as the difficulty of labelling '*from – to*' change class information, are inherent in the MCI approach (Deng *et al.* 2008). Additionally, the knowledge of the spectral characteristics of features in the study area and corresponding principal components are thus required for MCI approach, yet not required for WFMI approach (Macleod and Congalton 1998). While a few principal components (PCA result) based unsupervised classifier has been conducted for change detection analysis (Gluck *et al.* 1996), potentiality for classifying and detecting change is promising through cumulative capability of PCA and unsupervised classification techniques.

3.8.2.2 ICA based MLC

As mentioned in previous section, several challenges are inherent in MLC. This project however, attempted to constrain the negative effect derived from these challenges through hybrid approach scheme that applies the ICA for MLC to enhance accuracy of MLC result. Application of ICA for MLC is assumed to derive the strength of feature extraction technique and compensate the negative effects of MLC. Basic process of ICA basis supervised classifier approach is similar to the PCA basis unsupervised classifier. ICA is also subject to feature extraction to this WFMI approach like PCA. Yet, large difference between these two approaches is that the extracted features by ICA can be training samples for supervised classification unlike PCA. Extracted features by ICA contain single data value, yet each feature in the principal component images contains numerous data value like ordinal image. Since each independent component is statistically independent, extracted features allows analysts to determine training sample area easily without ancillary data and local knowledge of study area. Thus, when using ICA before image classification step, not only unsupervised classification but also supervised classification can be used. Additionally, ICA ensures that the improvement of image classification accuracy associated with the well extracted features by ICA. Multi-temporal thematic maps generated from the ICA based supervised classification is finally taken place in WFMI to detect *'from – to'* change in the object of interest. Shah et al. (2007) concluded the better accuracy of independent components based image classification than the use of conventional remote sensing feature extraction technique, such as PCA and Minimum Noise Function, as a base image for image classification. In their study, thematic map generated by K-means classifier based on 7 independent components represented significant improvement over the resultant thematic map generated based on original image in homogenous agricultural land cover area. They also indicated that application of ICA can enhance performance of several spectral analyses, including image classification. However, unless meaningful band combination for band dimensionality expansion takes place, sufficient capability of ICA for feature extraction is not performed (Shah *et al.* 2007). Statistically independent components generated from ICA are assumed to improve MLC performance for image classification in this project.

3.9 Accuracy Assessment

Generally, some kind of degree of error is subject to image analysis in remote sensing, especially in the procedure of geometric correction and image classification. Measurement of accuracy or remained error for these procedures is essential to ensure the data reliability or validation. This project also addressed with accuracy assessment for geometric correction and image classification. However, the accuracy assessment of the change detection was not undertaken due to the lack of ancillary data and time.

3.9.1 Assessment of geometric accuracy

Accuracy assessment for geometrically corrected images ensures not only the accuracy of the generated thematic maps but also the accuracy of change detection analysis. The approach used in this project calculated mean error values and standard deviation of residuals between objects in the rectified satellite image and objects in the reference data. Residual lines should be digitised throughout the image not only the area surrounding the immediate study site but also the areas close to the edge of the image to calculate unbiased value of residual means and standard deviation. The reason for this allocating pattern of the digitised residual lines was to ensure better overall geometric accuracy in the image. As the major aims of geometric correction is the production of a base image for the image analysis of seagrass habitat mapping and monitoring, high accuracy for the study site was the priority. Yet, on account of the cloud coverage and noise in the image, several corresponding points between the rectified image and validation data image is often difficult to be digitised for calculation in practice. Additionally, when using orthorectified aerial photography for validation data, the central area of orthorectified image has potentially lower distortion than the outer area. Thus, the area as much closer as central area should be used for digitising residual line in order to achieve higher quality of accuracy assessment.

3.9.2 Assessment of classification accuracy

Accuracy assessment of the thematic map is necessary when classification exercise is completed (Richard and Jia 2006; Deng *et al.* 2008). Appropriate accuracy assessment provides validation of the classification result (Richard and Jia 2006). The result of the accuracy assessment also gives a measurement or indicator for analyst to determine whether the research objective was achieved or not (Richard and Jia 2006). Additionally, the result of image classification accuracy is subject to the method selection of the either one of two (PCA based ISODATA or ICA based MLC) for WFMI change detection approach in this project. Conventional accuracy assessment approach, '*error matrix*' was employed to measure the accuracy of the image classification result in this project. Error matrix is a design based inference, which gives thorough probability assessment based on statistical principals (Jensen 2005). In short, error matrix infers the statistical characteristics of a limited population based on *sampling pixels* selected from the thematic map for this accuracy assessment (Jensen 2005; Richard and Jia 2006). After selecting the sampling pixel from the thematic map, the accuracy is determined based on *testing pixels*, selected from the reference data. Important factor for this process of the accuracy assessment is the total number of testing pixels from ground truth data (Deng *et al.* 2008). According to the rule of thumb by Congalton (1991), at least 50 samples should be taken for each land cover class in the error matrix. As the extent of study are or the number of feature class in the study area increases, the minimum number of samples should also be increased (Deng *et al.* 2008). By crosschecking their labels with feature classes determined from the testing pixels of the reference data (or ground truth data), the accuracy is eventually determined (Richard and Jia 2006). The percentage of the selected pixels from each feature class in the thematic map about whether it is labelled correctly is estimated through those checking procedures (Richard and Jia 2006). Conventional statistical measurements for remote sensing accuracy assessment are encompassing; overall accuracy, producer's accuracy, user's accuracy, and Kappa coefficient of agreement (Jensen 2005; Deng *et al.* 2008). Overall accuracy is the simplest descriptive statistics which is calculated by dividing the number of correct pixels by the total number of pixels checked in the error matrix (Congalton 1991; Banko 1998; Jensen 2005). Each error generated from the matrix is referred to as omission error (errors of exclusion), an omission from the correct category, and commission error (errors of inclusion), a commission to a wrong category (Jensen 2005). These errors are then represented by producer's accuracy and user's accuracy based on the matrix. Producer's accuracy is a measure of omission error, which indicates the probability of ground truth pixels being correctly classified (Congalton 1991; Jensen 2005). This accuracy is computed by dividing the number of correct pixels in a category by the total number of pixels in same category derived from ground truth data (Congalton 1991; Banko 1998). How much a certain area was well classified can be measured by the producer's accuracy (Banko 1998). User's accuracy is computed to indicate the probability of a pixel classified on the thematic map representing actual category for a measurement of commission error

(Congalton 1991; Banko 1998). Suppose if only a specific class is subject to the object of interest in the research, then, producer's accuracy and user's accuracy are more appropriate to measure the accuracy of the specific object than overall accuracy (Congalton 1991; Jensen 2005). Further, user's accuracy is usually more important since it indicates the actual percentage of the correctly labelled pixels on the thematic map (Jensen 2005; Richard and Jia 2006). Another parameter is the Kappa coefficient, a measure of overall agreement or accuracy between the thematic map derived from remote sensing and the reference data (Banko 1998; Jensen 2005). Large value of KHAT statistic, an estimate of Kappa, represents strong agreement or accuracy between the thematic map and the information of the reference data (Jensen 2005). Since this project addressed with seagrass meadows as object of interest, error matrix was therefore attempted to measure the accuracy of such a specific object through mainly focusing on the user's accuracy. Another consideration for accuracy assessment is sampling scheme. Jensen (2005, pp. 502) indicated "The location of the sample locations must be selected randomly without bias". As prejudiced sample location in the error matrix procedure results in the over or under estimation of accuracy of a thematic map, it is thus crucial to do unbiased random sampling (Jensen 2005).

Chapter 4 Case Study 1 – Comparison between remote sensing methods

4.1 Chapter overview

Chapter 4 introduces the Case Study 1; Comparison between two image classification methods, encompassing; (1) PCA based unsupervised classifier approach, and (2) ICA based supervised classifier approach. The comparison was performed for the purpose of identifying the ability of the methods to classify land cover features, especially SAV meadows. Production of multi-temporal thematic map series of the whole Boulanger Bay area is a secondary purpose for change detection analysis in Case Study 2. In order to investigate into the effectiveness of mapping SAV meadows, comparison between those two approaches associated with accuracy assessment was crucial. Results of thematic maps were subject to the accuracy assessment of '*error matrix*'. Description of the study area and data used for this case study was introduced. Image pre-processing and classification procedures and accuracy assessment were described.

4.2 Comparison between remote sensing methods

4.2.1 Introduction; Study area and Data

Study area of Case Study 1 includes the whole area of Boullanger Bay. It is located in 40.6°S and 144.6°E (Figure 4.1). As mentioned in the chapter 2, this area contains the large seagrass beds of approximately 8,000 ha (Rees 1993; Sprod *et al.* 2003). Many benefits and values in terms of environmental, social and economical significance are supported by this area (Crawford and White 2007). In order to perform image classification analysis for SAV distribution, Landsat TM, ETM+ and ALOS imagery were employed for this case study. In practice, high tide stage is not preferable for the image analysis of submerged object due to the interference of water (Macleod and Congalton 1998). Yet, the limitation of desirable image did not allow this project to arrange images with ideal status, such as low tide, low water turbidity and low noise together with similar anniversary acquisition date. The 5 images with acceptable quality for the whole Boullanger Bay, including: Landsat 5 1990; Landsat 7 2000; Landsat 5 2004; ALOS 2006 and Landsat 5 2008 for the above image classification analysis were prioritised for the tide stage, water clarity, noise coverage and acquisition date (Table 4.1).

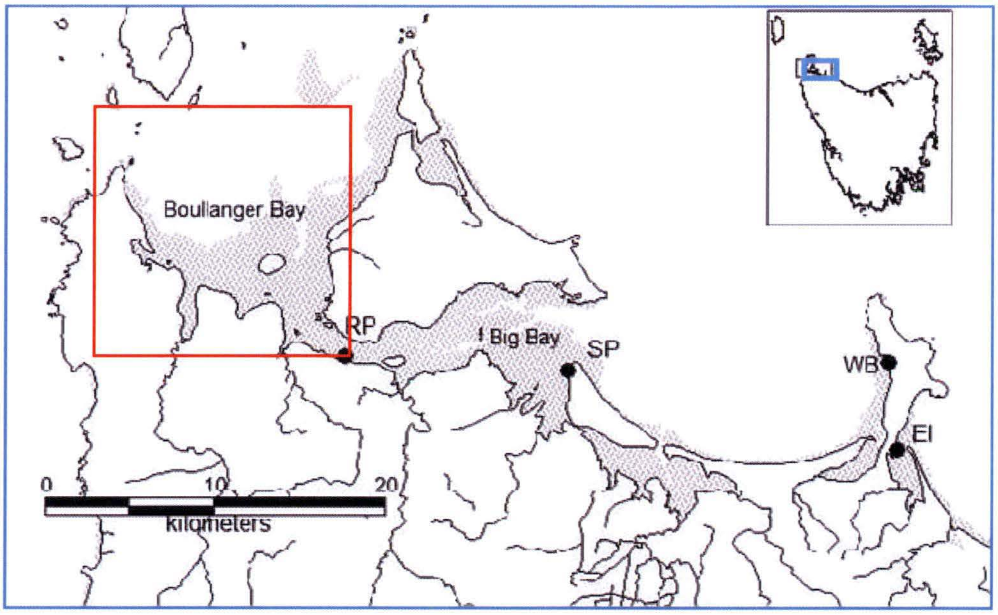

Figure 4.1 The Boullanger Bay Study Area is shown in the red square. This is also the study area for Case Study 1. Source: (Dunn 2000).

Table 4.1 Satellite data description for Case Study 1, '--'mark represents no data

Image date	Sensor	Processing level	Tide	Cloud cover (%)	Water turbidity	Other information
29/12/1990	Landsat 5 TM	L1G	High	--	Low	Image time at: -- Sun elevation at: 50 Sun azimuth at: 79
16/02/2000	Landsat 7 ETM+	L1G	High	--	Low	Image time at: -- Sun elevation at: -- Sun azimuth at: --
18/01/2004	Landsat 5 TM	L1T	High	0	Low	Image time at: 23: 43: 02 Sun elevation at: 49 Sun azimuth at: 73
19/10/2006	ALOS AVNIR - 2	Level1B2G	High	50	Low	Image time at: 00:22:05 Sun elevation at: -- Sun azimuth at: --
11/10/2008	Landsat 5 TM	L1T	High	4	Low	Image time at: 23:48:27 Sun elevation at: 45 Sun azimuth at: 52

4.2.2 Image pre-processing

Different status of systematic error was in the context of the acquired images, especially images distributed by U. S. Geological Survey (USGS) for this project. Generally, the most of Landsat 5 images distributed from USGS with L1T data were processed with standard terrain correction based on GCPs derived from GLS 2005 data set. However, the most of L1G data were only processed with systematic correction based on data collected by the sensor and spacecraft (USGS 2009). Additional geometric correction for most of L1G data, except for Landsat 1990 image (geometrically well corrected when it was distributed from USGS) were thus required to produce geometrically well corrected data for subsequent image analysis. Each Landsat scene of L1G data and ALOS imagery were then subject to '*image to image*' registration to match up with the geometry of Landsat 5, 1990. Less than the half a pixel of the Root Mean Square (RMS) errors, which is generally acceptable errors in georectification procedure for medium resolution satellite imagery were obtained in this case study. In order to produce corresponding pixel size over the acquired scenes derived from different sensors (Landsat and ALOS), each scene was resampled by '*nearest neighbour*' pixel resampling method to 25m. The radiometric consistency of corresponding objects over the different temporal scenes is crucial to ensure inter-image comparability for subsequent change detection analysis in Chapter 5. The Landsat 1990 scene was used as the reference image for radiometric normalisation. Equivalent blue, green and red bands from other scenes were radiometrically normalised with those corresponding bands of the reference image. '*Empirical line calibration*' technique, using Pseudo Invariant Feature (PIF) over the different time scenes was performed to not only remove atmospheric effects but also to reduce the radiometric discrepancy between two Landsat sensors, TM and ETM+. Adjacent upland area to coastal line was masked out using '*mask*' function of ENVI 4.6 based on the application of NDVI data to enhance the spectral value of the land cover of interests for image classification procedure. However, extensive variability of cloud layer density did not allow proper cloud removal processing in pre-processing procedure of this project. Pre-processed data were then subject to either the application for PCA based ISODATA image classification approach or the application for ICA based MLC image classification approach. Additionally, data dimensional expansion technique was required only for ICA based MLC method prior to the image classification and change detection procedures.

The dimensionality of original spectral bands was expanded to meet the number and spectral characteristics of proposed features of interests in the scene in accordance with the requirement for subsequent ICA image analysis. Non-linear operation for additional bands was required to detect additional information on underlying features in the image. Because of the concern over the water attenuation, bands between visible wavelengths were subject to the non-linear operation. The total of 18 additional bands, encompassing; (1) B1*B1, (2) B1*B2, (3) B1*B3, (4) B1*B7, (5) B2*B2, (6) B3*B3, (7) B3*B2*B1, (8) (B3*B2*B1)/ 3, (9) B1 - B2, (10) B1 - B3, (11) B2 - B3, (12) B1 / B2, (13) B1 / B3, (14) B2 / B3, (15) Normalised Red and Green Index (NRGI[3]), (16) Normalised Red and Blue Index (NRBI[4]), (17) Normalised Green and Blue Index (NGBI[5]), and (18) NDVI were then generated by using the function of '*Band math*' with ENVI 4.6 image software for each scene. These

[3] Modification ration of NDVI: (Red – Green)/ (Red + Green)
[4] Modification ration of NDVI: (Red – Blue)/ (Red + Blue)
[5] Modification ration of NDVI: (Green – Blue)/ (Green + Blue)

artificially generated bands were stacked with original bands for each scene. Each composite data consists of the original and additional bands were subject to ICA to extract the features of interests, such as dense SAV, sparse SAV, sand, sand, saltmarsh, deep water and cloud. Extracted features by ICA were assumed statistically independent, thus those were employed as training samples for image classification procedure of MLC.

4.2.3 Image classification

5 thematic map series of the whole Boullanger Bay area were produced by two different approaches, ICA based Maximum likelihood Classification (MLC) and PCA based Iterative self-organizing data analysis (ISODATA). ICA extracted features (independent components) from the acquired images for training areas. Independent components derived respectively from time 1 (T1) and time 2 (T2) images were employed to extract the endmember spectra of each class for each MLC analysis of T1 and T2 image. Each ROI for training pixels were digitised inside of the vector layer of the independent components from each feature class (Figure 4.2). Total of 6 classes (dense SAV, Sparse SAV, sand, deep water, saltmarsh, and cloud) were trained for classification stage of MLC (Figure 4.3). Only Landsat 5 1990, with no cloud coverage trained 5 classes. Based on the endmember spectra from each training sample, each feature class was classified by MLC procedure. PCA also extracted principal components from the acquired images. Unlike ICA approach, each principal component of T1 and T2 images were directly subject to ISODATA unsupervised classification procedure in this approach. For PCA based ISODATA approach, 25 classes were initially classified to obtain better classification result. These classes were then put together into 6 classes (Dense SAV, sparse SAV, sand, deep water, saltmarsh and cloud).

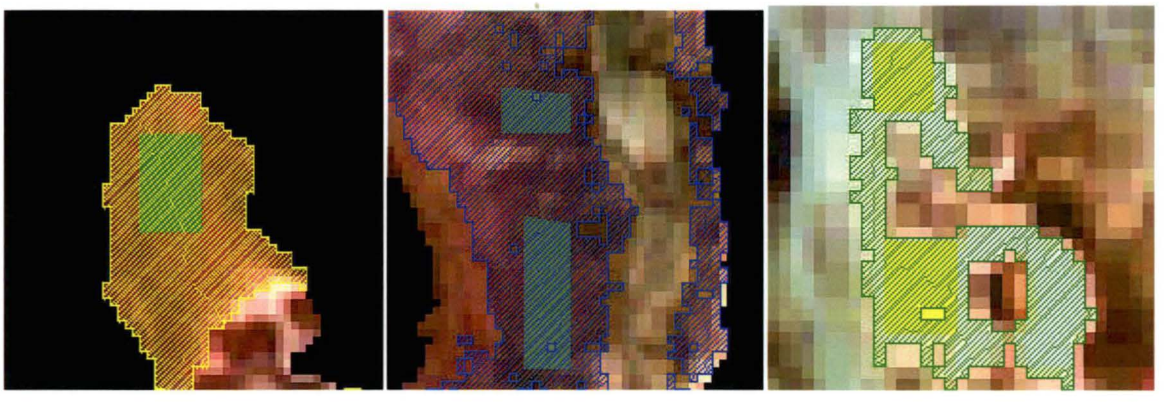

Figure 4.2 ROIs for training areas digitised inside of independent components

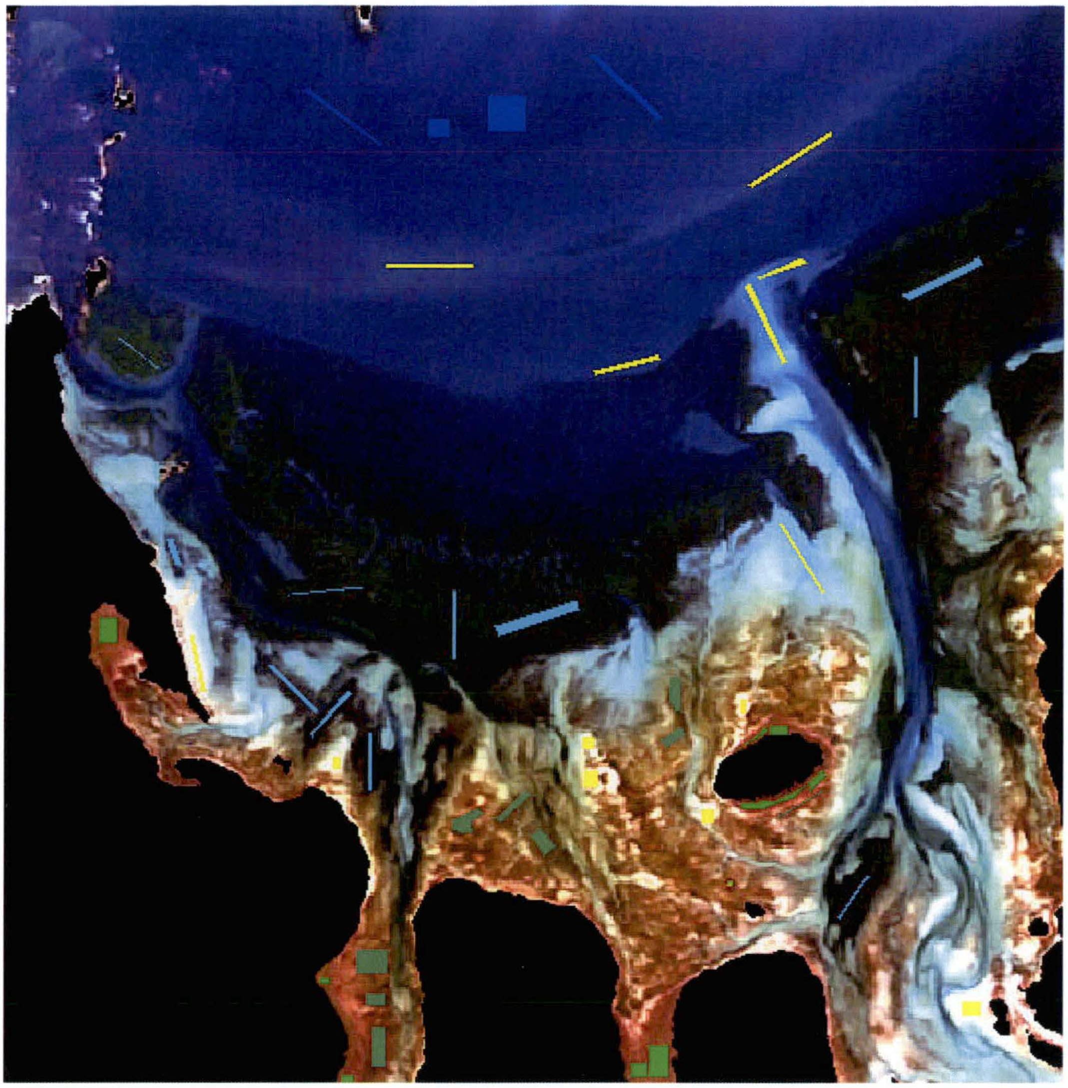

Figure 4.3 Training areas for MLC

4.2.4 Geometric accuracy assessment

Geometric accuracy assessment was conducted through ALOS 2006 images using ArcGIS 9.3 software (ESRI 2009). Vector layer data sets from the LIST map (LIST 2003) and orthorectified aerial photography (2006) were used as validation data for assessing geometric accuracy. Mean error values and standard deviation of residuals between objects in the rectified satellite image and objects in the orthorectified aerial photography and the state road layer of the LIST map were calculated. 70 residual lines were digitised for the calculation. Although potential objects or the places of the state road that that can be used for accuracy assessment were limited in the image due to the lack of outstanding landmarks in the natural environment, the digitised lines were assigned randomly to avoid unbiased assessment as much as possible.

4.2.5 *Accuracy assessment of image classification*

'*Error matrix*', known as conventional method for image classification accuracy assessment was performed for Case Study 1. Produced thematic maps generated from either PCA based ISODATA approach and ICA based MLC approaches were subject to error matrix. Vector layers, including; (1) sparse seagrass, (2) seagrass, (3) sand, and (4) saltmarsh, derived from SEAMAP Tasmania were employed for validation data. These layers were overlayed on the original image of ALOS 2006 to facilitate training sample data for the accuracy assessment of two approaches. While area of independent component and the vector layers from SEAMAP Tasmania were overlapped in most areas, training samples for accuracy assessment were picked up from different area from the area trained for two image classification approaches to avoid miss assessment. Classes that were not covered by the vector layers, including; deep water and cloud, were digitised simply in different places from the places used for training area in thematic map production procedures. All ROIs of the training areas were then subject to the calculation of error matrix between thematic maps and validation data. Statistical measurements, including; overall accuracy, producer's accuracy, user's accuracy, and kappa coefficient, were calculated between the sampling pixels derived from the ROI, used for the thematic map production and testing pixels, derived from the ROI, generated from the ground truth data.

4.3 *Results*

4.3.1 *Geometric accuracy assessment*

Geometric accuracy of less than a pixel size at mean residual (7.15m) was produced in the rectified image of ALOS 2006 through the geometric correction procedures via 70 digitised residual lines (Figure 4.5). Instantaneous field of view (IFOV) of ALOS imagery is 10m. Approximately the residual of 0.7 pixel size was thus considered as acceptable residual errors for ALOS imagery.

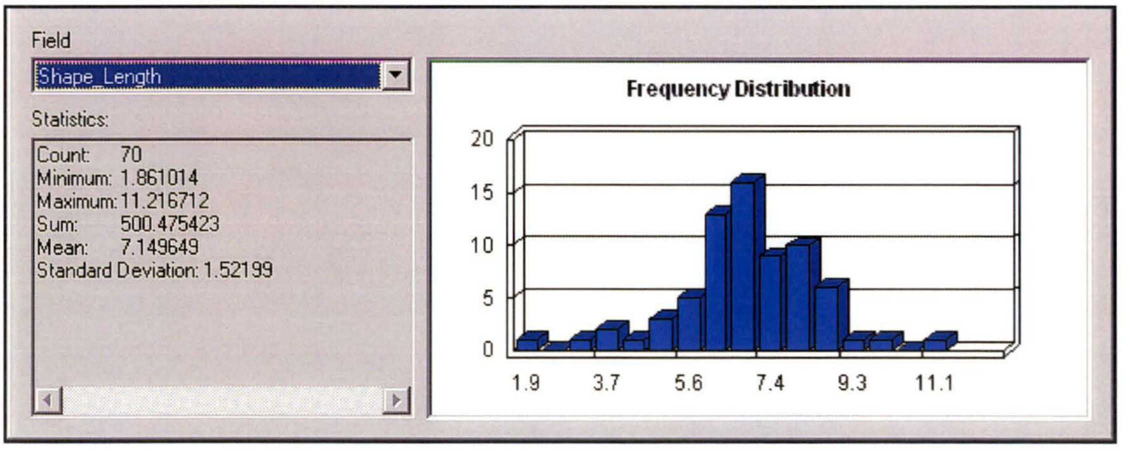

Figure 4.5 Mean residual errors

4.3.2 Case Study 1: comparison between remote sensing methods

Two thematic maps were produced from the reference image (19 October 2006 ALOS) through two image classification approaches, encompassing; ICA based Maximum likelihood Classification (MLC) and PCA based ISODATA (Figure 4.6 and 4.7). These thematic maps were then subject to accuracy assessment to investigate the better ability of mapping land cover classes, including SAV meadows in the Boullanger Bay.

The accuracy assessment was carried out through error matrix for the two methods of image classification. Overall accuracy of 82.7% and Kappa coefficient of 0.79 were obtained for PCA based ISODATA approach (Table 4.3). Producer's accuracy of saltmarsh was 100%, and user's accuracy of saltmarsh was 82.2%. For sparse SAV, producer's accuracy and user's accuracy were 75.9% and 100%. Additionally, the producer's accuracy and user's accuracy of dense SAV were 98.4% and 98.7%. As for the result of ICA based MLC approach, overall accuracy of 88.4% and Kappa coefficient of 0.86 were obtained (Table 4.2). The producer's accuracy and user's accuracy of 87.5% and 99.6% were obtained for saltmarsh. For sparse SAV, the producer's accuracy and user's accuracy of 54.1% and 85.4% were obtained. Additionally, the producer's accuracy and user's accuracy of 92.3% and 97.9% were obtained for dense SAV. Given overall accuracy and Kappa coefficient from ICA based MLC approach was higher than the approach of the PCA based ISODATA as the result. Producer's accuracy of saltmarsh represented higher in PCA based approach than ICA based approach. Yet User's accuracy of saltmarsh from ICA based approach obtained higher accuracy than PCA based approach. For the SAV category, almost equal accuracy, except for the producer's accuracy of ICA based approach, were obtained between two approaches. In all other classes, ICA based MLC approach obtained the accuracy of higher than or equal to the accuracy of PCA based ISODATA approach as the result. The main cause of the classification inaccuracy attributed to the high coverage of cloud associated with cirrus over the reference image.

While ICA based MLC approach obtained lower producer's accuracy and user's accuracy in sparse SAV than PCA based ISODATA approach, the accuracy of higher than or equal to PCA based ISODATA approach were obtained in other categories, which in turn, higher overall accuracy and Kappa coefficient. In accordance with the result, ICA based MLC approach was set out to image classification procedure for other images. The five reference images, 1990, 2000, 2004, 2006, and 2008, were classified into 6 classes: (1) Dense SAV; (2) Sparse SAV; (3) Saltmarsh; (4) Sand; (5) Deep water; (6) Cloud. Five thematic maps over 18 year time were produced by the ICA based MLC approach in Case Study 1 (Figure 4.8, 4.9, 4.10, 4.11 and 4.12).

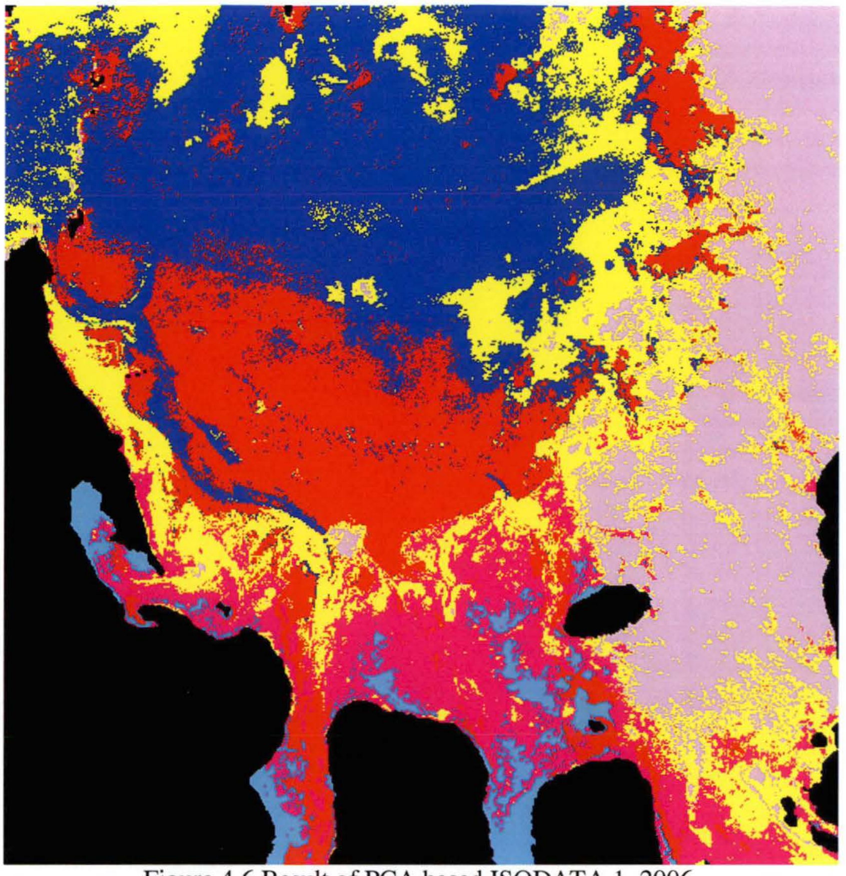
Figure 4.6 Result of PCA based ISODATA 1, 2006

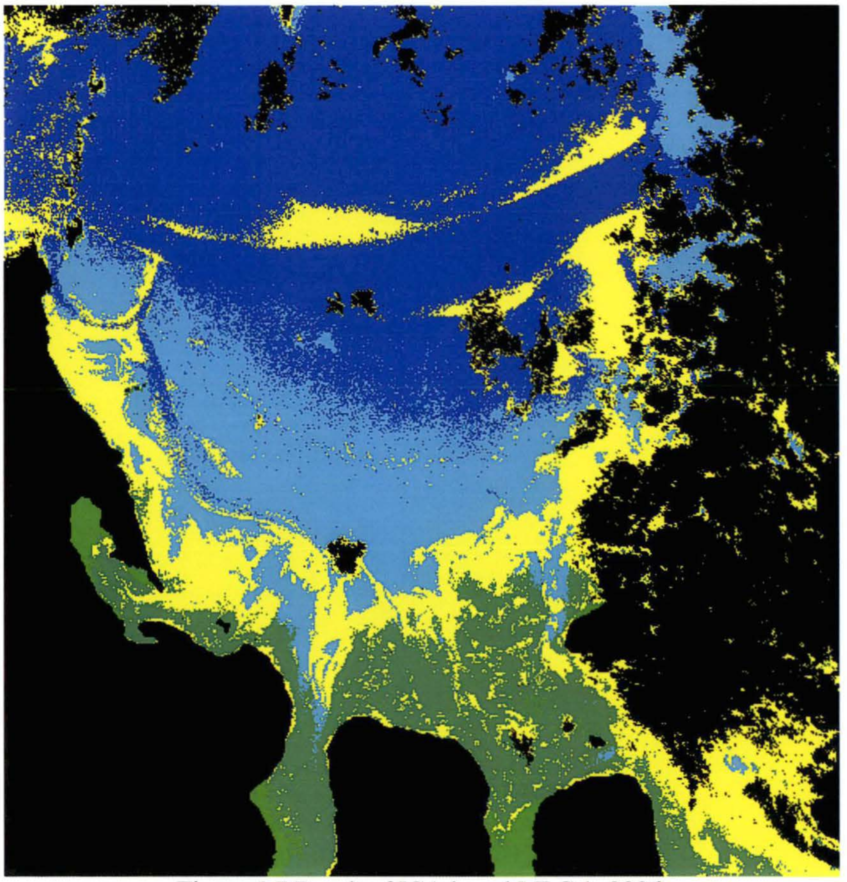
Figure 4.7 Result of ICA based MLC 1, 2006

Table 4.2 Error matrix result of ICA based MLC, 2006

Overall Accuracy = (1860/2102) 88.4872%
Kappa Coefficient = 0.8606

	Ground Truth (Pixels)				
Class	Saltmarsh	Sparse SAV	Sand	Dense SAV	Deep Water
Unclassified	0	0	0	0	0
Saltmarsh [Gr	259	1	0	0	0
Sparse SAV [S	28	164	0	0	0
Sand [Yellow]	8	136	347	3	0
Dense SAV [Cy	0	2	4	291	0
Deep Water [B	0	0	19	21	334
Cloud [White]	1	0	0	0	0
Total	296	303	370	315	334

	Ground Truth (Pixels)	
Class	Cloud	Total
Unclassified	0	0
Saltmarsh [Gr	0	260
Sparse SAV [S	0	192
Sand [Yellow]	19	513
Dense SAV [Cy	0	297
Deep Water [B	0	374
Cloud [White]	465	466
Total	484	2102

	Ground Truth (Percent)				
Class	Saltmarsh	Sparse SAV	Sand	Dense SAV	Deep Water
Unclassified	0.00	0.00	0.00	0.00	0.00
Saltmarsh [Gr	87.50	0.33	0.00	0.00	0.00
Sparse SAV [S	9.46	54.13	0.00	0.00	0.00
Sand [Yellow]	2.70	44.88	93.78	0.95	0.00
Dense SAV [Cy	0.00	0.66	1.08	92.38	0.00
Deep Water [B	0.00	0.00	5.14	6.67	100.00
Cloud [White]	0.34	0.00	0.00	0.00	0.00
Total	100.00	100.00	100.00	100.00	100.00

	Ground Truth (Percent)	
Class	Cloud	Total
Unclassified	0.00	0.00
Saltmarsh [Gr	0.00	12.37
Sparse SAV [S	0.00	9.13
Sand [Yellow]	3.93	24.41
Dense SAV [Cy	0.00	14.13
Deep Water [B	0.00	17.79
Cloud [White]	96.07	22.17
Total	100.00	100.00

Class	Commission (Percent)	Omission (Percent)	Commission (Pixels)	Omission (Pixels)
Saltmarsh [Gr	0.38	12.50	1/260	37/296
Sparse SAV [S	14.58	45.87	28/192	139/303
Sand [Yellow]	32.36	6.22	166/513	23/370
Dense SAV [Cy	2.02	7.62	6/297	24/315
Deep Water [B	10.70	0.00	40/374	0/334
Cloud [White]	0.21	3.93	1/466	19/484

Class	Prod. Acc. (Percent)	User Acc. (Percent)	Prod. Acc. (Pixels)	User Acc. (Pixels)
Saltmarsh [Gr	87.50	99.62	259/296	259/260
Sparse SAV [S	54.13	85.42	164/303	164/192
Sand [Yellow]	93.78	67.64	347/370	347/513
Dense SAV [Cy	92.38	97.98	291/315	291/297
Deep Water [B	100.00	89.30	334/334	334/374
Cloud [White]	96.07	99.79	465/484	465/466

Table 4.3 Error matrix result of PCA based ISODATA, 2006

Overall Accuracy = (1743/2107) 82.7243%
Kappa Coefficient = 0.7926

	Ground Truth (Pixels)				
Class	Saltmarsh	Sparse SAV	Sand	Dense SAV	Deep Water
Unclassified	0	0	0	0	0
Class 5	301	65	0	0	0
Class 6	0	230	0	0	0
Class 4	0	8	283	1	10
Class 1	0	0	0	310	4
Class 3	0	0	87	4	320
Class 15	0	0	0	0	0
Total	301	303	370	315	334

	Ground Truth (Pixels)	
Class	Cloud	Total
Unclassified	0	0
Class 5	0	366
Class 6	0	230
Class 4	185	487
Class 1	0	314
Class 3	0	411
Class 15	299	299
Total	484	2107

	Ground Truth (Percent)				
Class	Saltmarsh	Sparse SAV	Sand	Dense SAV	Deep Water
Unclassified	0.00	0.00	0.00	0.00	0.00
Class 5	100.00	21.45	0.00	0.00	0.00
Class 6	0.00	75.91	0.00	0.00	0.00
Class 4	0.00	2.64	76.49	0.32	2.99
Class 1	0.00	0.00	0.00	98.41	1.20
Class 3	0.00	0.00	23.51	1.27	95.81
Class 15	0.00	0.00	0.00	0.00	0.00
Total	100.00	100.00	100.00	100.00	100.00

	Ground Truth (Percent)	
Class	Cloud	Total
Unclassified	0.00	0.00
Class 5	0.00	17.37
Class 6	0.00	10.92
Class 4	38.22	23.11
Class 1	0.00	14.90
Class 3	0.00	19.51
Class 15	61.78	14.19
Total	100.00	100.00

Class	Commission (Percent)	Omission (Percent)	Commission (Pixels)	Omission (Pixels)
Class 5	17.76	0.00	65/366	0/301
Class 6	0.00	24.09	0/230	73/303
Class 4	41.89	23.51	204/487	87/370
Class 1	1.27	1.59	4/314	5/315
Class 3	22.14	4.19	91/411	14/334
Class 15	0.00	38.22	0/299	185/484

Class	Prod. Acc. (Percent)	User Acc. (Percent)	Prod. Acc. (Pixels)	User Acc. (Pixels)
Class 5	100.00	82.24	301/301	301/366
Class 6	75.91	100.00	230/303	230/230
Class 4	76.49	58.11	283/370	283/487
Class 1	98.41	98.73	310/315	310/314
Class 3	95.81	77.86	320/334	320/411
Class 15	61.78	100.00	299/484	299/299

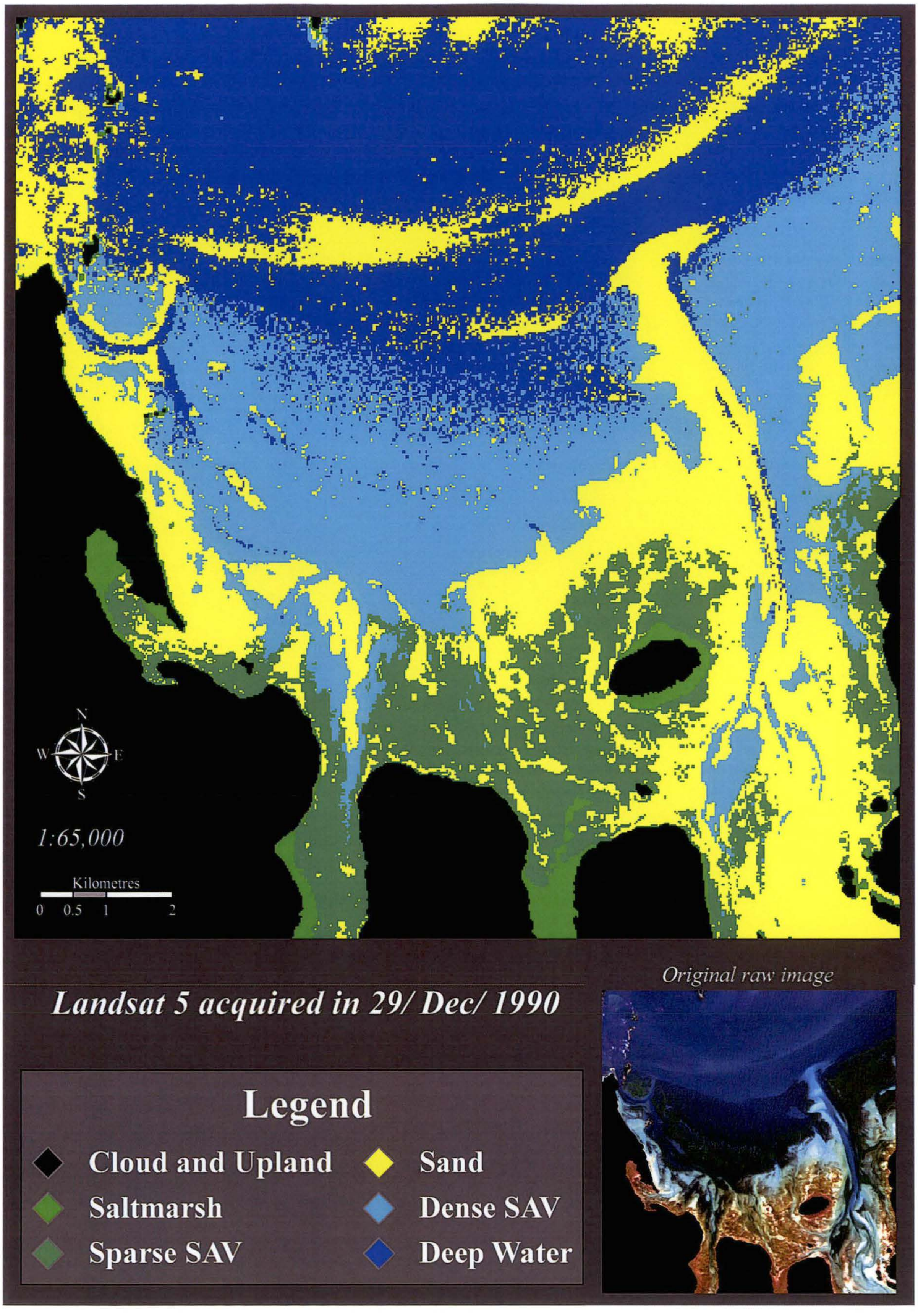

Figure 4.8 Thematic map of Landsat 5, 1990

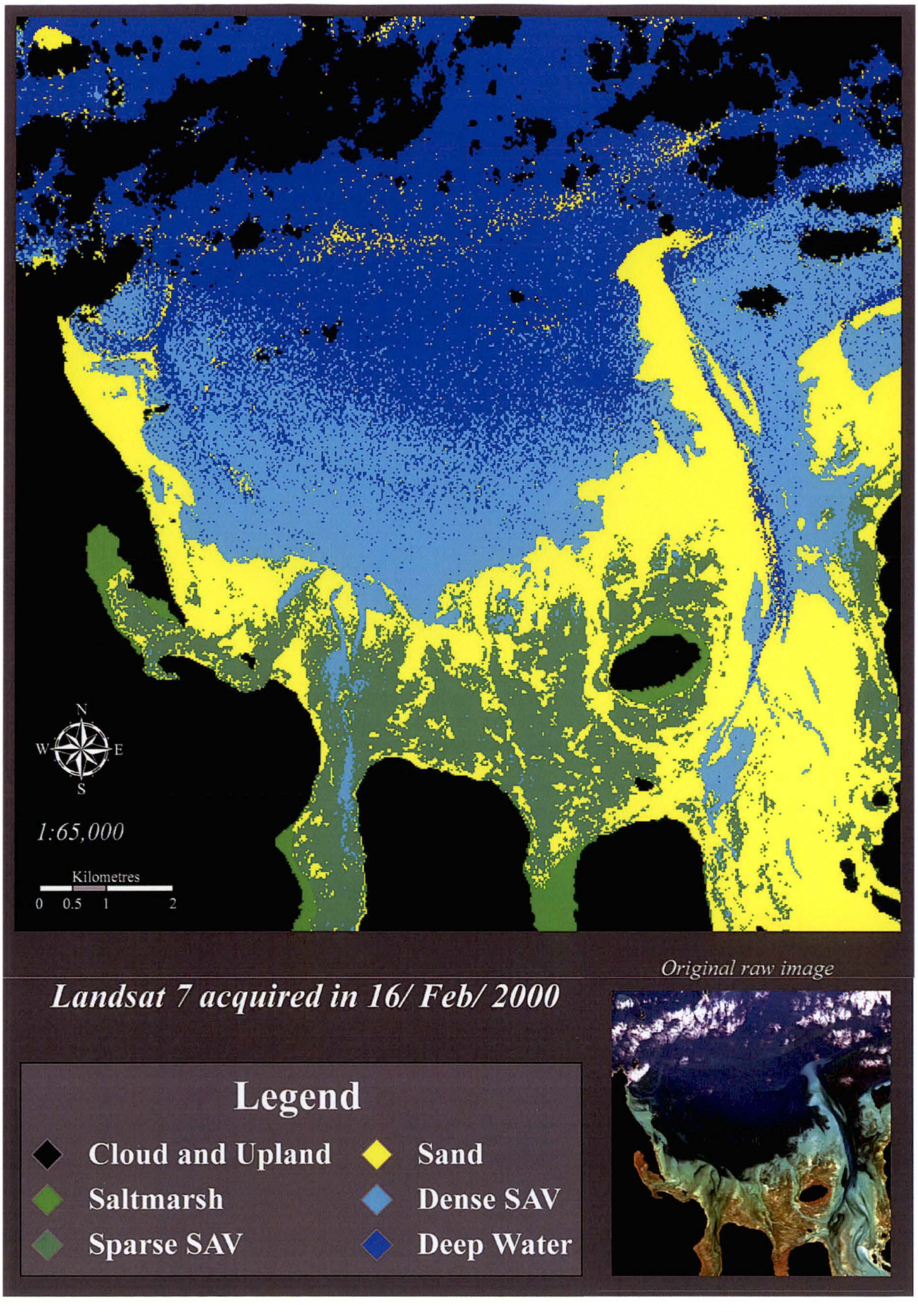

Figure 4.9 Thematic map of Landsat 7, 2000

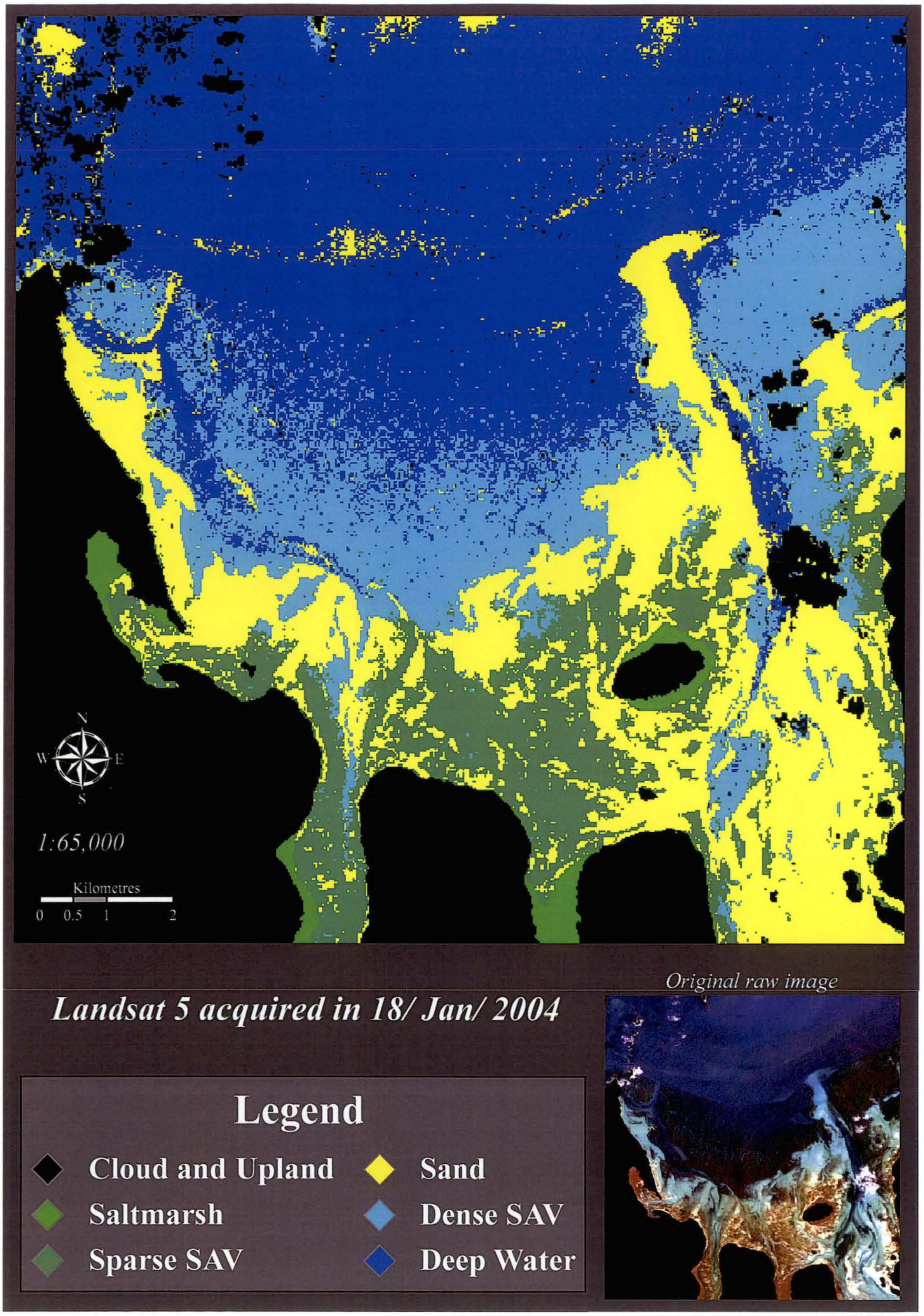

Figure 4.10 Thematic map of Landsat 5, 2004

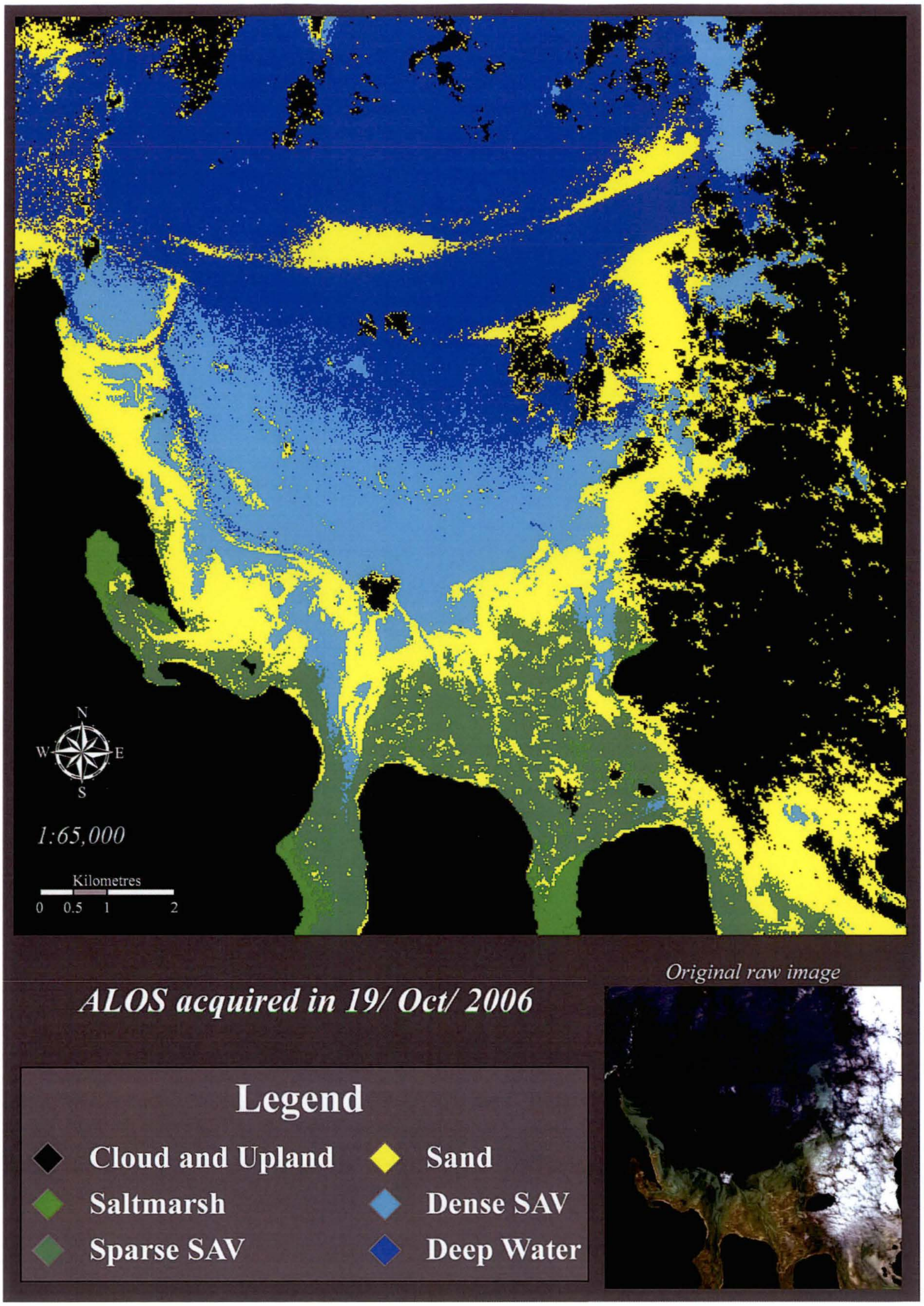

Figure 4.11 Thematic map of ALOS, 2006

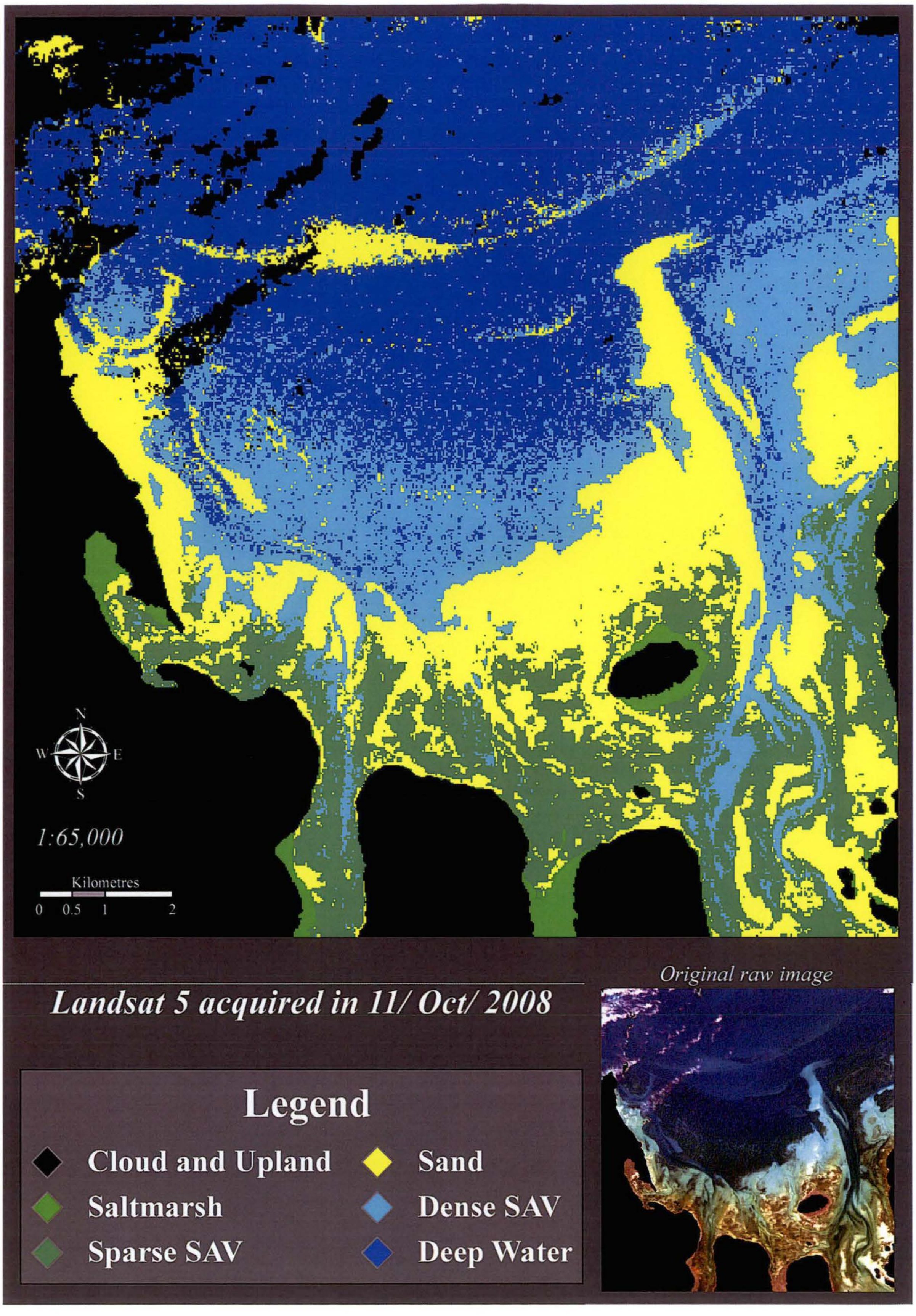

Figure 4.12 Thematic map of Landsat 5, 2008

Chapter 5 Case Study 2: Remote sensing change detection of submerged aquatic vegetation (SAV) at two spatial scales

5.1 Chapter overview

Chapter 5 introduces Case Study 2: change detection analysis based on the thematic maps generated from the Case Study 1. Aims of this case study is to detect '*from – to*' change between land cover features classified by Case Study 1. Two sub case study areas, encompassing; (1) whole Boullanger Bay, and (2) saltmarsh and sparse SAV boundaries were subject to the change detection analysis. Two different geographic scales were applied between the whole Boullanger Bay area and the saltmarsh and sparse SAV boundaries to obtain different spatial scale information on the distribution change in land cover classes. Whole Boullanger Bay area is firstly described. Area of saltmarsh and sparse SAV boundaries are then described.

5.2 Change in whole Boullanger Bay area

5.2.1 Introduction: Study area and data

Whole areal extent of Boullanger Bay area, which is same spatial subset as classification data was set out to identify '*from – to*' change in the synoptic distribution of the SAV meadows (Figure 5.1). Data employed for this case study were all derived from the Case Study 1. Tendency of the fluctuation in each land cover class classified in the Case Study 1 was identified at the scale of the large geographical area. Understanding the tendency of synoptic fluctuation was crucial for identifying natural dynamics of environmental features.

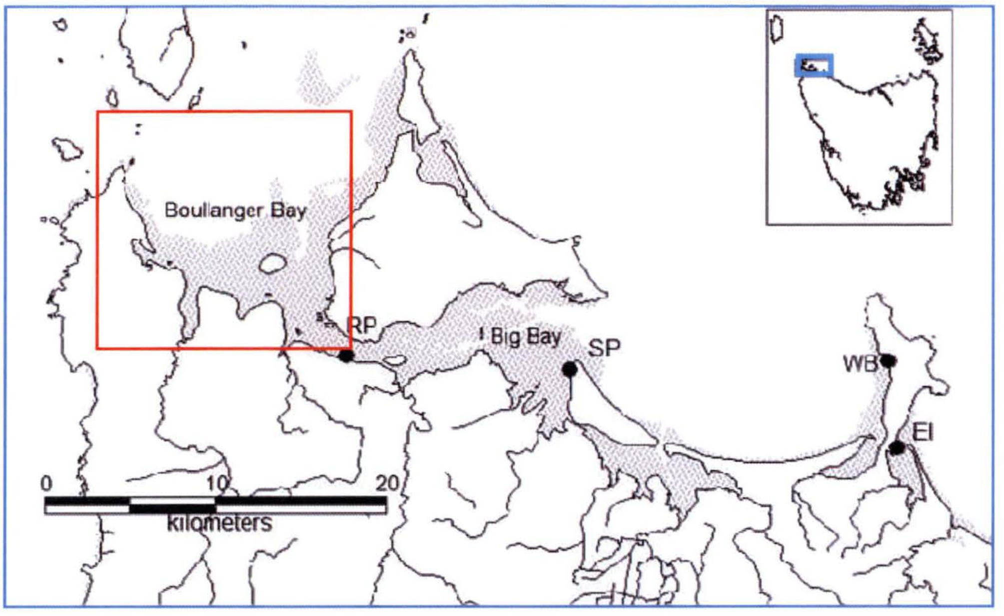

Figure 5.1 Study area of whole Boullanger Bay,

The red square depicts the case study site. Source: (Dunn 2000).

5.2.2 Change detection

In accordance with the results of accuracy assessment, ICA based MLC approach, which produced better accuracy through error matrix assessment was selected for change detection procedure of WFMI. Cloud class was removed from thematic map generated from the ICA based MLC approach after the classification to produce better visualisation of scene for the result of change detection. Additionally, equivalent subset size between the thematic maps of both Time 1 (T1) and Time 2 (T2) was set up to compose the T1 and T2 images into one file prior to change detection analysis. WFMI change detection approach was then performed using the composite file of T1 and T2 thematic map image. To detect change between the class features of interest over the 18 years, T1 image was assigned into the blue memory plane and time 2 (T2) image was assigned into the green and red memory planes. The potential area of change and non-change by difference with the indicative colors (Cyan and Red) on the output image were displayed. However, the result of the single usage of WFMI approach was not qualitative. '*From – to*' change in between the land cover classes were therefore identified by using '*Mask*' function with ENVI 4.6 to detect quantitative information. Individual data value of the each class from the thematic map were dealt to extract '*from – to*' change of each class. Additionally, change statistics, encompassing; pixel number of change, percentage of change and areal change, were calculated by ENVI 4.6 based on the result of the changed area.

5.3 *Change in Boundaries: Saltmarsh and Sparse SAV boundaries*

5.3.1 *Introduction: Study area and data*

Square subset area was used for identifying the correlation between SAV meadows and saltmarsh land cover classes at small geographic scale. Subset area located in the west part of the Boullanger Bay includes; location where contains the boundaries between saltmarsh and sparse SAV habitats (Figure 5.2 and 5.3). Classification results from the Case Study 1 were used for the change detection in this area as well. In order to facilitate the change detection at small scale, the spatial subset area size of approximately 1.5 km square was set up. The subset area was attempted to detect '*from – to*' change in the distribution between the two land cover classes in the boundary area for identifying the correlation. The boundary between saltmarsh and sparse SAV was clearly demonstrated based on the classification result over the years. This area was thus regarded as an appropriate area for identifying such a change at small geographic scale. Information on the biological relationship between the two-land cover classes associated with environmental change, such as sea level rise, were expected to be represented through the change in their habitats extent.

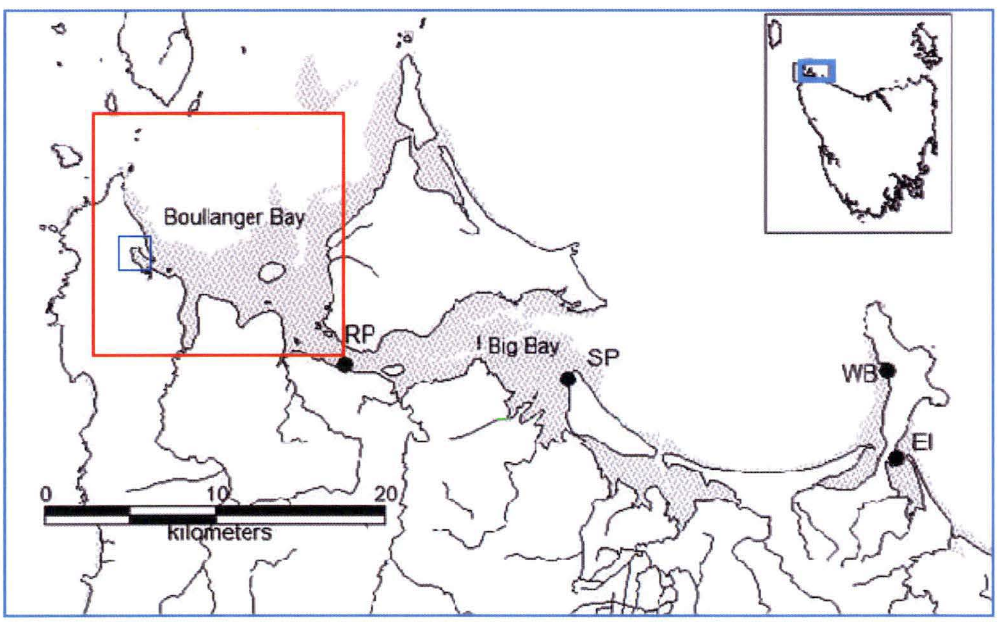

Figure 5.2 Saltmarsh and sparse SAV boundaries,

The Blue square depicts the case study site. Source: (Dunn 2000).

Figure 5.3 Boundary between *Sarcocornia quinqueflora* and *Zostera muelleri*

5.3.2 Change detection

Subset area was subject to the change detection procedure of WFMI approach same as change detection approach performed for the whole Boullanger Bay area. Additionally, change detection statistics for this area were also calculated for each land cover class over time series based on the change detection result.

5.4 Accuracy assessment

Accuracy assessment of change detection analysis was not performed in this case study due to the lack of validation data. The georectified data used for this case study were same as the Case Study 1.

5.5 Result

5.5.1 Change detection result: whole Boullanger Bay

In Case Study 1, image classification procedure was accomplished using ICA based MLC classification approach, which had higher accuracy. Total of 5 thematic maps produced by the approach were subject to a change detection procedure in Case Study 2. The "*WFMI*" change detection approach was performed using the 5 thematic map images. '*From – to*' changes in each land cover class between time 1 and time 2 images were identified based on the classification results (Figure 5.4, 5.5, 5.6, and 5.7). Change statistics of the '*from – to*' change in the whole Boullanger Bay area in terms of pixel counts, percentages and area over 18 years were presented in Appendix 1,2,3 and 4.

Areal change in 4 land cover classes, encompassing; sparse and dense SAV, saltmarsh, and sand cover occurred across the whole Boullanger Bay area during 1990 to 2008 (Figure 5.8). Land cover classes except for saltmarsh has represented similar tendency of decline in their extent throughout the period. Less area and percentage change in saltmarsh cover was represented compared to the other land cover classes in the area during the same period. Continual decline in the sparse and dense SAV distribution occurred between 1990 and 2006; however, increase in both land cover classes occurred from 2006 to 2008. Compared to the dense SAV, sparse SAV cover has continued to decrease with slower rate. While saltmarsh represented less change compared to other classes, repeat increase and decline was happened to this class during the period 1990 to 2008. The greatest decline in saltmarsh distribution occurred between 2004 and 2006. Additionally, the greatest increase in their distribution occurred between 2006 and 2008. Apparent major losses in all classes for the whole of Boullanger Bay occurred in 2006. That was assumed due to high cloud coverage in the reference image. Areas of changes in the sparse SAV distribution have not been uniformly associated with expansion of sand habitats across the whole Boullanger Bay over the period. On the other hand, changes in dense SAV distribution have been mostly occurred at the deeper water area across the dense SAV and sand edge over the period. These changes appear to be due to image classification issues, particularly a lack of a depth correction. Distributions of saltmarshes have been constant over the time series between 1990 and 2008.

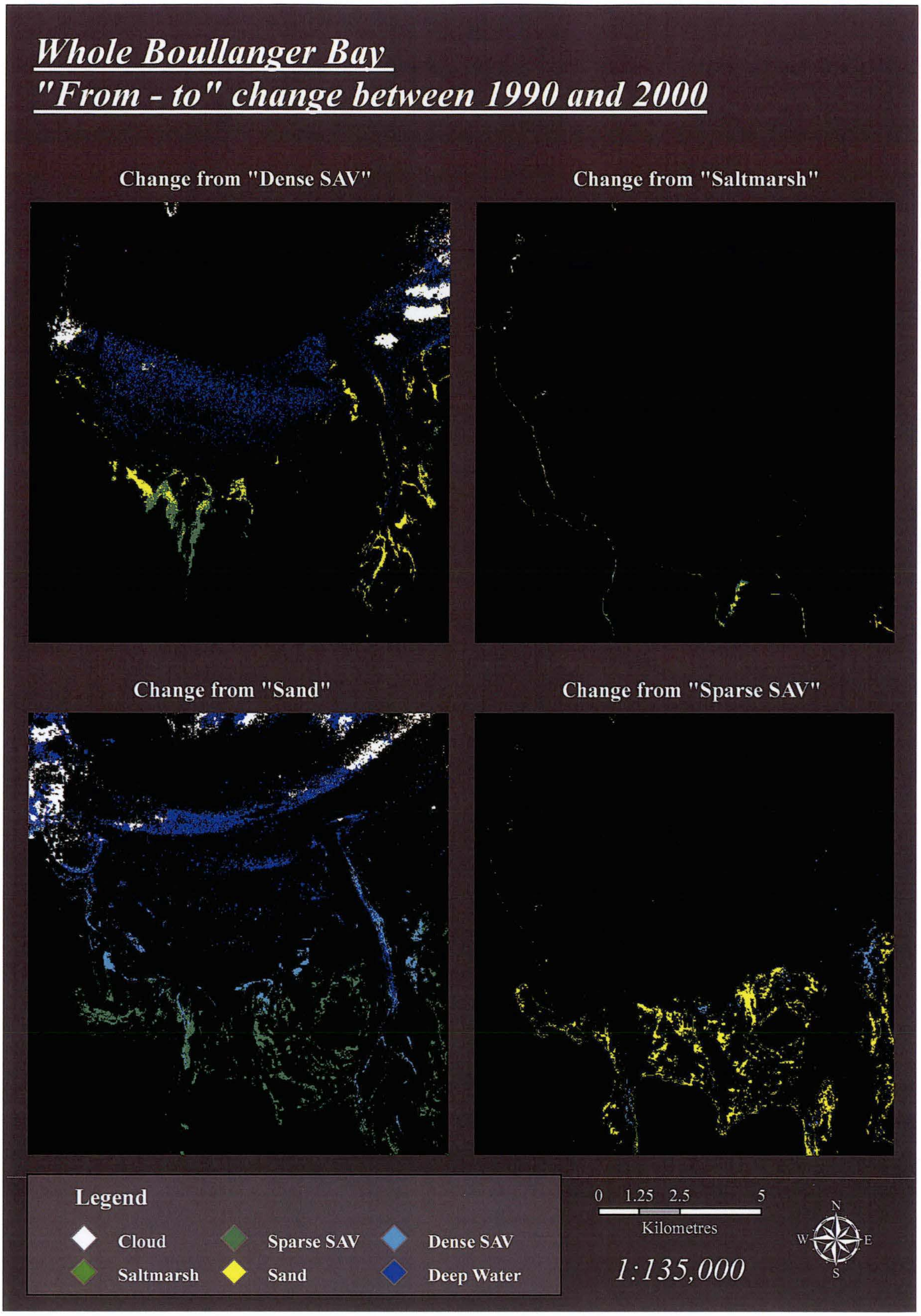

Figure 5.4 Whole Boullanger Bay "from – to" change between 1990 and 2000

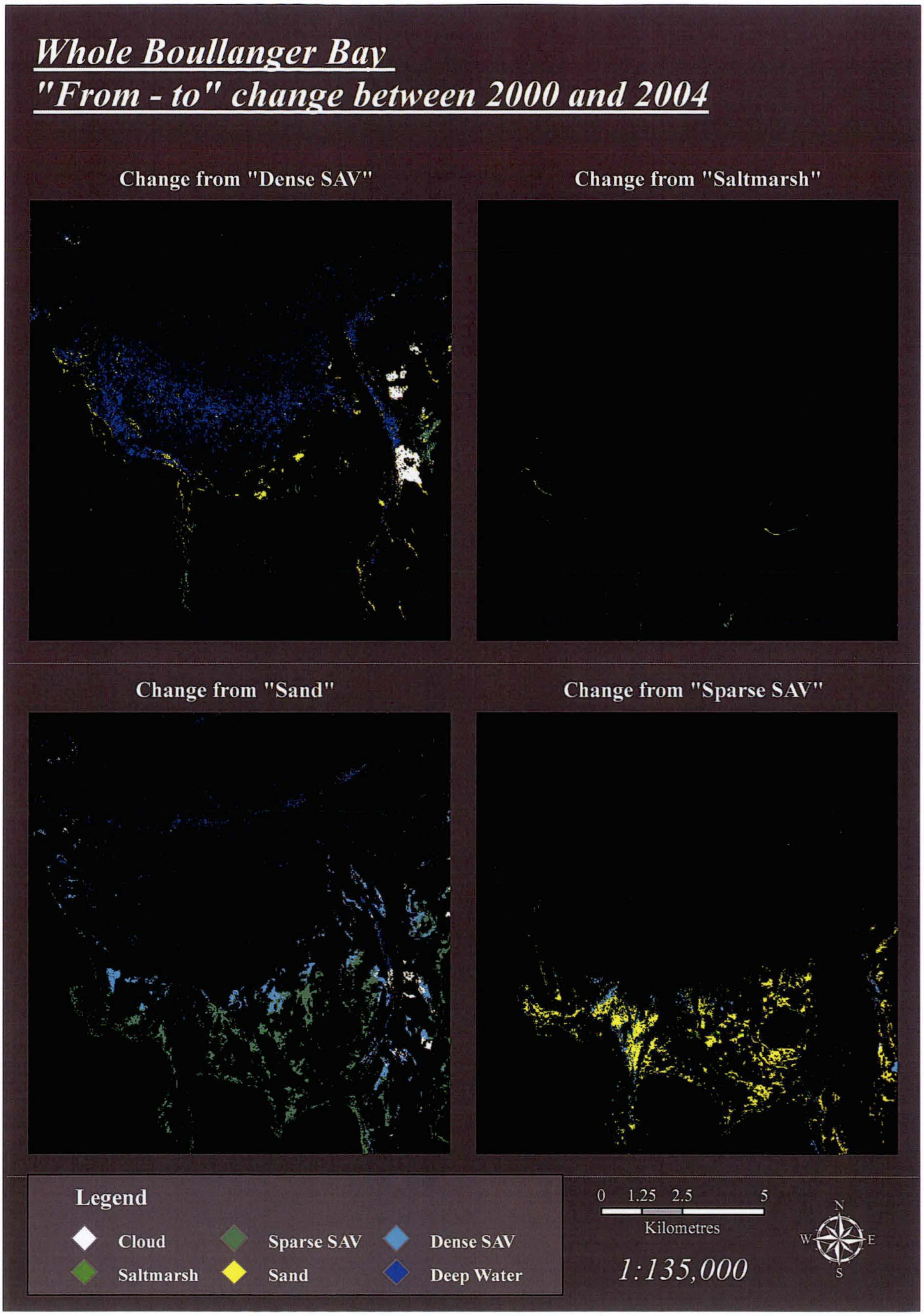

Figure 5.5 Whole Boullanger Bay "from – to" change between 2000 and 2004

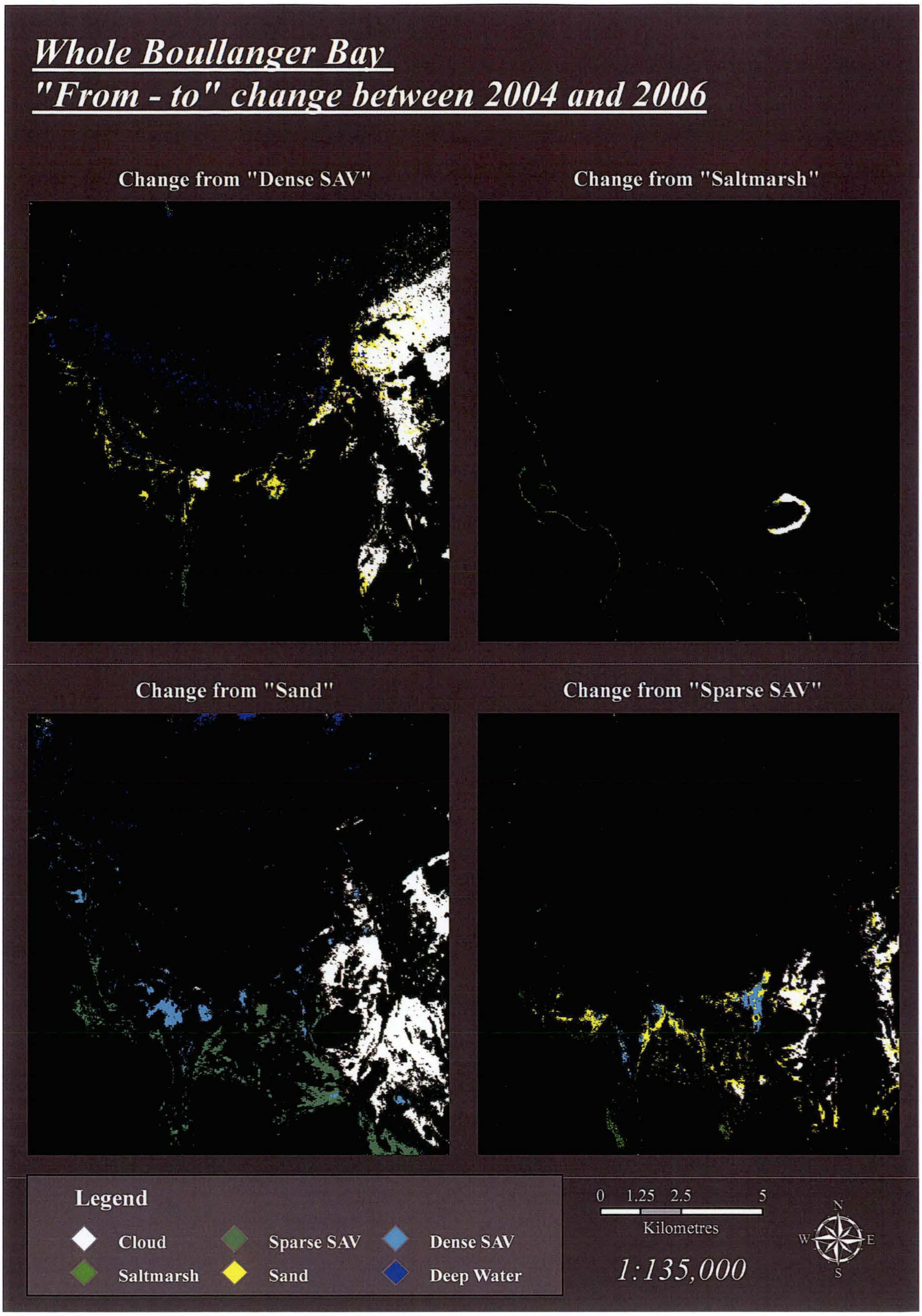

Figure 5.6 Whole Boullanger Bay "from – to" change between 2004 and 2006

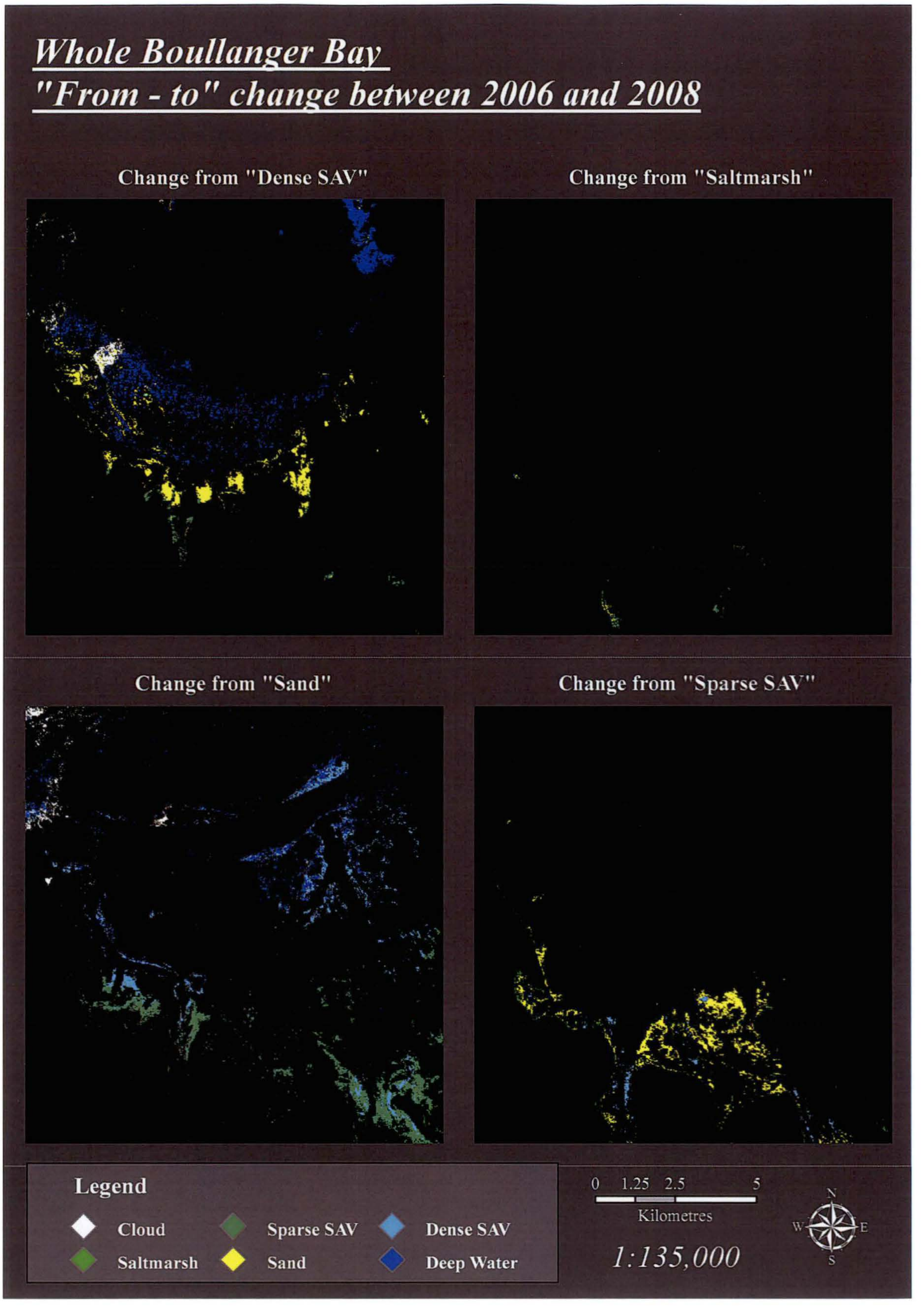

Figure 5.7 Whole Boullanger Bay "from – to" change between 2006 and 2008

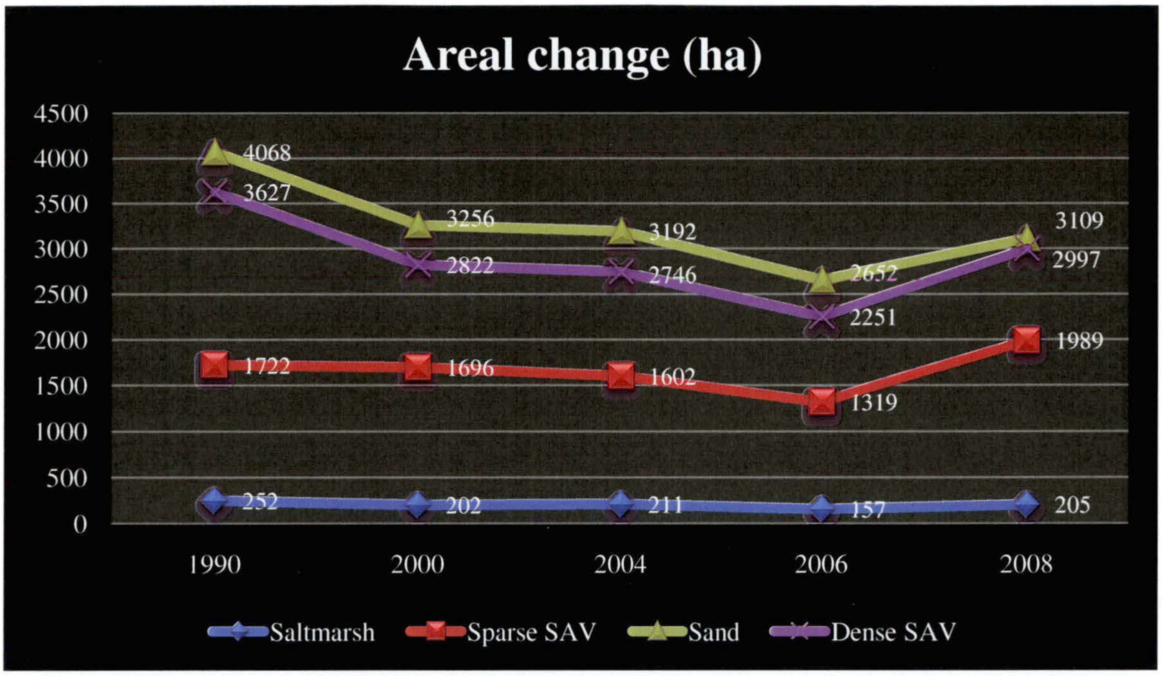

Figure 5.8 Areal changes in each class in the Whole Boullanger Bay between 1990 and 2008

5.5.2 Change detection result: Saltmarsh/ Sparse SAV boundaries

"*WFMI*" change detection approach was performed using the 5 thematic map images across the boundaries between saltmarsh and sparse SAV, mainly consists of intertidal seagrass community. '*From – to*' change between saltmarsh and sparse SAV was identified based on the classification results. Change statistics of the '*from – to*' change across this area in terms of pixel counts, percentages and area were presented in Appendix 5,6,7 and 8.

Inconsistent increase and decrease in saltmarsh cover were observed in this area at each subset of time 1 and time 2 images between 1990 and 2008. In particular, the changes in their distribution occurred mainly across the boundary area between other land cover classes, encompassing; sparse SAV and sand (Figure 5.9 and 5.10). However, small areal changes that was two hectares differences between minimum (38 ha) and maximum (40 ha) in saltmarsh cover occurred on this area over the period of time (Figure 5.11). The change rate and the areas were not uniform over the boundary. Classification results of saltmarsh area represented the increase in their extent between 1990 and 2000. Since 2000, the distribution of saltmarsh has decreased gradually. On the other hand, the extent of sparse SAV and sand has repeated the increase and decrease in their extent between 1990 and 2008 period. Unlike saltmarsh, large areal changes in sparse SAV cover was represented on this area. Additionally, inconsistent change rate of sparse SAV was also observed. Relatively consistent correlation between sparse SAV and other two land covers in terms of opposite change rate, however, was found across the area except for 2008, which represented significant increase in sand cover. In other words, the rate of change in sparse SAV extent has demonstrated consistently opposite to the rate of change in saltmarsh and sand extent throughout the monitoring period. In particular, this consistent correlation has been found between saltmarsh and sparse SAV extent. While repetition of increase and decrease in the extent of three land covers were defined at each subset of change detection transection, saltmarsh has represented relative decline at long term point of view from 1990 to 2008. Additionally, as for the stability in saltmarsh and sparse SAV extent, the north and south part of the area has represented during the period.

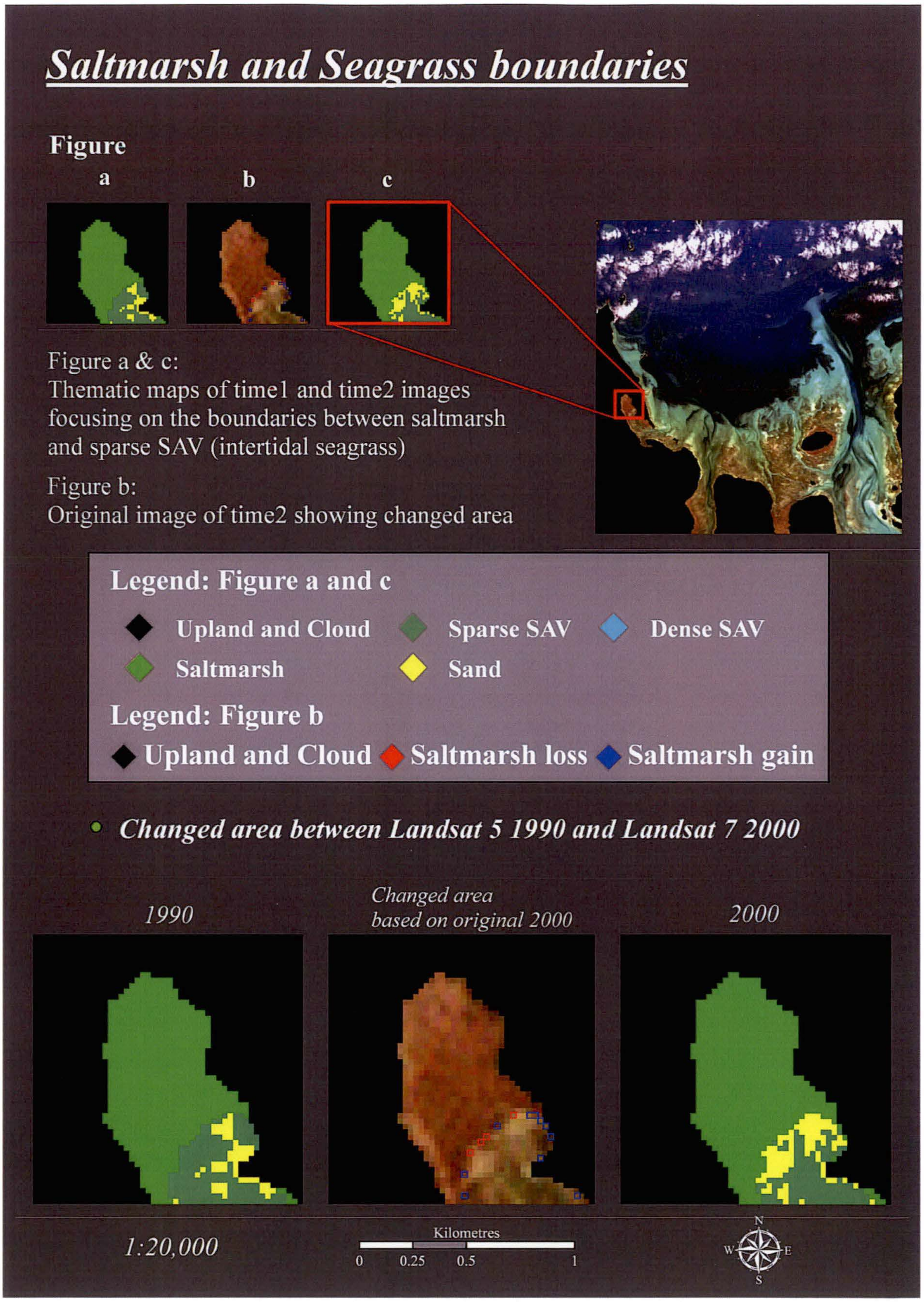

Figure 5.9 Saltmarsh and SAV boundary change between 1990 and 2000

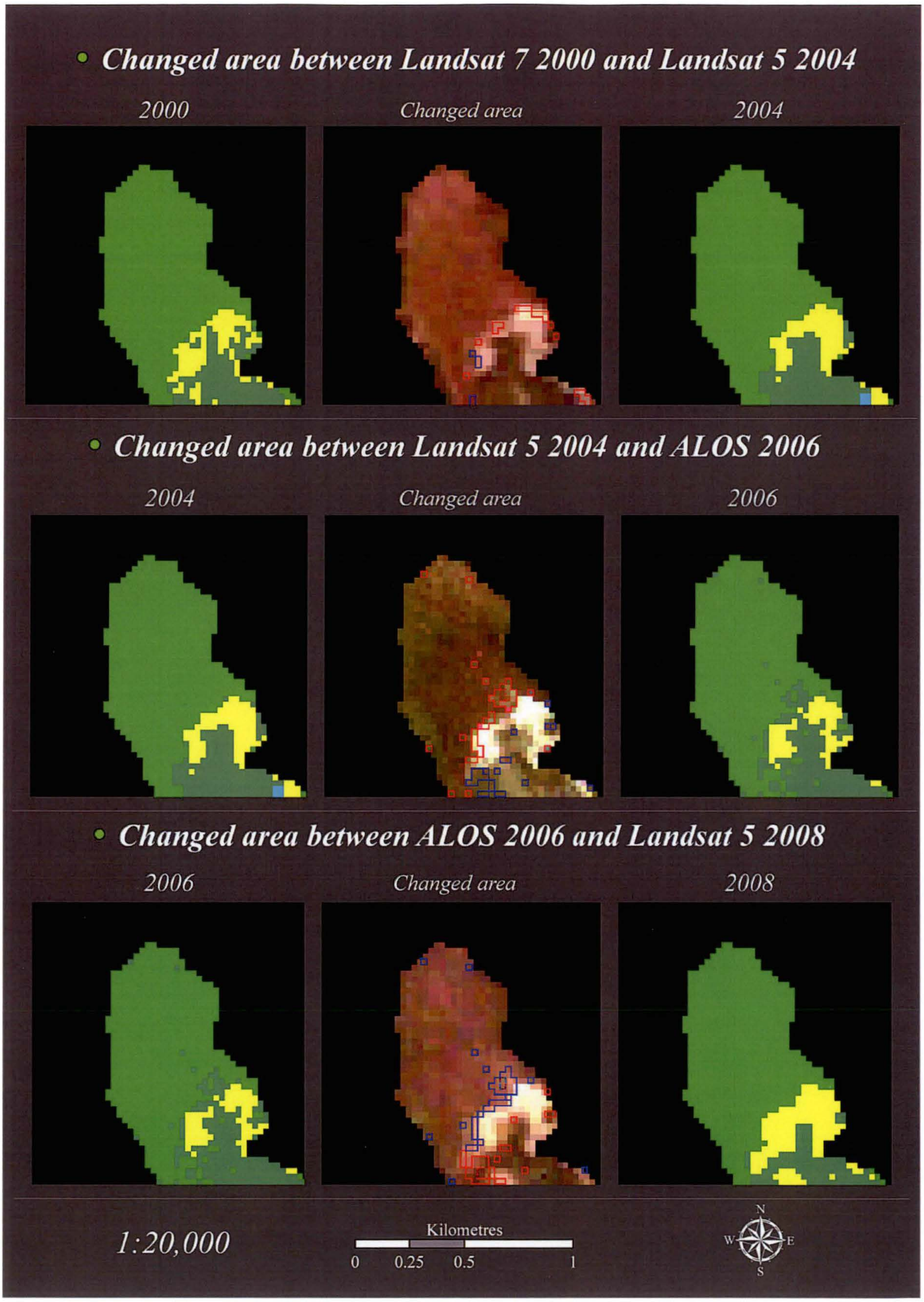

Figure 5.10 Saltmarsh and SAV boundary change between:
(1) 2000 and 2004, (2) 2004 and 2006, and (3) 2006 and 2008

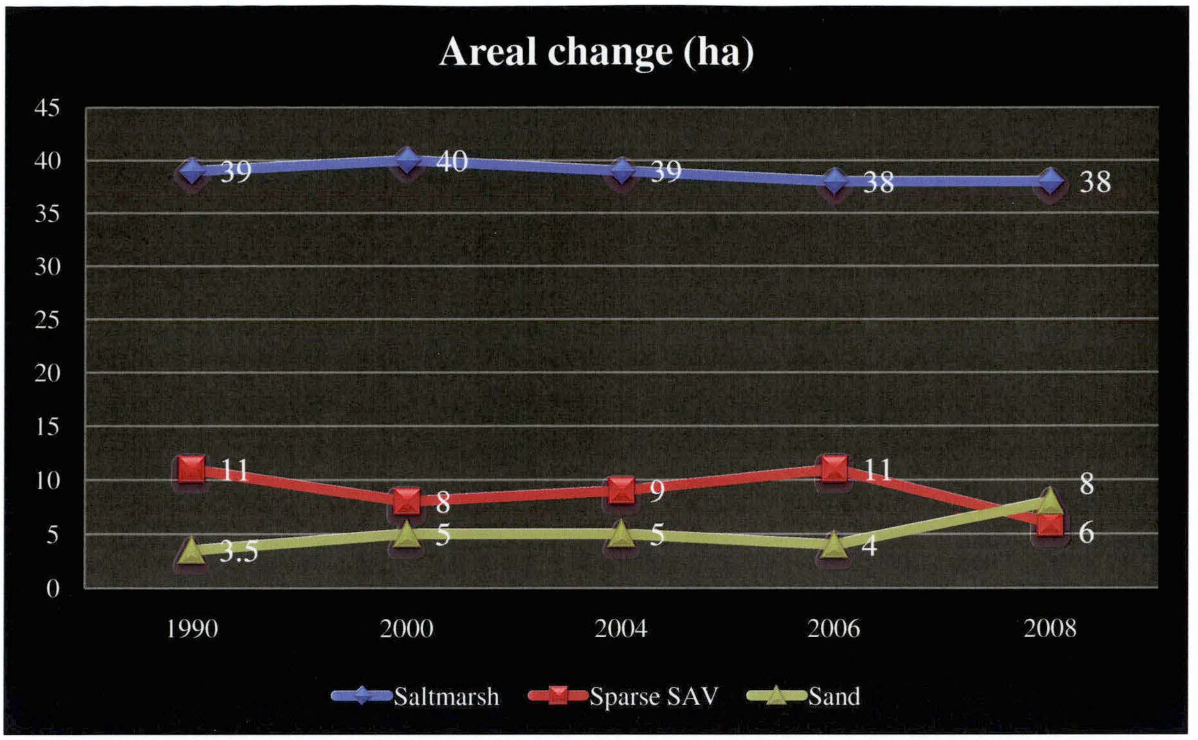

Figure 5.11 Areal changes in each class in saltmarsh and SAV border area between 1990 and 2008

Chapter 6 Case Study 3: Time series change detection in subtidal and intertidal areas via MCI and WFMI

6.1 Chapter overview

Chapter 6 introduces the Case Study 3: Change detection analysis for two sub case study areas, encompassing; (1) Welcome Inlet, and (2) subtidal open water area. Case Study 3 sets out to detect the change in the distribution of SAV communities at a local geographic scale. Change detection in the distribution of intertidal SAV was performed in the area of the Welcome Inlet. MCI change detection approach was applied for this sub case study area. Subtidal open water area was subject to the change detection in the distribution of subtidal SAV, such as subtidal seagrass. WFMI change detection approach was performed for this sub case study area. Different biological characteristics are in the context of the different natural dynamics in the habitats distribution of intertidal and subtidal seagrasses. Set up of two sub case study areas were thus crucial to identify the change derived from such a different natural dynamics. The context of mapping and monitoring scheme in Welcome Inlet area was firstly introduced. Then, subtidal open water area was described.

6.2 Welcome Inlet: Intertidal SAV habitat change

6.2.1 Introduction: Study area and data

Welcome river inlet is located in the south of the Boullanger Bay (Figure 6.1). Intertidal area of this estuarine contains large intertidal seagrass and macro algae meadows. Information on the SAV distribution, especially seagrass community at local area is now regarded as significant information for environment management system. Yet, mapping and monitoring scheme at single spatial or temporal scale results in the insufficient information on the natural dynamics of seagrass community. In this regard, it has been identified that to map and monitor the SAV distribution of not only present location but also potential recolonisation areas are crucial (Short *et al.* 2001). This is particularly the case for SAV species which have high recolonisation capability and numerous threats to them. Additionally, the ability of remote sensing techniques varies depending on the correlation between proposed object and the spatial scale of study area. In particular, ICA is assumed as the highly spatial scale dependent technique as the number of features in the image influences on the analysis. Investigation of the ICA technique effectiveness is then crucial for future research into SAV at same area. In order to detect such small areal information on SAV distribution change and to identify the effectiveness of remote sensing computational techniques, the study region needed to be focused. The aim of the Case Study 3 was to detect the small areal change in the distribution of intertidal SAV meadows and to identify the capability of ICA technique for this spatial scale of study area. Hypothesis of this case study is the detection of spatial and temporal change in intertidal SAV meadows. Landsat TM and ETM+ imagery from 1990 to 2008 were employed for this case study. For image selection, the anniversary date of the acquired image was prioritised, rather than the tide stage. It was assumed that the tide stage variation did not have such large effect on this case study as different temporal image. This is because the proposed object, the intertidal seagrass meadows were located in the intertidal area where is very shallow water area where even longer wavelength of the sun radiation can often reach the substratum. Total of 10 images with reliable quality were selected to meet the annual term difference as much as possible (Table 6.1). A simple method for comparing every date with every other date was also devised in the form of a image visualisation comparison matrix (IVCM) similar to a multivariate statistical tool, the scatter plot matrix (Mount, 2007).

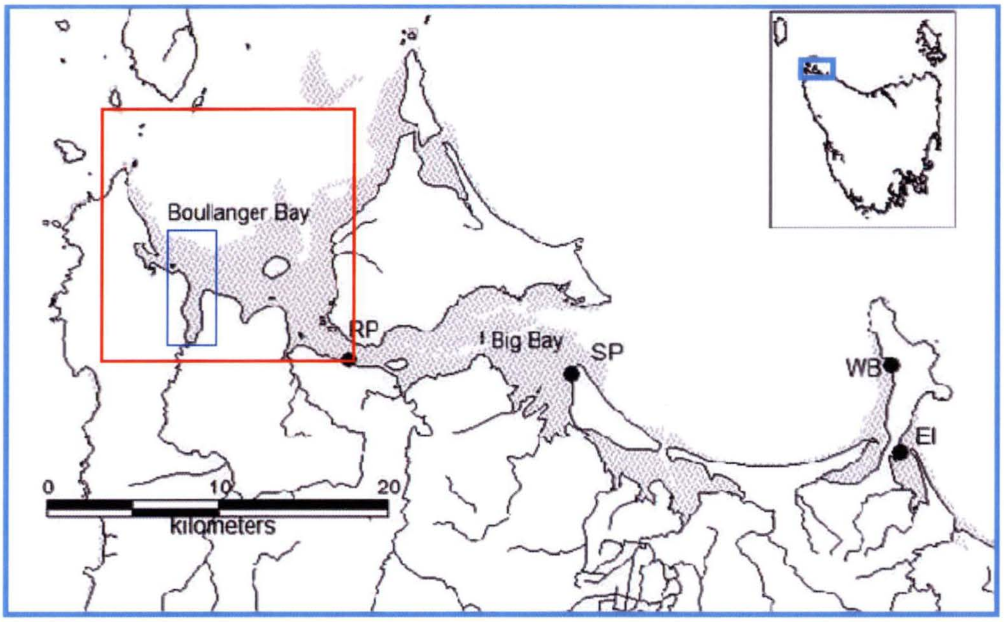

Figure 6.1 Welcome Inlet study area,

The Blue rectangle depicts the case study site. Source: (Dunn 2000).

Table 6.1 Satellite data for Welcome Inlet case study, '--'mark represents no data

Image date	Sensor	Processing level	Tide	Cloud cover (%)	Water turbidity	Other information
29/12/1990	Landsat 5 TM	L1G	High	--	Low	Image time at: -- Sun elevatino at: 50 Sun azimuth at: 79
16/02/2000	Landsat 7 ETM+	L1G	High	--	Low	Image time at: -- Sun elevatino at -- Sun azimuth at --
9/05/2001	Landsat 7 ETM+	L1G	Low	25	Low	Image time at 23:54:14 Sun elevatino at: 23 Sun azimuth at 37
26/04/2002	Landsat 7 ETM+	L1T	Low	12	Low	Image time at: 23:53:03 Sun elevatino at: 26 Sun azimuth at: 39
15/05/2003	Landsat 7 ETM+	L1T	Low	21	Low	Image time at: 23:52:57 Sun elevatino at: 21 Sun azimuth at 36
10/06/2004	Landsat 5 TM	L1G	Low	30	High	Image time at 23:45:34 Sun elevatino at 17 Sun azimuth at 36
4/11/2005	Landsat 5 TM	L1T	Low	0	High	Image time at: 23:52:22 Sun elevatino at: 52 Sun azimuth at: 58
22/10/2006	Landsat 5 TM	L1T	Low	0	Low	Image time at 23:58:27 Sun elevatino at 49 Sun azimuth at 52
7/09/2007	Landsat 5 TM	L1T	High	0	Low	Image time at: 23:57:24 Sun elevatino at: 33 Sun azimuth at 43
11/10/2008	Landsat 5 TM	L1T	High	4	Low	Image time at: 23:48:27 Sun elevatino at 45 Sun azimuth at: 52

6.2.2 Image pre-processing

As case study area 1, each image of L1G data was geometrically corrected (image to image registration) based on the image of Landsat 5, acquired in 1990. Less than half RMS errors, were obtained for each registered image. Each scene of pixel size was resampled from 30m to 25m to make corresponding pixel size for all, using "*nearest neighbour*" resampling technique. 25m were set up for this case study area due to the concern over the miss estimation of resampled pixel values from large scale resampling like from 30m to 10m, although nearest neighbour resampling maintains the original value of the original pixels for resampled image. Only the images that have no cloud and cloud shadow in the area were selected; thus, cloud removal from the images were not performed. Radiometric normalisation using PIFs were performed to make radiometric consistency over the scene based on the reference image of Landsat 5, 1990. Since this case study also employed ICA based approach, data dimensional expansion was required prior to the image classification and change detection procedures.

This case study was also subject to band dimensional expansion for ICA approach. Dimensionality of original spectral bands derived from the both T1 and T2 images was expanded to meet the number and spectral characteristics of proposed objects, including intertidal seagrass meadows. Total of 15 additional bands, encompassing; (1) B1*B1, (2) B1*B2, (3) B1*B3, (4) B2*B2, (5) B3*B3, (6) B3*B2*B1, (7) (B3*B2*B1)/ 3, (8) B1 - B2, (9) B1 - B3, (10) B2 - B3, (11) B1 / B2, (12) B1 / B3, (13) B2 / B3, (14) Normalised Green and Blue Index (NGBI), (15) NDVI, were generated by '*Band math*' with ENVI 4.6 image software. Composite image of T1 and T2, consists of original and additional bands were combined into one file for ICA based MCI approach for change detection analysis.

6.2.3 Change detection

Each pre-processed composite image was subject to the change detection stages. ICA based MCI approach was performed for change detection analysis procedures for this case study area. MCI approaches needed a composite image of T1 and T2, yet consists of original bands with additional bands generated from the data dimensional expansion for ICA application. ICA was performed to extract change area from the multiple date composite images. Image interpretation was performed subjectively through the optical comparison between two original images and the generated independent components to identify the change in the distribution of intertidal SAV habitats. The change areas where had the increase and decrease of SAV meadows, were extracted. These extracted features of raster data was converted to vector data to overlay on the original image of T2 for better visualisation in the resultant images.

6.2.4 GIS application

ArcGIS software was employed to extract additional information from the resultant data of vector layers in this project. Vector layers produced from the change detection procedure was exported from ENVI 4.6 to ArcGIS 9.3. Areas of single time change over 18 years were calculated by SQL query function of ArcGIS based on the attribute of the resultant vector layers. Additionally, the areas representing the total counts of the times of change were also calculated. '*Kernel density*' function of ArcGIS was performed to produce the area density representing the single times changed areas and stable land cover areas between 1990 and 2008. In order to identify the natural dynamics of SAV population in the Welcome Inlet, annual growth of SAV was also calculated.

6.2.5 Accuracy assessment

Accuracy assessment of change detection was not attempted in this case study due to the lack of validation data. The rectified data used for this case study was same as the Case Study 1.

6.3 *Subtidal open water area SAV habitat change*

6.3.1 *Introduction: Study area and data*

Open water near shore area is located between the Robbins Island and Woolnorth point (Figure 6.2). Extensive subtidal seagrass meadows of dominant *P. australis* range over the open water area. Recolonisation ability of such a highly stabilised seagrass varies depending on the environmental condition of the surrounding area. Therefore, information on the recolonisation rate is crucial for seagrass conservation and management. There is the patchy configuration of uncolonised areas, which is about 25m radius in the beds of *P. australis,* in the area. These uncolonised areas in meadows were identified as an ideal target to investigate their recolonisation rate and stability of their meadows over different temporal scale. Meehan and West (2000) conducted the research into the recovery rates of *P. australis* through mapping circular uncolonised areas. Similarly, the aim of this case study was to detect any changes or non-change in the subtidal seagrass meadows for identification of their recolonisation ability. Hypothesis of this case study is non-change in the patchy uncolonised area based on the high stability of the subtidal seagrass specie in their habitats terms. A series of Landsat TM and ETM+ images over the 18 years was employed to produce the information. Since this case study attempted to identify the change in the subtidal seagrass meadows based on the geometry of the un-colonised area, important concern was clear appearance of the uncolonised area for image selection. It is noteworthy that the dominant subtidal seagrass, *P. australis* has few seasonal phenotypic changes. Image selection of this sub-study area simply needed to avoid high cloudy coverage. Therefore, water clarity, cloud coverage, and noise coverage over the study area in the acquired image associated with the similar anniversary date were mainly concerned for image selection. However, identical tide levels and regularly annual term basis were also concerned for image selection to arrange the appropriate combination of acquired images. Then, the total of 11 images with reliable quality was eventually selected for image analysis in this case study (Table 6.2).

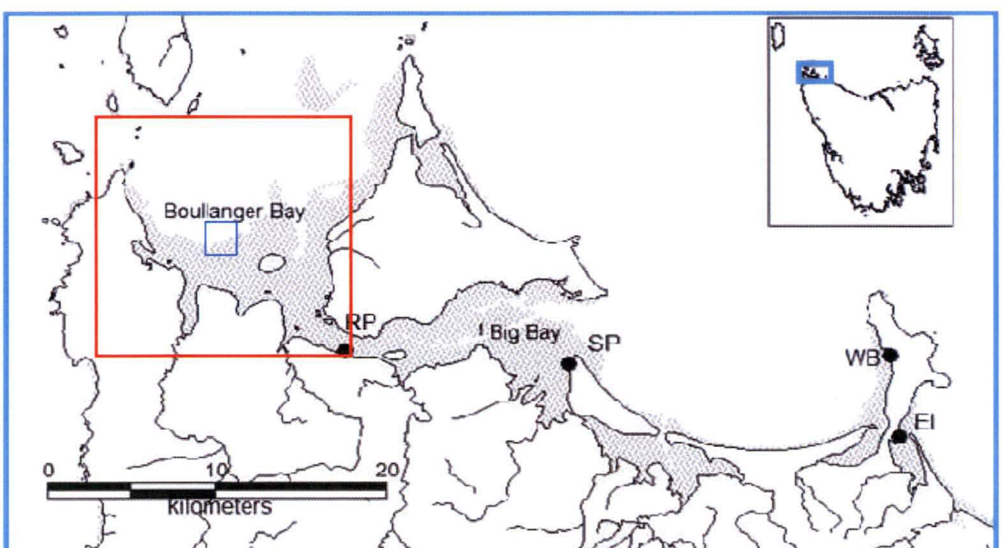

Figure 6.2 Subtidal open water study area,

The Blue rectangle depicts the case study site. Source: (Dunn 2000).

Table 6.2 Satellite data for subtidal open water case study, '--'mark represents no data

Image date	Sensor	Processing level	Tide	Cloud cover	Water turbidity	Other information
29/12/1990	Landsat 5 TM	L1G	High	--	Low	Image time at -- Sun elevatıno at 50 Sun azımuth at 79
28/11/1999	Landsat 7 ETM+	L1T	Low	0	Low	Image tıme at: 23:57:02 Sun elevatıno at: 56 Sun azimuth at: 65
16/02/2000	Landsat 7 ETM+	L1G	Hıgh	--	Low	Image time at: -- Sun elevatıno at: -- Sun azimuth at: --
28/07/2001	Landsat 7 ETM+	L1T	Low	17	Low	Image time at. 23:53.26 Sun elevatıno at: 20 Sun azımuth at: 38
5/02/2002	Landsat 7 ETM+	L1T	Low	40	Low	Image time at 23 53:06 Sun elevatino at: 47 Sun azımuth at 66
23/01/2003	Landsat 7 ETM+	L1T	Low	4	Low	Image tıme at· 23:52 45 Sun elevatino at: 50 Sun azimuth at: 70
2/01/2004	Landsat 5 TM	L1G	Low	40	Low	Image time at. 23 43:00 Sun elevatino at: 51 Sun azimuth at: 75
5/02/2005	Landsat 5 TM	L1G	High	--	Low	Image time at: 23:50:39 Sun elevatino at: 46 Sun azimuth at 67
22/10/2006	Landsat 5 TM	L1T	Low	0	Low	Image time at: 23:58:27 Sun elevatıno at. 49 Sun azimuth at 52
7/09/2007	Landsat 5 TM	L1T	High	0	Low	Image time at: 23:57:24 Sun elevatino at: 33 Sun azimuth at· 43
11/10/2008	Landsat 5 TM	L1T	High	4	Low	Image tıme at: 23:48:27 Sun elevatino at: 45 Sun azımuth at: 52

6.3.2 Image pre-processing

Each original images of L1G data were geometrically corrected (image to image registration) based on the image of Landsat 5, 1990. Less than half RMS errors were obtained for each image registered. Original pixel size of 30m was resampled to 10m pixel size for this case study so that discernible change was easily to be detected in optical identification. For the better visualisation of image, '*cubic convolution*' resampling approach was performed. Finer pixel size was assumed more suitable for the size of the patchy un-colonized area that was around 25m radius. The assumption of the pixel size was involved in the two reasons; the characteristics of the subtidal seagrass colonisation and optical based change detection. Generally, recolonisation rate of the subtidal seagrass species were low, which in turn, the change in the distribution of such species were assumed very small areal scale. Additionally, this case study underwent change detection method based on visual interpretation; thus, 10m pixel size was assumed more suitable than coarser pixel size to detect small areal change by optical interpretation through the results produced from the change detection procedure. Same subset size was set up for all resampled image for subsequent WFMI procedure. Composite image consists of time 1 and time 2 images were produced for change detection analysis.

6.3.3 Change detection

Change detection procedure of WFMI approach was performed in this case study. Image classification for this case study area was not performed due to the concern over the miss-estimated brightness values generated from the "*cubic convolution*" approach that cannot maintain the original brightness values. Visual based change detection was thus performed to detect change in the subtidal seagrass meadows. Although numerous change detection techniques have been developed, the human interpretation based on visual evidence still plays an important role for change detection (Mount 2007). WFMI approach underwent with ENVI 4.6 to provide the trend of seagrass distribution and information on whether there are anomalies in the time series. Visible green band of Landsat TM and ETM from each T1 and T2 image were allocated to the write function memory banks. This is part of the reason that the light attenuation of longer wave length than visible green and the higher spectral response of visible green from submerged plant community. As Case Study 1, visible green band from T1 image was inserted into the blue memory plane and the band from T2 image was inserted into the green and red memory planes. The potential area of change and non-change by difference with the indicative colours (Cyan and Red) on the output image were going to be displayed as the results.

6.3.4 Accuracy assessment

Accuracy assessment of change detection was also not attempted in this case study due to the lack of validation data. The rectified data used for this case study was also same as the Case Study 1.

6.4 *Result*

6.4.1 *Welcome Inlet intertidal SAV habitat change: MCI approach*

10 reference images over 18 years were subject to change detection procedure (Figure 6.3). ICA based MCI approach was performed to detect change in the distribution of SAV meadows, mainly consists of intertidal seagrasses over the Welcome Inlet. 9 subsets composed of the two different temporal reference images and resultant image were produced by the change detection method (Figure 6.4, 6.5, 6.6, 6.7 and 6.8). The presented results of mapping and monitoring SAV meadows in the Welcome Inlet has demonstrated that either increases or decreases in their population density occurred over the 18 year period from 1990 to 2008 (Figure 6.9).

Inconsistent change in the distribution of SAV was found across the Welcome Inlet area over the 18 year period through the each set of change detection results. However, a couple of area, the centre part and the north-west part of the Welcome Inlet represented the high stability of SAV colonisation. Inconsistent change rate of the gain and loss of SAV meadows was also observed. Gain and loss of SAV meadows varied dependent upon the places on the area and the observed year. Significant changes in SAV cover occurred during the subset period of '1990 – 2000', '2000 – 2001', '2001 – 2002', '2005 – 2006' and '2006 – 2007' (Figure 6.12). Maximum change of both increase and decrease in SAV cover was observed during the period 2001 to 2002 in this area.

Area observed single change was demonstrated by GIS application based on the result of MCI approach. Additionally, derivative results, encompassing: (1) stable area of 2008; (2) area of total change count; (3) density of single change area; and (4) density of stable area 2008 were produced through GIS application (Figure 6.10, 6.11). While the total of single change areas occurred broadly across the Welcome Inlet area, single change areas of individual year were relatively clustered. Additionally, many single changes were observed relatively around stable area. Stable area represented large coverage of SAV meadows. This was assumed as a part because of misclassification in 2008 image. As for the total count of change, change area with higher count mainly occurred in the north part of the image where is next to the deep water stream and closer to the open water area in the Welcome Inlet.

The Image Visualisation Comparison Matrix (IVCM) is presented in Appendix 10. It enables the user to compare processed images from any date with a processed image from any other date. This is a powerful method for finding patterns through time and identifying anomalous years.

Figure 6.3 Original images, red rectangle represents the areas of SAV meadows with high stability

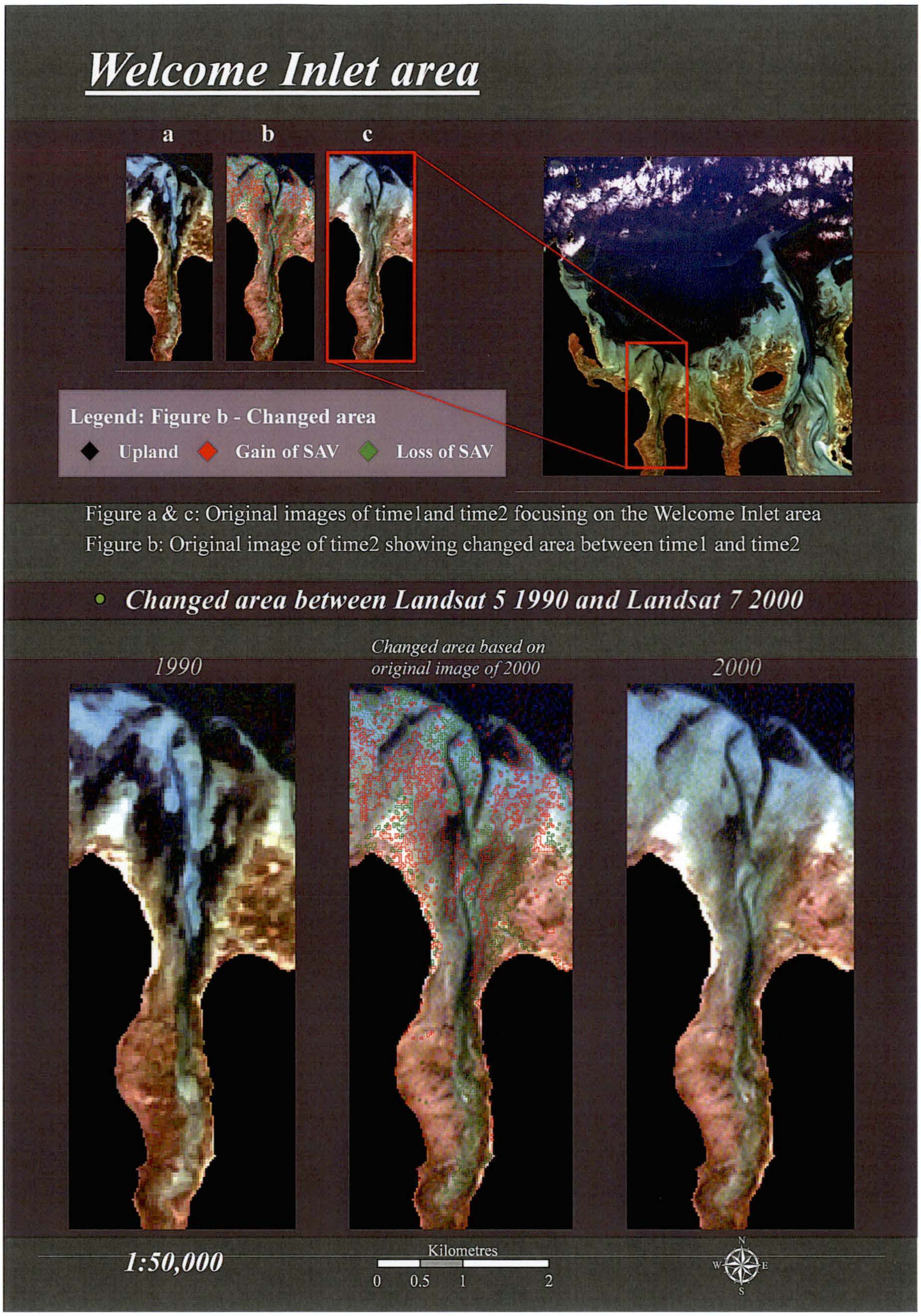

Figure 6.4 Welcome Inlet change detection result between 1990 and 2000

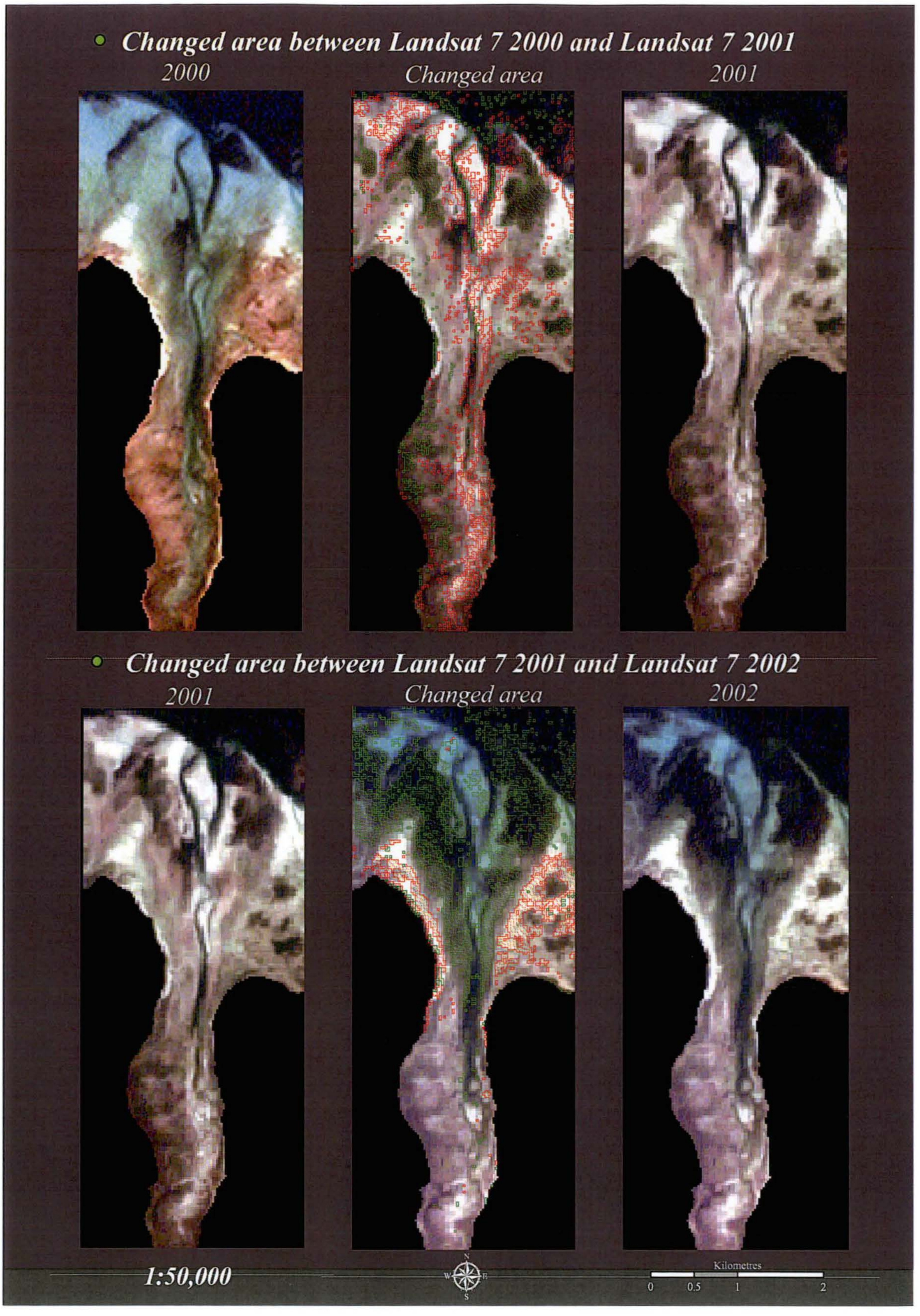

Figure 6.5 Welcome Inlet change detection results (1) between 2000 and 2001, and (2) between 2001 and 2002

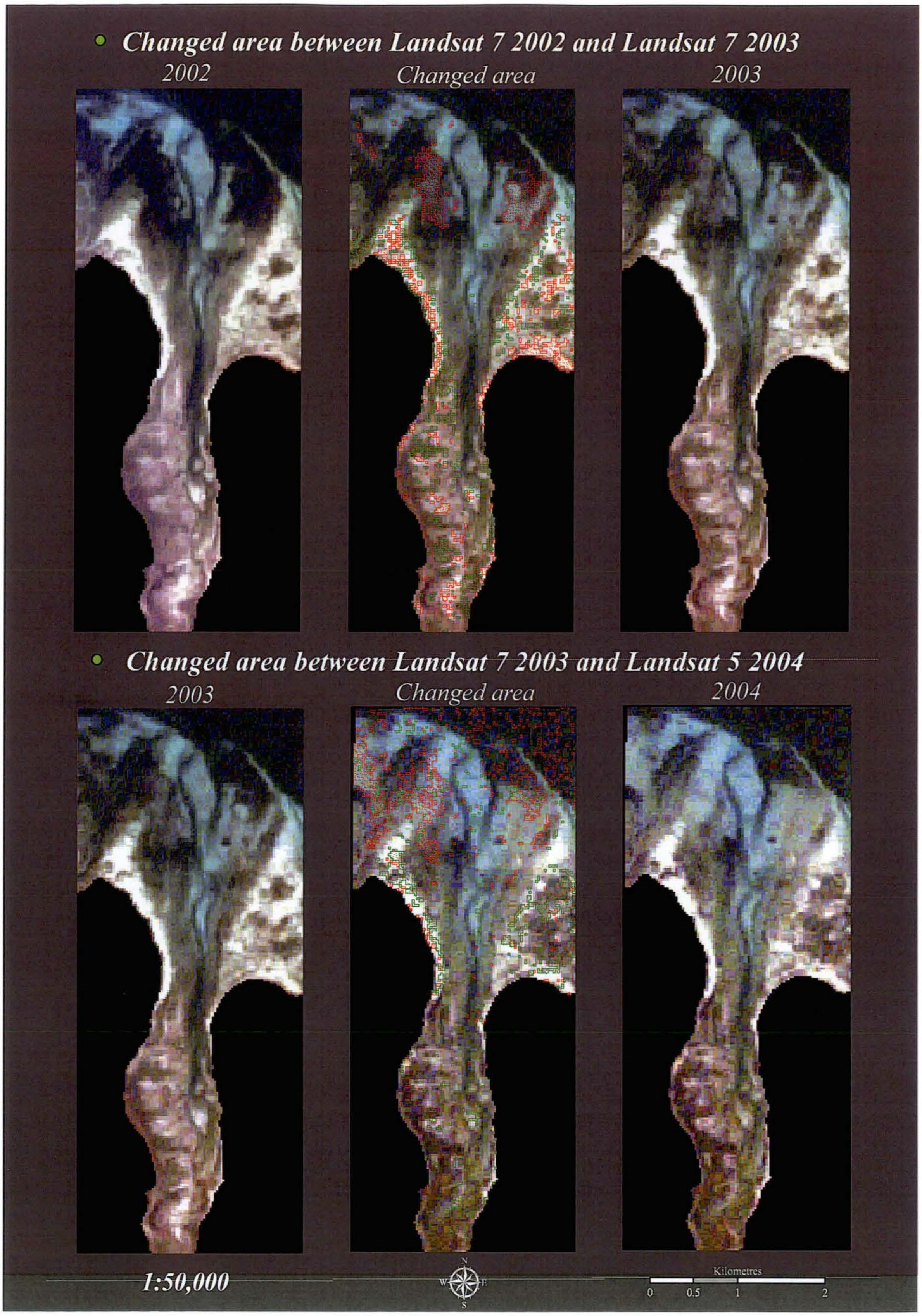

Figure 6.6 Welcome Inlet change detection results (1) between 2002 and 2003, and (2) 2003 and 2004

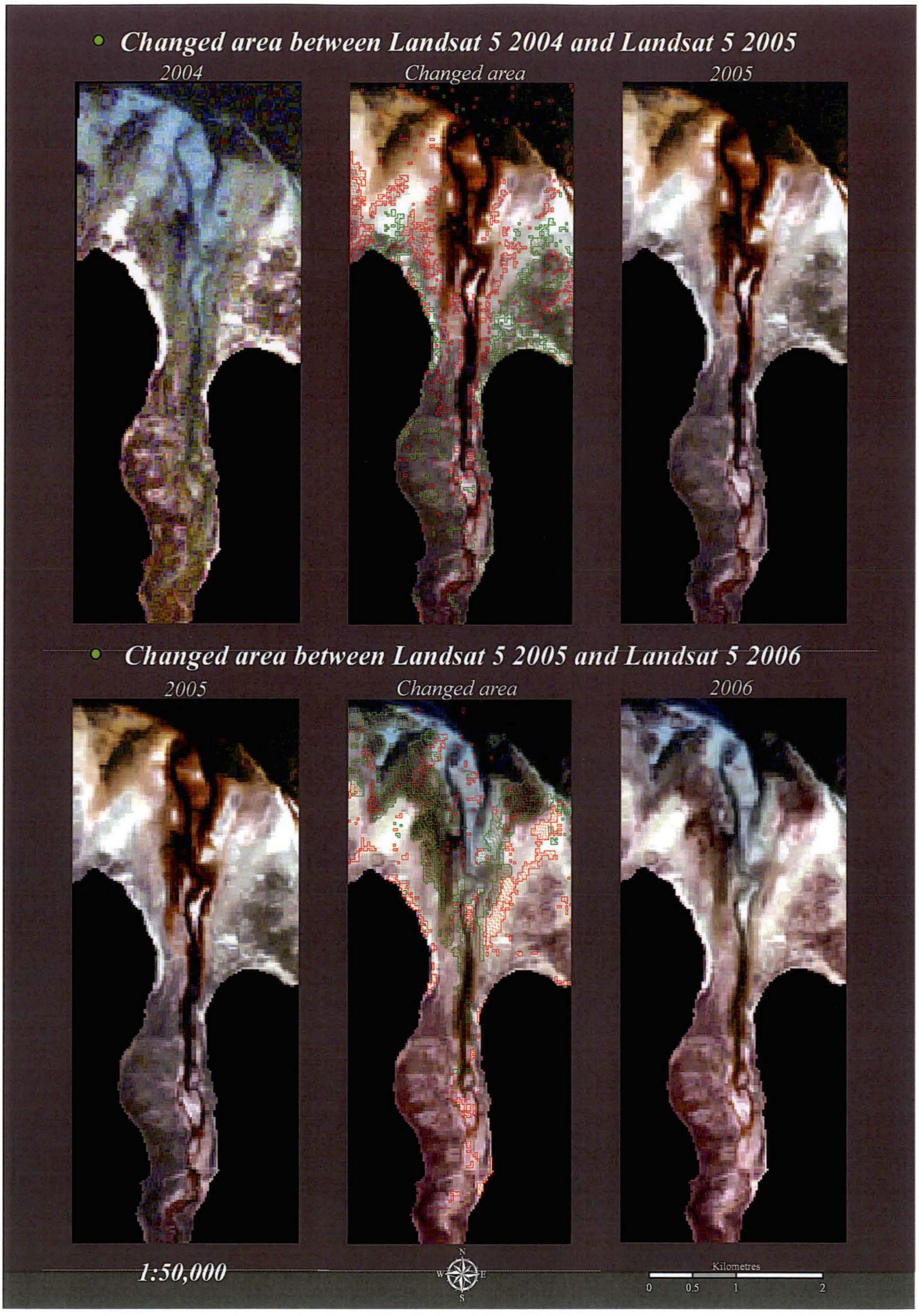

Figure 6.7 Welcome Inlet change detection results (1) between 2004 and 2005, and (2) 2005 and 2006

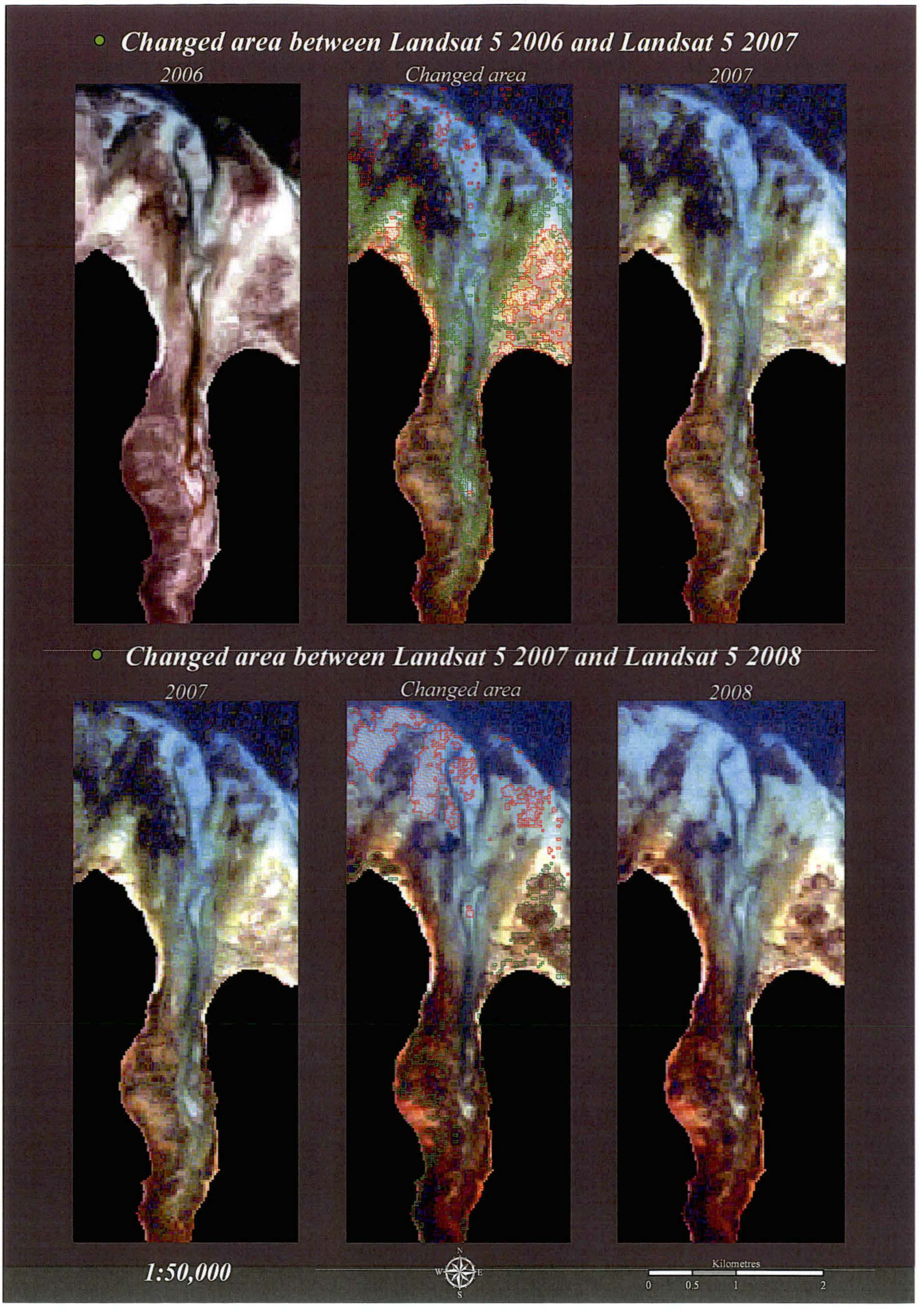

Figure 6.8 Welcome Inlet change detection results (1) between 2006 and 2007, and (2) between 2007 and 2008

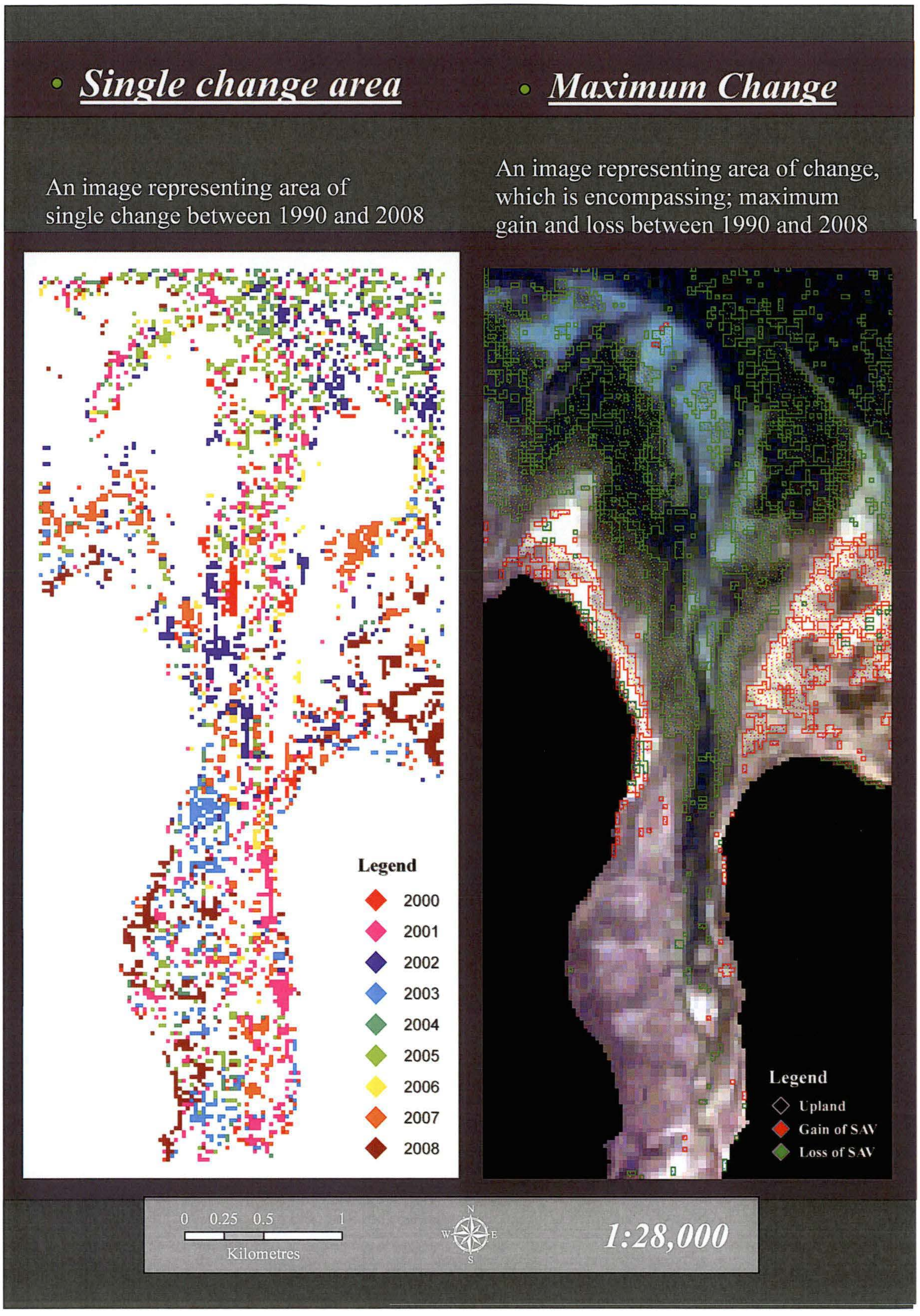

Figure 6.9 Single count change area and change detection result between 2001 and 2002

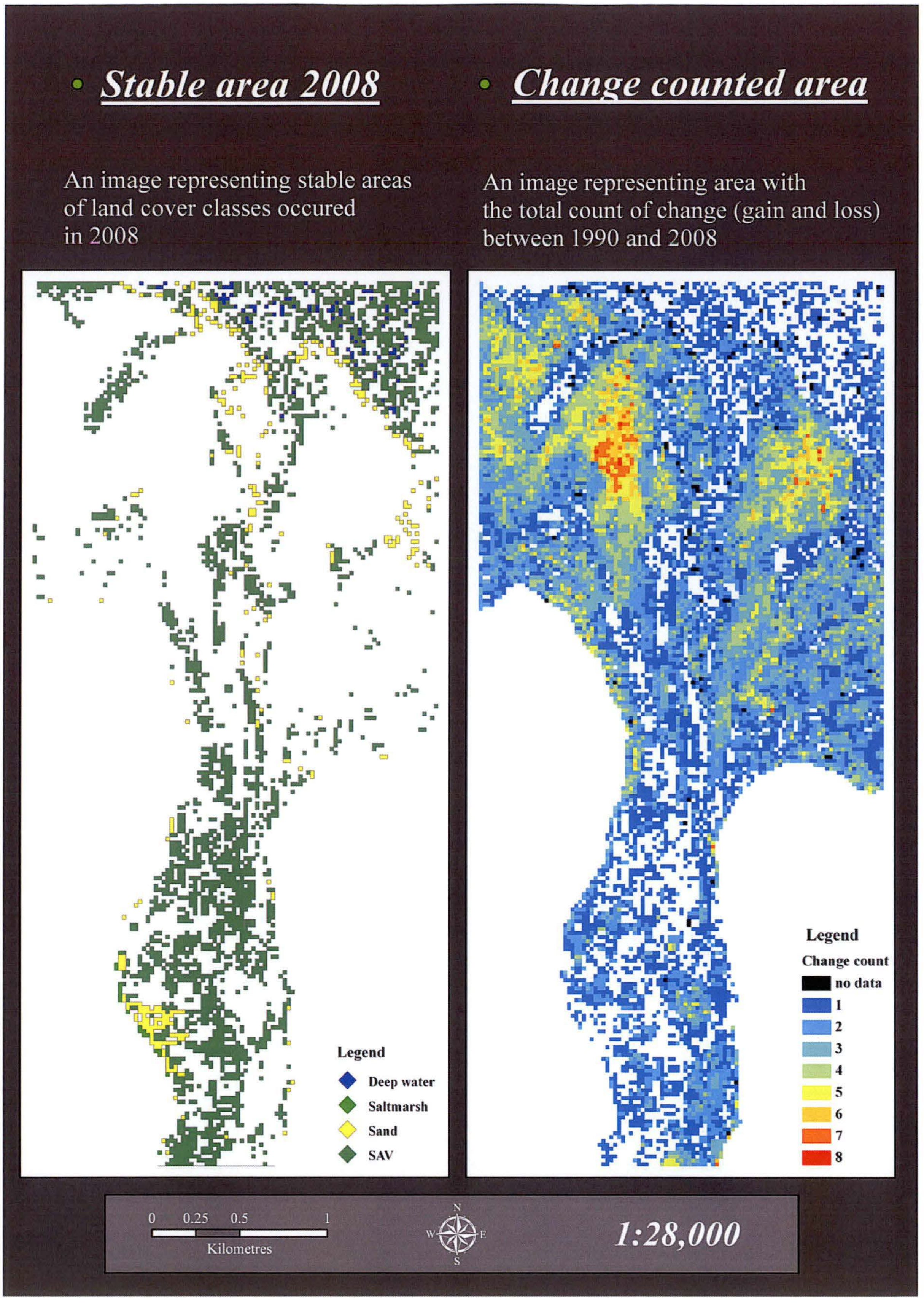

Figure 6.10 Stable area and change counted area

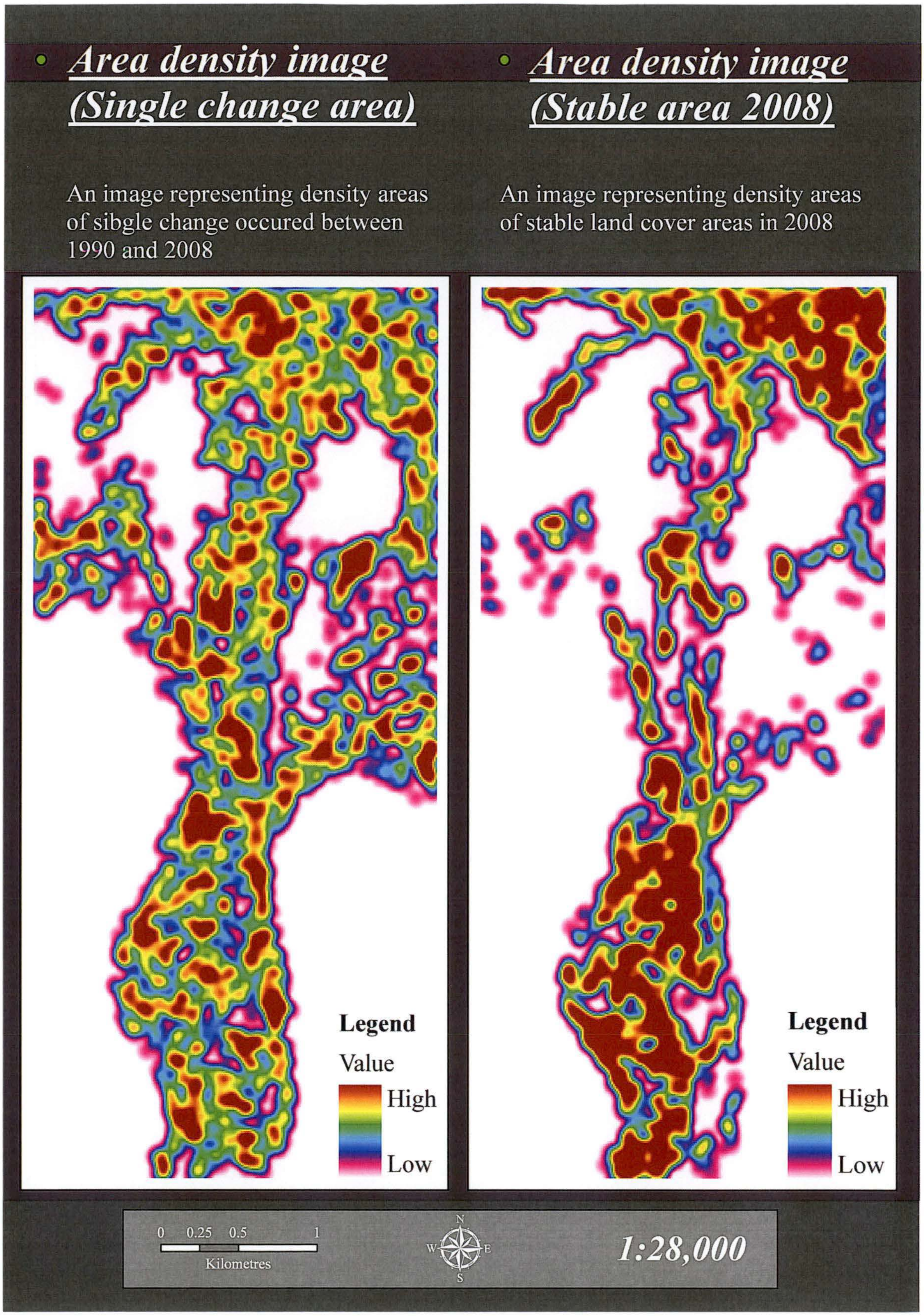

Figure 6.11 Area density images of single count change area and stable area

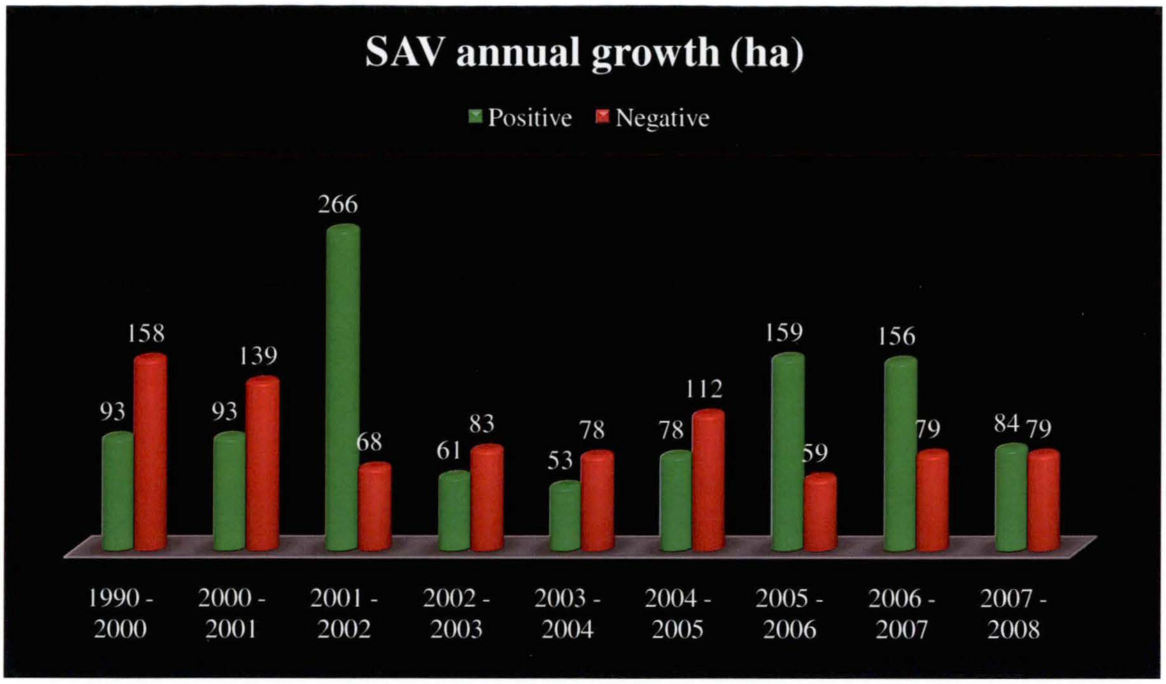

Figure 6.12 Welcome Inlet SAV annual growth

6.4.2 Subtidal open water area SAV habitat: WFMI approach

The 11 reference images over 18 years were subject to change detection procedure (Figure 6.13). WFMI approach was performed to detect change in the distribution of SAV meadows, mainly consists of subtidal seagrasses over the subtidal open water area on the Boullanger Bay. 10 resultant images based on the subsets composed of time 1 and time 2 original images were produced by the change detection method (Figure 6.14, 6.15, 6.16, and 6.17). The presented SAV meadows monitoring has demonstrated change and un-change areas of their meadows over the 18 year period from 1990 to 2008. Increase and decrease of the brightness values based on the visible Green band varied dependent area on the image and the individual year.

Particular finding of this sub-case study was the high stability of un-colonised area rather than change in their distribution. Changed area was displayed by red and cyan, and unchanged area was displayed by gray scale colors from white to black. Consistency of the patchy un-colonised meadows was represented by white in the subtidal open water area of the Boullanger Bay over the 18 year period. While the un-colonised areas displayed the consistent white color, which represents consistent stability, changed areas were represented by the inconsistent density of color through red and cyan with dotted appearance. In short, changed areas have demonstrated inconsistent change. Those changed areas were represented around the patchy un-colonised area. In practice, these changed areas displayed around the patchy un-colonised areas were unexpected result in this sub-case study since the assumption of the subtidal seagrass meadows is high stability that is changeless.

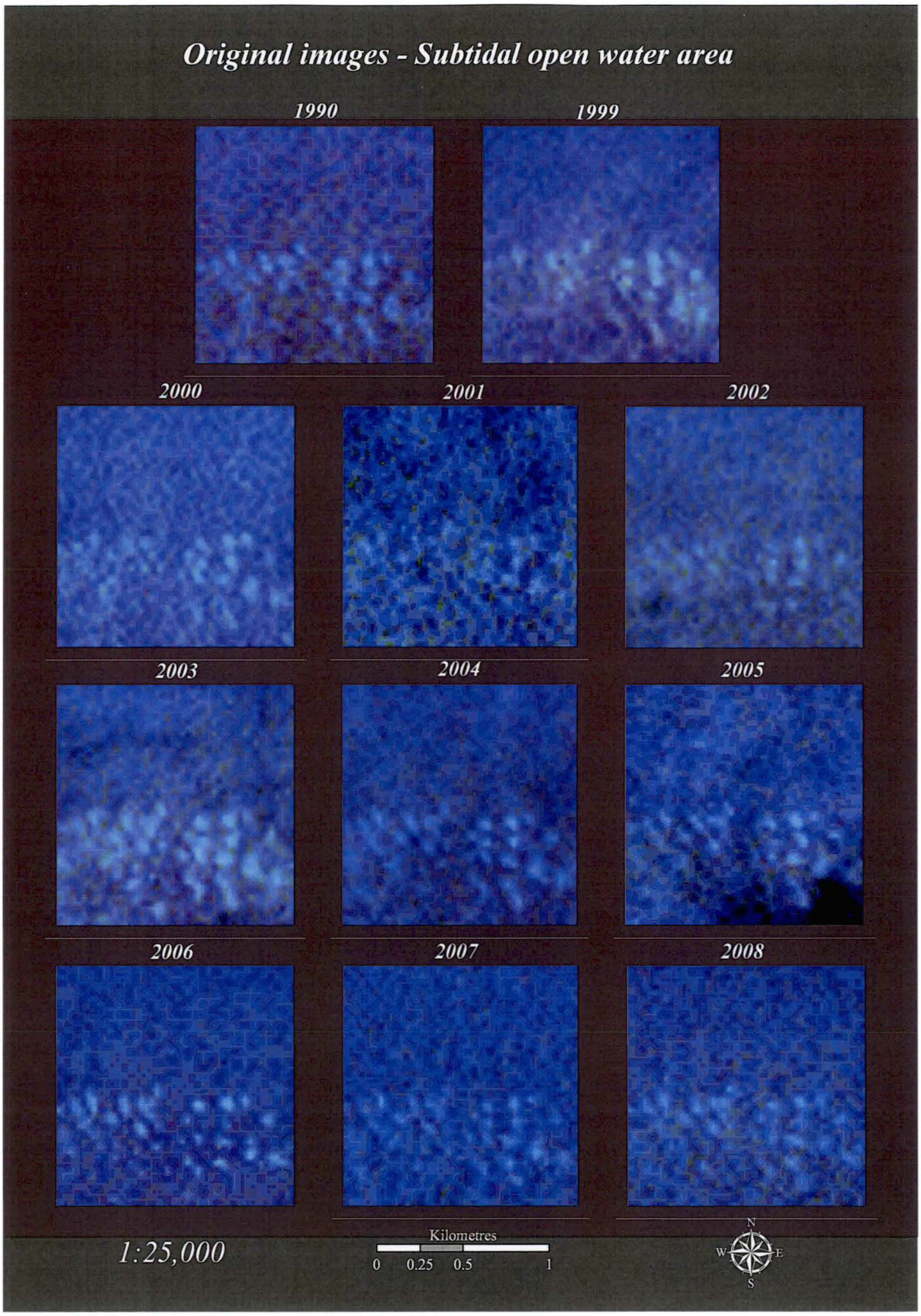

Figure 6.13 Subtidal open water area original images, red rectangle focuses on several patchy uncolonised areas

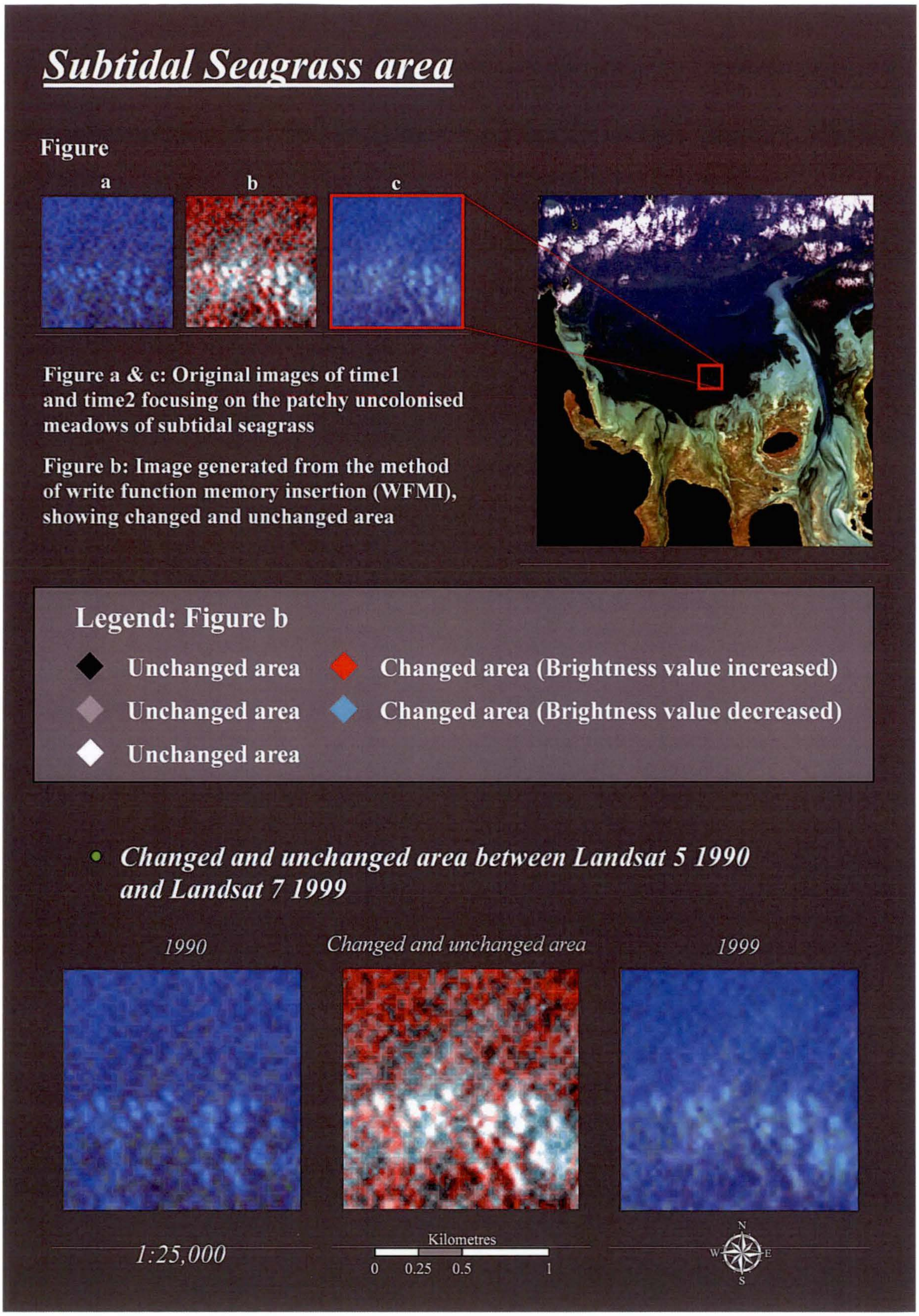

Figure 6.14 Subtidal open water area change detection result

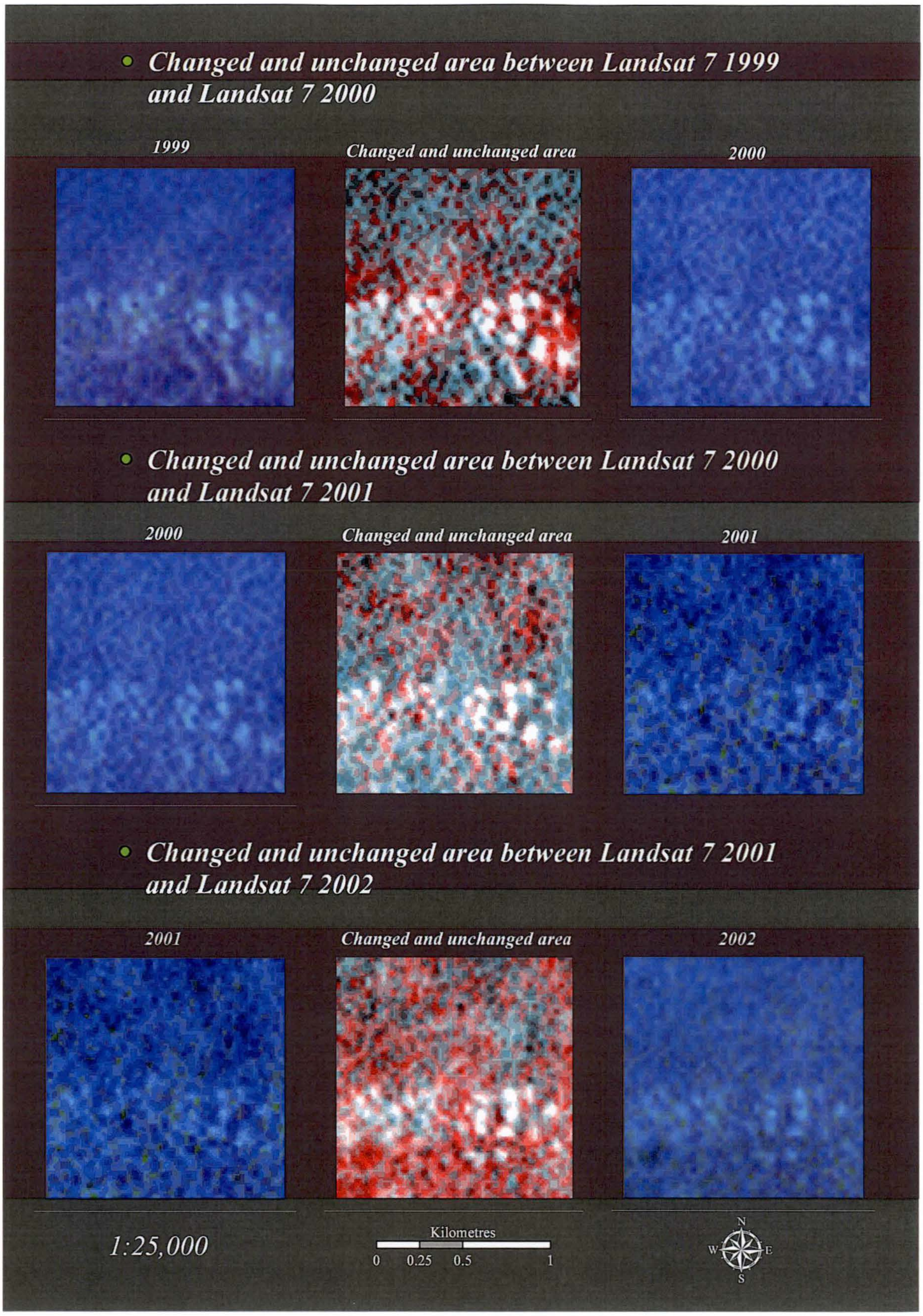

Figure 6.15 Subtidal open water area change detection results

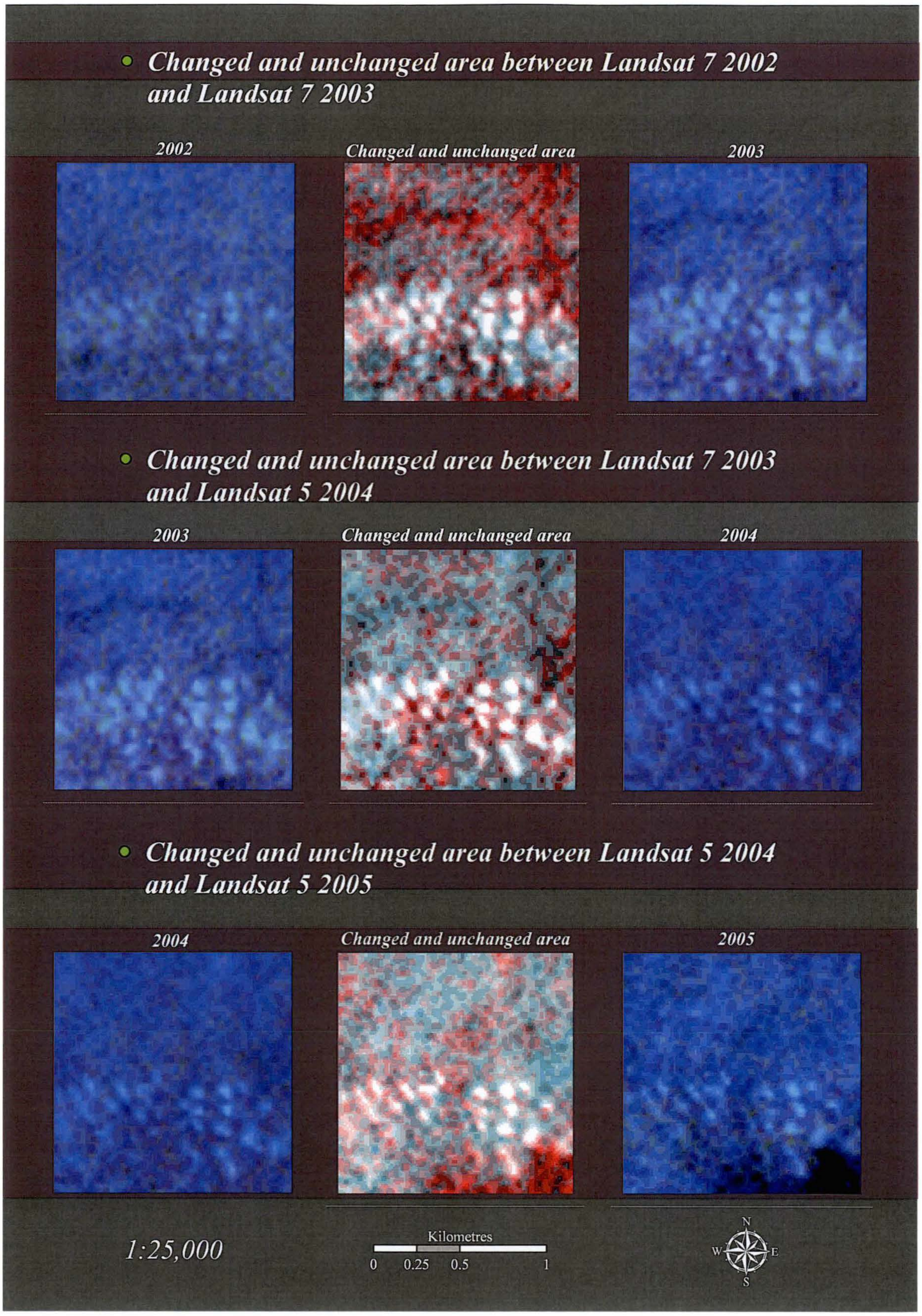

Figure 6.16 Subtidal open water area change detection results

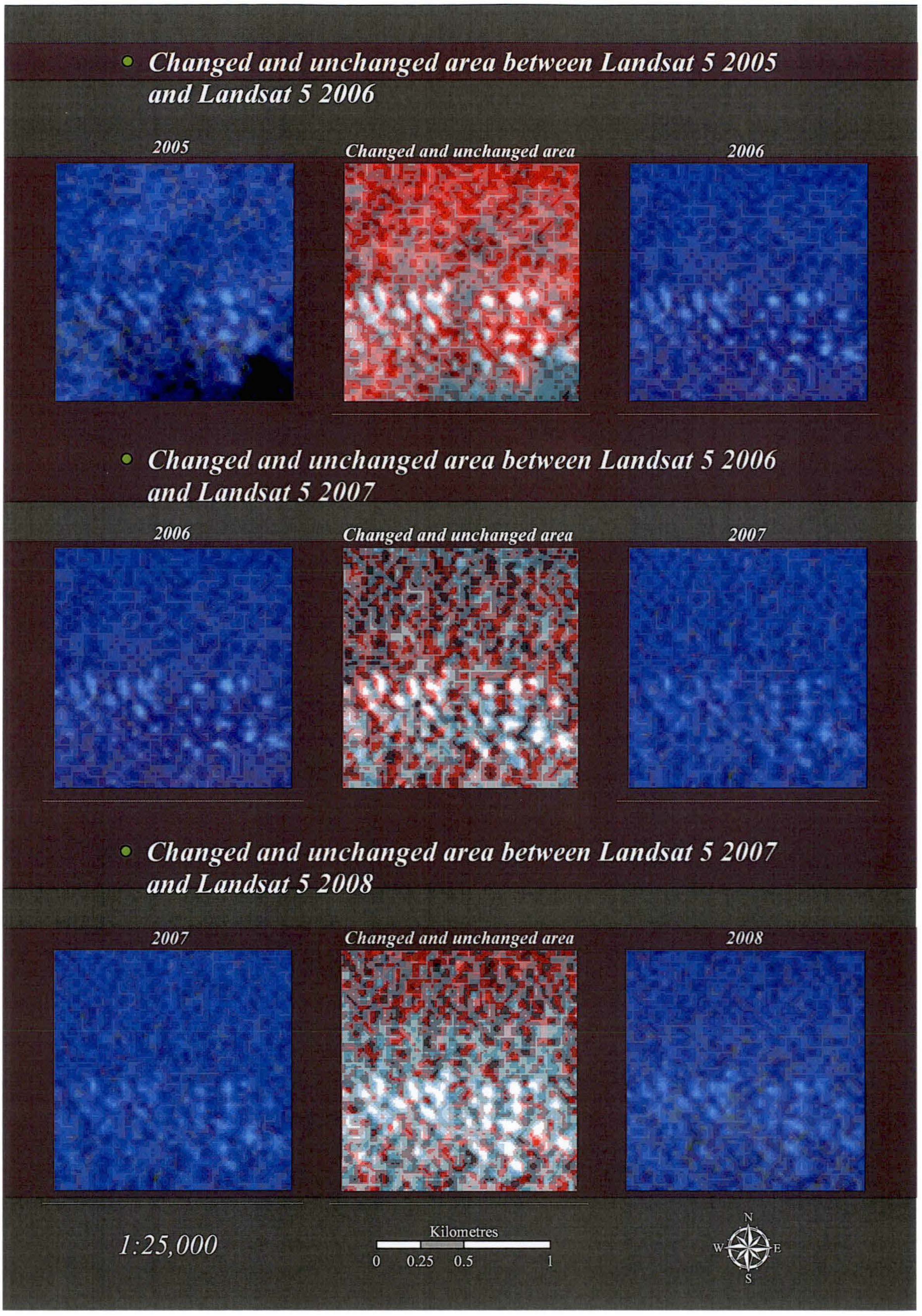

Figure 6.17 Subtidal open water area change detection results

Chapter 7 Discussion

7.1 Chapter overview

Chapter 7 discusses the findings of the case studies. The learnings from the image pre-processing stage are described first and then the case studies are discussed in detail. Key findings are highlighted and potential techniques applicable to SAV mapping and monitoring are proposed for future research.

7.2 Pre-processing

Some issues became apparent during the image analysis that could not be addressed during the study, including problems with cloud removal and radiometric differences between images over time. These issues are discussed and some alternative approaches presented.

Many types of clouds ranged over some of the acquired images, including semi-transparent cirrus cloud and dense cumulus cloud. That high variety of cloud type brought the challenges of cloud removal procedure in this project. There are three main concerns arising from cloud coverage, including: (1) the mixture of spectral value between cirrus cloud and other object in cirrus cloud; (2) similar brightness value between cloud and other objects; such as beaches; and (3) cloud shadow coverage. The procedure of cloud removal from the acquired images with using '*mask*' function of ENVI 4.6 was confounded due to spectral and radiometric overlap, especially between the clouds and beaches. The lack of cloud removal procedures at the pre-processing stage led in the part to misclassification between the classes of 'Dense SAV' and 'Deep water' in the image classification analysis of Case Study 1. In order to improve the accuracy of classification and change detection analysis, several pre-processing techniques could have been attempted instead of the techniques used for this project. For instance, the method developed by Hoan and Tateishi (2008) reportedly removes not only cloud coverage but also the shadow coverage from the image. This method is performed based on an interpolation from Synthetic Aperture Radar (SAR) data and uses several algorithm techniques, including; Total Reflectance Radiance Index and Cloud-Soil Index for defining cloud coverage. Although they used ALOS data, the advantage of this method is the ability to apply it to other satellite data, such as Landsat TM and ETM+. This method is potentially effective at producing a time series of free cloud and shadow data for change detection analysis (Hoan and Tateishi 2008). Although it was not possible to employ this method in this study due to limitations of data, it is one potential technique to consider using in future research.

Relative radiometric correction using pseudo-invariant features (PIFs) was accomplished in this project based on medium spatial resolution satellite imagery, i.e., Landsat TM and ETM+. The empirical line calibration approach based on the PIF of deep open water area and sand dune were effective for this project. The reason for using this radiometric correction technique is that the pixel size of the imagery highly influences on the measurements taken of the PIF. While small objects in any particular area, such as open water or a sand dune cannot be detected by moderate resolution images, these objects can be detected by high resolution imagery and will influence the empirical line technique (Hong and Zhang 2008). Therefore, the empirical line calibration using the PIF is more applicable to moderate resolution imagery; and high resolution imagery requires another procedure to remove those small objects from PIF prior to application of empirical line calibration approach (Hong and Zhang 2008). However, the manual selection of each PIF by visual inspection was dependent on the local knowledge of the study area and the skill of the researcher in this project. In short, the relative radiometric correction performed in this project was a subjective approach. However, the PCA method for selecting the PIF could be more accurate and applicable to regions that contains few PIFs. PCA based PIF selection could not be used for this project due to the limitations indicated by Paolini et al. (2006) when applying the method for Landsat data. Potentially, the multi-dimensional PIFs selection (MDPS) method developed by Paolini et al. (2006) could be an effective Landsat image pre-processing procedure. They found that this method provides a quality of radiometric image comparable to the absolute correction method. The method is based on a three-dimensional principal component analysis. A cylinder generated by the calculation of 3D PCA is defined by the major axis and its radius with an arbitrary threshold (Paolini *et al.* 2006). All pixels contained are defined as PIFs, and the radiometric discrepancy between Landsat TM and ETM+ sensors are reduced by this method. An objective approach is generally more preferable unless researcher has sufficient information on the study area. MDPS, a particular method for objective radiometric normalisation, especially for images acquired by different sensors would be a potential approach for change detection research into coastal area that have limited PIF sources.

A variety of pre-processing techniques are potentially applicable to the image analysis for seagrass mapping and monitoring. Geometric correction for the acquired images is critical. In addition, radiometric correction is also critical in multi-temporal multi-sensor change detection analysis, especially for the coastal regions where is often in the context of the various environmental conditions. The several methods mentioned in the previous paragraphs could be the next steps to improve image correction accuracy for image analysis.

7.3 Case Study 1: Remote Sensing method comparison

An investigation of hybrid methods of image classification were performed in Case Study 1 a PCA based ISODATA approach and an ICA based MLC approach. Both were subject to an accuracy assessment by '*error matrix*'. The hypothesis of this case study was that the ICA based MLC approach has a better accuracy than that of the PCA based ISODATA approach. This hypothesis is based on the reasoning that while ICA will detect a linear representation of non-Gaussian data, the PCA depends on an assumption of a Gaussian distribution which satellite data often doesn't exhibit.

According to the result of the error matrix for the two image classification results, the ICA based MLC approach obtained an accuracy higher than or equal to the PCA based ISODATA approach except for the producer's accuracy and user's accuracy of the sparse SAV class. The lower accuracy for this class was assumed due to the lack of water depth correction that eliminates the water column effect from reference images. ICA extracts mutually independent components underlying the acquired image based on the spectral characteristics. However, the lack of water depth correction procedure resulted in the miss-transformation of ICA for land cover classes, such as 'Dense SAV' and 'Sparse SAV'. For instance, misclassification of land cover class between 'Deep water' and 'Dense SAV' in deep water area, especially around the sand edge and subtidal SAV meadows was assumed due to this problem. Additionally, this problem contributed to the misclassification between 'Dense SAV' and 'Sparse SAV' in shallow water area as well. While water depth correction could not be performed in this project due to time limitations of research, this procedure would be useful to consider for SAV mapping in future research. The water attenuation effect resulting from absorption and scattering of light in the water column should be corrected in order to extract a more accurate classification result of submerged objects. The water depth correction method, developed by the Lyzenga (1978; 1981) has been a common approach for the application for SAV (Mumby *et al.* 1998; Ciraolo *et al.* 2006; Mount 2007). Previous research into SAV mapping by Mumby et al. (1998) and Ciraolo et al. (2006) found the method highly effective. Generally, removal of the water attenuation effect requires two factors; (1) a digital elevation model of depth in study area and (2) water attenuation characteristics of water column in study area (Mumby *et al.* 1998). However, the water depth correction method developed by the Lyzenga (1978; 1981) is a simple image based approach. In other words, no ancillary data or *in situ* data are required for this method (Mumby *et al.* 1998). It produces a depth invariant index of bottom type from two spectral band pairs instead of predicting the reflectance from the underwater objects (Mumby *et al.* 1998; Ciraolo *et al.* 2006). Therefore, Lyzenga's water depth correction method would be a potential approach to compensate the water attenuation effect on the SAV mapping in coastal area for future research on the condition that the water column has consistent light attenuating characteristics across the entire image scene.

In practice, the lack of ground truth data and other ancillary data was also implicated in the inconsistent accuracy results between the two approaches. Only the year of 2006 had adequate data to enable an accuracy assessment. This meant that the accuracy assessment of change detection was not able to be performed in this project due to the lack of the validation data for other years. While the error matrix accuracy assessment accomplished the identification of the appropriate method, an accuracy assessment with further ancillary data is needed to investigate the effectiveness of the two methods for mapping SAV meadows.

ICA was found to be an effective technique for extracting statistically independent components. The Regions of Interest (ROI), digitised based on the independent components, are required to be statistically independent to be useful as training samples for image classification. The accuracy of the MLC approach was thus improved by application of ICA for mapping SAV meadows in this project. While PCA based ISODATA demonstrated lower accuracy than ICA based MLC approach, PCA application for ISODATA was also considered an effective process of feature extraction and improved the accuracy of the unsupervised classification. For the hybrid classification approach, numerous researches have supported the value of a hybrid approach combining supervised or unsupervised classifier with other image processing technique land cover classification to improve the accuracy of classification result (Li and Yeh 1998; Lu and Weng 2007; Deng *et al.* 2008; Deng *et al.* 2009). Deng et al. (2009) used a combination method between PCA and MLC, and Deng et al. (2008) used the integrated method of a PCA based hybrid image classification approach using the combination of supervised and unsupervised classifier. Both studies indicated the ability of the integrated method of PCA based hybrid image classification approach to extract the information on the direction, nature, rate, and location of land use and land-use changes. Li and Yeh (1998) found application of a hybrid method using MLC based on PCA for the Pearl River Delta in China enhanced the accuracy of an image classification of land use. In turn, it reduced potential errors inherent in change detection due to low image classification accuracy. Therefore, further research could be conducted to identify the most effective hybrid approach for SAV mapping in the Boullanger Bay. However, the difficulty inherent in the arrangement of additional bands was also identified during the application of ICA in this project. Identifying the appropriate number of additional bands and appropriate spectral characteristics of additional bands to extract features of interest was critical. Additionally, identifying the appropriate thresholds of data value for extracting independent component was also challenging.

For PCA based ISODATA approach, 25 land cover classes were designated for the classification procedure in advance. However, further attention could fruitfully be given to the selection process for an appropriate number for the unsupervised classification. For example, Macleod and Congalton (1998) tested two sets of clusters of 100 and 255 with ISODATA to identify the population of eelgrass, *Zostera marina* in Great Bay, New Hampshire based on a Landsat TM image. Everitt et al. (2009) also employed ISODATA with 75 clusters for black mangrove mapping, and Gluck et al. (1996) used 250 clusters for PCA based ISODATA to map wetlands. These researchers employed a much larger number of clusters for the classification procedure than that used in this case study. In particular, Macleod and Congalton (1998) identified that 255 clusters produced a better result for the change detection of the eelgrass meadows in their result. While the appropriate number is not necessarily large, further investigation into the appropriate number for unsupervised classification procedure will potentially improve the accuracy of the change detection approach.

The mixed pixel problem is a major challenge for image classification or change detection procedures and is inherent in medium or coarse spatial resolution of satellite imagery. Heterogeneity of complicated landscapes in study location and large instantaneous field of view (IFOV) are often major sources of the mixed pixels in the acquired image (Lu and Weng 2007). Since this project employed medium spatial resolution imagery of Landsat, the problem of mixed pixels in the image was assumed. Mixed pixels between subtidal seagrass, intertidal seagrass and macroalgae contributed to misclassification between dense and sparse SAV. Although two classification approaches were performed based on image transformation techniques to improve accuracy of the resultant data, this problem eventually remained in the resultant thematic maps. Mixed pixels are another challenge for future seagrass mapping and monitoring research when using medium spatial resolution imagery. Subpixel and soft image classification is one of the potential approaches to deal with the mixed pixel problem. Major aims of subpixel and soft classification are to provide a more appropriate representation of feature class a more precise estimation of feature class area compared to the per-pixel classification approach (Lu and Weng 2007). This approach is potentially effective for the study area, especially using medium and coarse spatial resolution for a complex landscape region, such as Boullanger Bay area and could achieve better accuracy (Lu and Weng 2007). Among the subpixel classification techniques, the fuzzy classification approach is producing good results for vegetation classification and is reducing the mixed pixel problem using fuzzy logic (Lu and Weng 2007). However, the challenge of evaluating the accuracy of classification result remains in this approach due to the difficulty of obtaining adequate reference data. In spite of these difficulties, this approach is a noteworthy method for seagrass mapping.

7.4 Case Study 2: Remote sensing change detection of submerged aquatic vegetation (SAV) at two spatial scales

The '*from – to*' change between the distribution of land cover classes, especially dense and sparse SAV meadows, saltmarsh, and sand were demonstrated by the WFMI approach over the 18 year period from 1990 to 2008 in Case Study 1. Over short time periods (i.e. year to year) many changes were found in the habitat distribution between land cover classes in the whole Boullanger Bay area throughout the 18 years. The change detection results have shown that there is a consistent rate of change across the whole Boullanger Bay over the 18 years. This result also applies to the boundary between saltmarsh and sparse SAV. Overall, saltmarsh has been in gradual decline in extent in this area over the long term between 1990 and 2008.

The rapid switching from one form of land cover to another was not unexpected for the sparse SAV distribution (usually switching between seagrass and sand) since the recolonising ability of the intertidal seagrass (here, *Z. muelleri)* in the sparse SAV class, is high. Yet, the high rate of change in the dense SAV distribution was also identified across the boundary between dense SAV and deep water edge in deep open water area. This finding in the dense SAV distribution results was not expected since the dominant subtidal seagrass *P. australis* has the assumption of high stability in their meadows. However, this apparent change in the distribution of the dense SAV does not necessary demonstrate actual change in the distribution of dense SAV over the years. As mentioned in Chapter 2, *P. australis* occurs in about 1– 15 m of water depth. Light attenuation due to high tide level was attributed to the misclassification of the subtidal seagrass meadows in the subtidal water area. Further, the dense SAV class might have contained not only dense intertidal seagrass but also macroalgae, which has a high recolonising rate. Therefore, the rapid change in the distribution of dense SAV class was mainly attributed to the part of misclassification due to water column light attenuation.

In another respect, the misclassification of objects in deep water areas is also related to the limitations of moderate spatial resolution sensors, such as Landsat and ALOS, to resolve underwater features. Seagrass meadows located in deep water areas (around 7m depth; Appendix 9) could not be detected well by the moderate resolution sensors in this case study. Change detection for *Posidonia* spp. beds by Anstee et al. (2009) found higher stability of *Posidonia* beds when analysing the QuickBird imagery than when analysing the ALOS imagery. Since, this case study used ALOS and Landsat TM imagery, the low stability of the subtidal seagrass meadows may partly be attributed to the spatial resolution. Additionally, Larkum and West (1990) selected shallow bay (Botany Bay, which is covered by 4,600ha seagrass beds) for change detection of *P. australis* using aerial photographs. They detected a loss of 58% of the seagrass meadows between 1942 and 1986. Gullström et al. (2006) successfully performed change detection of tropical intertidal SAV meadows (*Halimeda* spp. and macroalgae) in Chwaka Bay, Tanzania, which is relatively shallow (average depth 3.2 m).

For the image classification of underwater objects using moderate resolution sensor, the depth of the study location is a critical factor, and a compromise between depth range of objects and spatial resolution of sensor may be required to select an appropriate spatial subset area, within which subsurface features can be detected by moderate spatial resolution sensor.

The lack of a water depth correction procedure appears to have impacted the change detection results. Less area and percentage change in saltmarsh cover compared to the other land cover classes were identified. However, correlation in area and percentage change between saltmarsh and other land cover classes, especially sparse SAV has not been identified in the results for the whole Boullanger Bay. The main reason for this is that the other cover types were changing so rapidly that no reasonable correlation could be found either with any one cover type or any grouping of cover types.

For saltmarsh and sparse SAV boundary area, increases and decreases in each land cover class distribution were observed at each pair of consecutive images between 1990 and 2008. Since this area contains sparse SAV class, mainly composed of the intertidal seagrass and macroalgae, the rapid change in their extent was expected. However, the saltmarsh loss and gain in other areas remote from the boundary was not expected. Although change detection in consecutive images between 1990 and 2000 and between 2000 and 2004 showed a pattern of loss and gain of saltmarsh cover across the boundary, other consecutive image pairs have shown losscs in places other than the seagrass/saltmarsh boundary. Such saltmarsh cover loss and gain in areas remote from the boundary were assumed due to the misclassification of saltmarsh with sparse SAV caused by the different tidal level in channels within the saltmarsh. However, correlation between land cover classes has shown a constant relationship of change in their distribution in this area (see Figure 5.8). A consistent negative correlation between sparse SAV and the two other land cover types ("Sand" and "Dense SAV") was found except for 2008, which showed a significant increase in sand cover. These rapid changes and the consistent correlation between land cover classes were considered mainly to be driven by the quick response of intertidal seagrass community to environmental change. The influence of the intertidal seagrass community on the habitat extent of saltmarsh plant community during the recolonisation activity of the intertidal seagrasses resulted in the correlation between the land cover classes in their distribution change. The tendency of distribution change in these three classes has demonstrated their response to the natural disturbances or indirect human induced disturbances, such as sea level rise or current flow change. Relative decline of saltmarsh cover from 1990 to 2008 must be viewed in the context of these disturbances. A gradual increase in the frequency of such disturbances could have an effect on the distribution of intertidal seagrass meadows, which in turn, led to a gradual change in their distribution over the long term. For the satellite remote sensing efficacy in this case study, the different capability to map the land cover classes has been demonstrated between Landsat TM and ALOS. ALOS has detected more particular land objects than Landsat TM. This indicates that spatial resolution influences the image classification accuracy. Phinn et al. (2006b) and Anstee et al. (2009) have also identified such an impact on the classification accuracy. Higher spatial resolution is better for mapping and monitoring more particular seagrass beds (Phinn *et al.* 2006b; Anstee *et al.* 2009). However, they concluded that Landsat TM is potentially capable for mapping and monitoring seagrasses or saltmarshes at broad scale. This case study has also represented the general stability of saltmarsh by broad scale monitoring through the classification results. In this regard, the potential capability of Landsat TM for broad scale mapping and monitoring, especially for saltmarshes was also indicated in this case study.

7.5 Case Study 3: Time series change detection in subtidal and intertidal areas via MCI and WFMI

The results presented of SAV meadows mapping and monitoring in the Welcome Inlet has demonstrated that both increases and decreases in their abundance occurred over the 18 year period from 1990 to 2008. Frequent changes in the distribution of SAV were found at both short and long periods of change detection throughout the time series. However, two of areas of the Welcome Inlet study site, namely the centre and northwest parts, were found to have high stability SAV throughout the 18 year period (Figure 6.10 and 6.11). For subtidal open water area change detection, consistency of the patchy un-colonised meadows was found in the subtidal open water area of the Boullanger Bay over the 18 year period.

7.5.1 Welcome Inlet: Intertidal SAV habitat change

A high rate of change was expected for intertidal SAV, such as intertidal seagrass (*Zostera muelleri)* and macroalgae. Frequent change in the distribution of SAV meadows is as a result of their quick response to the rapid environmental change, such as eutrophication events or pulses of smothering sediments or shading turbidity. For example, eutrophication promotes algal epiphyte cover on intertidal seagrass communities and can, eventually shade the seagrass out (Figure 7.1). This is consistent with the findings of Abal and Dennison (1996) in southern Moreton Bay, Queensland, Australia. A relatively high correlation between light attenuation and the depth range of *Zostera capricorni* were observed in their research. They indicated that a significant decrease in seagrass depth range over the two-year duration was linked to the deterioration of water quality, especially higher light attenuation (Long Island and Victoria Point, 9 and 18 km from the Logan River mouth, respectively). A significant decrease in the intertidal SAV was also observed in Welcome Inlet, for example between 2002 and 2004 (Appendix 10). In this regard, the frequent population changes in the intertidal SAV meadows in Welcome Inlet could be also attributed to the decrease of water quality, possibly caused by eutrophication that promotes epiphyte bloom. The population change of the intertidal SAV thus could be a sensitive bio-indicator of water quality in Welcome Inlet. The areas experiencing frequent change of sparse SAV and high stable areas of sparse SAV were compared in a GIS. According to the results, the areas with frequent change were located in the north part of the Welcome Inlet, and area with smaller count of change and stable areas were located relatively close to the Welcome Inlet.

This moderate spatial resolution case study has shown that this is an environmentally sensitive area of SAV meadows subject to natural and or human-induced disturbances. Gullström et al (2006) also found that the overall seagrass cover to be stable between 1986 and 2003 in change detection analysis for tropical intertidal SAV meadows using Landsat imagery. However, temporally dynamic losses and gains were also observed through their mapping results. According to them, this population dynamics of the SAV meadows was attributed to less intense environmental deterioration, such as coastal development and nutrient discharge, in Chwaka Bay. While upland farming may be a potential source of nutrient discharge through fertiliser that promotes epiphyte growth (Figure 7.2), relatively stable overall coverage with fluctuations in intertidal SAV distribution on Welcome Inlet may imply both the vulnerability of the area to environmental change and the less intense environmental deterioration in Welcome Inlet. Additionally, the presence of the apparently stable area of intertidal SAV in the results has several implications. First of all, the stability of the SAV might have been supported by consistent environmental conditions and the intertidal SAV community was not unduly influenced by any kind of disturbances or environmental change. If the area supports such high environmental stability, the area could be a potential location of a marine parks or reserves (Kirkman 1997) or could be a useful reference site for monitoring at particular time scales – e.g. decadal.

Lack of the change detection accuracy assessment due to the lack of ground truth data and ancillary data for each consecutive pair of time 1 and time 2 images was hence involved in the problems associated with drawing conclusive results in this case study. However, the ICA for MCI approach represented sufficient ability to extract change area in intertidal SAV distribution from an overall point of view. In particular, the strength of the ICA technique, the change area extraction of individual features from the image was represented in this case study. As this technique produces statistically independent components based on the spectral characteristics of each pixel, small areal change in the intertidal SAV distribution that occurred in the time 2 image was also extracted well. Therefore, the ICA based MCI approach was demonstrated as an effective method for SAV mapping and monitoring, especially intertidal seagrass compared to the PCA and unsupervised classification approach that cannot extract such a feature.

However, the limitation of ICA technique relates to the difficulty of subjective optical "*image interpretation*" for identifying the change and non-change area. The WFMI technique using original bands was used to assist the image interpretation in this project. Subtle differences of change area due to the problem of different spectral characteristics between original bands used for the WFMI and independent components generated from ICA using non-linear spectral characteristics bands produced the difficulties in image interpretation via optical decision for identifying change area in some independent components. The ICA algorithm deals with each pixel in the image. Noise condition in the image thus highly influences the ICA procedure. Landsat 5, 2004 and 2005, involved in the ICA procedure represented the large amount of noise in the produced independent components, which in turn, the vector layers generated from the extracted features of changed area were also noisy (Figure 6.6 and 6.7). Although along track scanners generally produce smaller amounts of noise than across track scanners like Landsat TM, application of noise removal techniques could improve the production of independent components.

Additionally, the extracted features in several independent components were overlapped each other in their extent due to the subtle spectral difference of input bands for ICA. Vector layers generated from this overlapped features eventually produced visually complicated images. As the result, the application of GIS was required to consolidate the changed area into a single polygon. Adequately distinct spectral characteristics and appropriate number of bands thus should be taken into account for future seagrass mapping and monitoring research using ICA technique. In this regard, masking out the adjacent area should also be performed properly to control the number of features in the study area for improving the extraction of proposed features with desirable extent. Arrangement of the number of features in the image and the number of the additional bands with sufficient spectral difference is crucial. High spatial resolution multispectral sensor satellite, such as World View-2, would be a major source for land cover mapping analysis. Hence, appropriate non-linear operation technique to produce additional bands will be critical to enhance the ability of such high resolution satellite imagery for land cover analysis, including intertidal and subtidal seagrass mapping.

Figure 7.1 Epiphyte loading on *Zostera muelleri*

Figure 7.2 Intertidal seagrass beds and upland farm

7.5.2 *Subtidal open water area SAV habitat*

High stability of the colonisation area was the assumption of the subtidal seagrass species, such as *P. australis* (Clarke and Kirkman 1989). Each subset of time 1 and time 2 images for change detection represented the non-change of un-colonised patch of the subtidal SAV over the 18 year period except for the 2006 image. Slow recolonisation of *P. australis* has also been identified by Meehan and West (2000) through mapping circular uncolonised areas over 25 years. While Meehan and West (2000) employed a series of historical aerial photographs to map the uncolonised areas for estimating the recovery time for *P. australis*, the slow recolonisation characteristics of the subtidal seagrass meadows have also been identified by satellite remote sensing technique of the WFMI approach in this case study. The presence of the subtidal seagrass community in the subtidal area of Boullanger Bay over 18 year period was in included in the assumption from published slow elongation and spreading rates for *Amphibolis* and *Posidonia* species of 200–500 and <100–200 mm year_1, respectively (Clarke & Kirkman, 1989). However, the patchy appearances of change areas over the SAV meadows around the un-colonised area were also demonstrated in the results of this case study. While the high stability of the subtidal seagrass meadows is general idea, Kendrick et al. (2000) reported the dynamic increase of such subtidal seagrass meadows consists of *Posidonia coriacea* and *Amphibolis griffithii,* on Success and Parmelia Banks over the past 30 years. Recruitment of *P. australis* has been identified by Campbell (2003) as a possible factor for the maintenance and the expansion of their meadows. Additionally, the presence of intertidal seagrass community was basically difficult due to the environmental condition of the area (subtidal and average water depth of 4m; Appendix 9). Nevertheless, this change was considered due to another factor, which is an atmospheric distortion. This change in their meadows was attributed to the problem derived from the method applied for this case study. Few waves and surface reflection on the sea surface enabled data to detect clearly the subtidal seagrass habitat. However, the slight remain of waves and surface reflection influenced WFMI approach, especially in this case study. WFMI change detection approach is straightforward in terms of the spectral discrepancy as it is based on the spectral value difference between bands from time 1 and time 2 images. Even slight difference of brightness values can be thus distinguished by WFMI approach as Red or Cyan for changed area. Correction procedure of water depth, surface reflection, sun glitter, and volumetric scattering or absorption effect in the water column (O'Neill *et al.* 1988) were not performed in this project. While the stability of the patchy un-colonised area of subtidal seagrass meadows over the time series were identified by WFMI approach, those atmospheric corrections would be other challenges to distinguish actual change from the change affected by those atmospheric effect in future research into mapping seagrass meadows. WFMI approach employed in this project was visual change detection approach. Cubic convolution resampling technique produced visually better image than nearest neighbour resampling technique although little change of original data value was occurred. Conventional pan sharpening techniques, including; Hue, Saturation, Value (HSV), Color Normalized (Brovey), Principal Components, and Gram-Schmidt, were considered to apply for this optical based method. Yet practical problem about the fluctuation of original data value did not allow using this method in practice. However, recently developed pan sharpening technique using ICA is in the context of the assumption to produce the pan shrpened image with very little difference of data value between pre-processed and post-processed data (Wang *et al.* 2008). Therefore, this pan sharpening method could be a possible pre-processing technique for WFMI approach instead of the cubic convolution resampling to obtain better visual and data value.

7.6 *Overall project*

SAV meadows in Boullanger Bay have shown the changes over the 18 years of the study that are consistent with the biological assumptions. Sprod *et al.* (2003) and CCNRM (2005) reported that many seagrass meadows in Tasmania have already been destroyed by eutrophication from sewage and fertiliser discharge and imply that these processes may be active in the north west of Tasmania including the study area. As they indicate, the main cause of the decline in SAV meadows is considered to be as eutrophication that promotes epiphyte growth, and then reduces light penetration to the seagrass plants. However, according to the result of Case Study 3, the meadows do not only decline but increase over the change detection period as well. The rapid recovery of intertidal SAV was observed in this project a number of time following substantial losses. Additionally, the stability of subtidal seagrass was demonstrated in Case Study 3. While the subtle change in the meadows surrounding the sand patches (i.e. the uncolonised areas) was attributed to the technical problem of image analysis, the sand patches were highly stable throughout the monitoring period. Case Study 2 has produced what appear to be pseudo-changes in the 'Dense SAV' class (i.e. mainly subtidal seagrass), particularly in deep water areas. This inconsistency with the biological assumption was probably caused by technical problems of image analysis, especially the lack of water depth correction. While several technical problems attributed to some of the results, the change detection analysis performed in both Case Study 2 and Case Study 3 appears to be useful for monitoring SAV meadows in Boullanger Bay.

Landsat TM, ETM+ and ALOS both have a proven ability to map SAV meadows, yet the accuracy of the mapping varies dependent upon the case study area and the analysis applied. Results not corresponding to the biological assumptions of the SAV meadows were generated from the different sensors. According to some researchers, higher spatial resolution is more likely to obtain results that are more consistent with the biological assumptions. For example, Matarrese et al. (2008) compared the ability of different spatial resolution sensors to map *Posidonia oceanica* meadows. They indicated Landsat ETM+ has the ability to produce more accurate maps than ASTER sensor. However, IKONOS demonstrated a better result than Landsat ETM+ in their study. Nevertheless, many scientists indicated the Landsat TM and ETM+ have the ability to map and monitor seagrasses (Ferguson and Korfmacher 1997; Shapiro and Rohmann 2006). This study showed that the moderate spatial resolution Landsat imagery has superior temporal resolution compared to any other satellite archive of similar or higher spatial resolution. For this reason alone, Landsat must be considered for time series analyses. Further, the higher resolution imagery can have its own challenges such as the problems associated with selecting PIFs as discussed earlier.

Thus, moderate spatial resolution sensors are applicable to most part of Boullanger Bay, yet high spatial resolution sensors would be required to map and monitor the areas if the features of interest or the dimensions of change are smaller than the spatial resolution of the moderate spatial resolution sensors.

7.7 *Limitations in this project*

The limitations of this research project are mainly related to the research methodology employed and stem from a lack of ancillary data. It was not possible to conduct a field survey to 'ground truth' remotely sensed data due to budget and time limitations. Along with aerial photography, vector layer of land cover classes produced from TAFI and the expert knowledge of Dr. Mount, the lack of the ground truth data was offset. Some image analysis, including water depth collection and more precise image classification were also restricted due to time limitations. Second, this research could not address the accuracy assessment of the change detection carried out in two of case studies since only aerial photography acquired in 2006 was available. Thus, although the one year (2006) of the thematic mapping was assessed for accuracy using the aerial photography, change detection accuracy assessment that requires at least two images acquired at different time was not addressed in this research. Additionally, ideal combination of satellite imagery was not managed due to the limited budget for research. Satellite imagery is generally less expensive than aerial photography, yet when a number of data is required, for instance, for annual change detection, it can still be costly. This research only employed cost free imagery distributed by U. S. Geological Survey; thus there was a limitation of available data, ideal for image analysis.

Chapter 8 Conclusion

Submerged aquatic vegetation (SAV) plays an important role in Australia's marine ecosystems. Seagrass meadows have an environmentally important relationship with ambient coastal environments in terms of geographical configuration, water flow, water nutrient component, and biological relationship with other species (Short and Wyllie-Echeverria 1996; Butler and Jernakoff 1999; Kemp 2000; Orth *et al.* 2006). Information on the extent and status of SAV meadows at multi-spatial and temporal scale is crucial factors for conservation and management (Kirkman, H., 1990; Kirkman 1996; Kirkman 1997; Butler and Jernakoff 1999; Kemp 2000; McKenzie *et al.* 2001b). Information on the natural dynamics in seagrass species with environmental variability leads to successful conservation and management program. The overall aim of this study is to determine the contribution that remote sensing change detection methods can make to meet these information needs.

A series of objectives were devised and are presented in Chapter 1. The first objective was to identify and select satellite image a data and methods related to the study needs. The findings of the study have supported the choice of Landsat imagery for temporal change detection of shallow coastal waters. Landsat is particularly suitable for large area mapping and is especially useful because it is readily available and is a large historical archive. A large number of the recent developments in satellite remote sensing methods were evaluated. These include: Write Function Memory Insertion (WFMI); Multiple-Date Composite Image (MCI), Independent Components Analysis (ICA) and Principal Components Analysis (PCA).

The second objective of this study was to subject two key hybrid classification methods to investigation: the ICA based supervised classification approach and PCA based unsupervised classification approach. The investigation into the effectiveness of application for mapping SAV was reported in Case Study 1. Comparison between the two image classification approaches was performed using '*error matrix*', known as a conventional accuracy assessment method in Case Study 1. Result showed that ICA based MLC approach represented equal or better accuracy than PCA based ISODATA approach.

The third objective of the study was to perform change detection on habitats at two different spatial scales to determine whether the moderate spatial resolution of Landsat is effective. This objective was addressed in Case Study 2. In Case Study 2, the WFMI change detection approach was performed to identify the '*from – to*' change for two different sized study sites, one the whole of the Boullanger Bay area and one on a small inlet focussed on the changes between saltmarsh and intertidal seagrass. '*From – to*' changes in the distribution and change rate were found between feature classes of interest at short periodic change detection over the 18 years. Relatively stable fluctuation in overall coverage with discontinuous increase and decrease in both land cover distributions were observed in the saltmarsh/ seagrass boundary area at each subset of time 1 and time 2 images between 1990 and 2008.

The forth objective of the study was to perform change detection on habitats to determine whether the moderate spatial resolution and annual temporal resolution of Landsat is effective (Case Study 3) in either intertidal or subtidal seagrass dominated environments. ICA based MCI change detection analysis was performed to identify the spatial and temporal changes in the occurrence of intertidal SAV coverage in the Welcome Inlet area in Case Study 3. The presented SAV distribution monitoring has demonstrated that either increases or decreases in their population density occurred over the 18 year period from 1990 to 2008. Discontinuous changes in the distribution of intertidal SAV habitats were found at both short and long period through time series. Single approach of WFMI was used for change detection analysis in open subtidal area of the Boullanger Bay to identify the stability of subtidal SAV habitats over the period of time. Consistency of the patchy un-colonised SAV meadows was demonstrated in the subtidal open water area of the Boullanger Bay over the 18 year period. According to the results, the presence of subtidal seagrasses and their high stability in colonisation were proven in this area.

The overall aim of the thesis was achieved in this research project. Landsat TM and ETM+ are able to be used to detect SAV in shallow (less than 5m depth), sheltered and low turbidity water environment with large geographic scale. The long temporal span of these image data makes this sensor highly suitable for multi-temporal change detection analysis. The SAV habitat mapping capability of ALOS was also demonstrated. The higher spatial resolution of this satellite's imagery enabled detailed information on the land cover class distribution to be detected than the moderate spatial resolution images of the Landsat sensor. While the hybrid ICA based MLC image classification approach obtained better results in overall accuracy compared to the PCA based ISODATA, both approaches were effective for classifying land cover classes in Boullanger Bay. Additionally, it is considered that there is room for improvement in their accuracy with further improvements in the image analysis procedures. The ICA based MCI change detection approach is a useful technique to detect change in the abundance of intertidal SAV habitats at annual and decadal scales. Derivative data, such as change rate of their abundance can be derived from the independent components. The Image Visualisation Comparison Matrix (Appendix 10) was based on these results and enables comparisons of any date to any other date. WFMI change detection approach was straightforward to detect subtle change in subtidal SAV habitats. High stability of patchy sand areas in subtidal seagrass meadows was clearly identified by optical analysis over 18 years. Additionally, WFMI approach can be performed as a post-classification change detection approach to detect '*from – to*' change. This research project therefore has shown the ability of satellite imagery and remote sensing methods used in this project to detect changes through time in the distribution of intertidal and subtidal SAV habitats, especially seagrass in Boullanger Bay. Rapid changes in intertidal SAV coverage and the high stability of subtidal SAV coverage derived from multiple spatial and temporal scales monitoring could be a baseline data for a successful conservation and management program or a future research into SAV mapping and monitoring in the Boullanger Bay area.

Underwater objects detection has been a weakness of optical remote sensing technology. However, with ongoing technological development, satellite remote sensing techniques have been becoming important problem solving instrument for mapping and monitoring under water objects. As the improvement of technology proceeds, further objects located in deep underwater areas will be potentially applicable for the target of observation. Further information on the objects like seagrasses detected by remote sensing will facilitate their use within interdisciplinary studies or environmental conservation and management programme. Further studies about remote sensing technique for underwater object detection will be required with the improvement of satellite sensor and sensor technology so that sufficient information can be detected appropriately.

References

Abal, E. G., Dennison, W. C., 1996; Seagrass depth range and water quality in Southern Moreton Bay, Queensland, *Australia.Marine and Freshwater Research,* 47, 763 – 771.

Ackerman, S., Strabala, K., Menzel, P., Frey, R., Moeller, C., Gumley, L., Baum, B., Schaaf, C., & Riggs, G., 1997; Discriminating Clear – Sky from Cloud with MODIS Algorithm Theoretical Basis Document (MOD35). Version 3.2, Available at: <http://sky.ccny.cuny.edu/wc/atbd_mod06.pdf>, [Accessed 10th Aug]

Alphan, H., Doygun, H., & Unlukaplan, Y. I., 2009; Post-classification comparison of land cover using multitemporal Landsat and ASTER imagery: the case of Kahramanmaraş, Turkey, Environ Monit Assess, 151, 327–336.

Anstee, J. M., Botha, E. J., & Dekker, A. G., 2009; Study on the remote sensing of estuarine macrophytes and Saltmarsh vegetation on Wallis Lake, CSIRO Water from a Healthy Country Science Report, Department of Primary Industries, NSW.

Banko, G., 1998; *A Review of Assessing the Accuracy of Classifications of Remotely Sensed Data and of Methods Including Remote Sensing Data in Forest Inventory*, INTERIM REPORT IR-98-081, International Institute for Applied Systems Analysis, Laxenburg, Austria.

Bajjouk, T., Guillaumont, B., & Populus, J., 1996; Application of airborne imaging spectrometry system data to intertidal seaweed classification and mapping, *Hydrobiologia,* 326, 463 – 471.

Beck M.W., et al. 2001; The identification, conservation, and management of estuarine and marine nurseries for fish and invertebrates, *BioScience*, 51: 633–641.

Behrens, R. J., 1998; *Change Detection Analysis with Spectral Thermal Imagery*; Naval PostGraduate School, Monterey, California; Thesis, Available at: <http://www.nps.edu/Faculty/Olsen/Student_theses/Behrens_Thesis.pdf>, [Accessed 20th July].

Benlin, X., Fangfang, L., Xingliangc, M., & Huazhong, J., 2008; Study on Independent Component Analysis' Application In Classification And Change Detection of Multispectral Images, *The International Archives of the Photogrammetry, Remote Sensing and Spatial Information Sciences.* Vol. XXXVII. Part B7. Beijing.

Boese, B. L., Kaldy, J. E., Clinton, P. J., Eldridge, P. M., Folger, C. L., 2009; Recolonization of intertidal Zostera marina L. (eelgrass) following experimental shoot removal, *Journal of Experimental Marine Biology and Ecology*, 374, 69–77.

Bortone, S. A., 2000; *Seagrasses: Monitoring, Ecology, Physiology, and Management*, CRC Press LLC, USA.

Bos, A. R., Bouma, T. J., Kort, G. L. J., & Katwijk, M. M., 2007; Ecosystem engineering by annual intertidal seagrass beds: Sediment accretion and modification, *Estuarine, Coastal and Shelf Science*, 74, 344 – 348.

Brivio, P. A., Giardino, C., & Zilioli, E., 2001; Determination of chlorophyll concentration changes in Lake Garda using an image-based radiative transfer code for Landsat TM images, *International Jounal of Remote Sensing*, 22, 487 – 502.

Bryant, S., 2002; *Conservation Assessment of Beach Nesting & Migratory Shorebirds in Tasmania:* Natural Heritage Trust Project No NWP 11990, Nature Conservation Branch, Department Primary Industries Water and Environment.

Butler, A., & Jernakoff, P., 1999; *Seagrass in Australia: strategic review and development of an R & D plan*, CSIRO publishing, Victoria, Australia.

Cambridge, M. L., & Kendrick, G. A., 2009; Contrasting responses of seagrass transplants (Posidonia australis) to nitrogen, phosphorus and iron addition in an estuary and a coastal embayment, *Journal of Experimental Marine Biology and Ecology,* 371, 34 – 41.

Campbell, M. L., 2003; Recruitment and colonisation of vegetative fragments of Posidonia australis, Aquatic Botany, 76, 2, 175 – 184.

Campbell, S. J., & McKenzie, L. J., 2004; Flood related loss and recovery of intertidal seagrass meadows in southern Queensland, Australia, *Estuarine, Coastal and Shelf Science*, 60, 477 – 490.

Chang, C. W., Lim, K. H., & Liew, S. C., 2001; Cloud Mask for MODIS, *Centre for Remote Imaging, Sensing and Processing*, Faculty of Science, National University of Singapore.

Ciraolo, G., Cox, E., Loggia, G. L., & Maltese, A., 2006; The classification of submerged vegetation using hyperspectral MIVIS data, Annals of Geophysics, 49, 1.

Clarke, S. M., & Kirkman, H., 1989; Seagrass dynamics. In *Biology of Seagrasses: A Treatise on the Biology of Seagrasses with Special Reference to the Australian Region,* ed. Larkum, A. W. D., McComb, A. J. & Shepherd, S. A., Elsevier, Amsterdam, 304 – 345.

Congalton, R., 1991; A Review of Assessing the Accuracy of Classi_cations of Remotely Sensed Data, *Remote Sensing of Environment*, 37, 35 – 46.

Coppin, P., Jonckheere, I., Nackaerts, K., & Muys, B., 2004; Digital change detection methods in ecosystem monitoring: a review, *International Journal of Remote Sensing*, 25, 9, 1565–1596.

Cradle Coast Natural Resource Management (CCNRM), 2005; *Cradle Coast Natural Resource Management Strategy*, Cradle Coast Natural Resource Management Committee.

Crawford, C., & White, C., 2007; Establishing key estuaries and coastal waters for monitoring in the Cradle Coast NRM region, Marine Research Laboratories – Tasmanian Aquaculture & Fisheries Institute, Nubeena Crescent, Taroona, Tasmania.

Dekker, A., Mount, R., & Jordan, A., 2007; *Satellite and Airborne Imagery including Aerial Photography for Benthic Habitat Mapping*, in Todd, B. J., & Green, H. G., eds., Mapping the Seafloor for Habitat Characterization: Geological Association of Canada, Special Paper 47, 11 – 27.

Deng, J. S., Wang, K., Deng, Y. H. and Qi, G. J., 2008; PCA-based land-use change detection and analysis using multitemporal and multisensor satellite data, *International Journal of Remote Sensing*, 29, 16, 4823 – 4838.

Deng, J. S., Wang, K., Li, J., & Deng, Y. H., 2009; Urban Land Use Change Detection Using Multisensor Satellite Images, *Pedosphere*, 19, 1, 96 – 103.

Department for Environment, Heritage and Aboriginal Affairs (DEHAA) 1998; Change in Seagrass Coverage: and links to the water quality off the Adelaide metropolitan coastline, Environment Protection Agency, Government of South Australia.

Department of Primary Industries, Water and Environment (DPIWE), 2003; *State of the River Report for the Montagu River Catchment,* Water Assessment and Planning Branch, Department of Primary Industries, Water and Environment, Hobart. Technical Report No. WAP 03/09.

Department of Primary Industries, Water and Environment (DPIWE), 2003b; *State of the River Report for the Montagu River Catchment.* Water Assessment and Planning Branch, Department of Primary Industries, Water and Environment, Hobart. Technical Report No. WAP 03/09.

Department of Primary Industries, Water and Environment (DPIWE), 2005; *Waterways monitoring report, Welcome catchment.* Water Resources Division, Department of Primary Industry, Water and Environment.

Department of Primary Industries, Parks, Water and Environment (DPIPWE), 2009; Tasmania's Nature Conservation Strategy 2002 – 2006 Final Report: An action plan to protect Tasmania's natural diversity and maintain ecological processes and systems, Biodiversity Conservation Branch, Department of Primary Industries, Parks, Water and Environment, Available at:
< http://www.dpipwe.tas.gov.au/inter.nsf/WebPages/JCOK-5KZTT4?open>, [Accessed 1st Oct].

Dierssen, H. M., Zimmerman, R. C., Leathers, R. A., Downes, T. V., & Davis, C. O., 2003; Ocean color remote sensing of seagrass and bathymetry in the Bahamas Banks by high-resolution airborne imagery, *Limnol. Oceanogr.*, 48, 444- 455.

Dobson, J. E., Bright, E. A., Ferguson, R. L., Field, D. W., Wood, L. L., Haddad, K. D., Iredale, H., Jensen, J. R., Klemas, V. V., Orth, R. J., & Thomas, J. P., 1995; *NOAA Coastal Change Analysis Program (C-CAP): Guidance for Regional Implementation.* NOAA Technical Report NMFS 123. U.S. Department of Commerce, Seattle, WA.

Dorigo, W. A., Zurita-Milla, R., de Wit, A. J. W., Brazile, J., Singh, R., & Schaepman, M. E., 2007; A review on reflective remote sensing and data assimilation techniques for enhanced agroecosystem modeling, *International Journal of Applied Earth Observation and Geoinformation,* 9, 165- 193.

Du, Y., Teillet, P.M., & Cihlar, J., 2002; Radiometric normalization of multitemporal high-resolution satellite images with quality control for land cover change detection. Remote Sensing of environment, 82, 123 - 134.

Du, Q., Kopriva, I., & Szu, H., 2004; Independent Component Analysis For Classifying Multispectral Images With Dimensionality Limitation, *International Journal of Information Acquisition,* 1, 3, 201 – 216.

Duarte, C. M., 1991; Seagrass depth limits, *Aquatic Botany*, 40, 4, 363 – 377.

Duarte, C. M., 2002; The future of seagrass meadows, *Environmental Conservation,* 29, 2, 192 – 206.

Dunn, H., 2000; Boullanger Bay/Robbins Passage Ramsar Nomination: Report of a Natural Heritage Trust Project, *Natural Heritage Trust*, Hobart.

Earth Observation Research Centre (EORC), 1997; About ALOS: Overview and Objectives, Earth Observation Research Centre, JAXA, Available at:
< http://www.eorc.jaxa.jp/ALOS/en/about/about_index.htm>, [Accessed 1st Aug].

Eckhardt, D.W., Verdin, J.P., & Lyford, G.R., 1990; Automated update of an irrigated lands GIS using SPOT HRV imagery, *PhotogrammetricEngineering and Remote Sensing*, 56, 1515 – 1522.

Edgar, G.J., Barrett, N.S., & Graddon, D.J., 1999; *A classification of Tasmanian estuaries and assessment of their conservation significance using ecological and physical attributes, population and land use.* Technical report series no 2. Marine Research Laboratories – Tasmanian Aquaculture and Fisheries Institute, University of Tasmania.

Edyvane, K., 2003; *Conservation, Monitoring and Recovery of Threatened Giant Kelp (Macrocystis pyrifera) Beds in Tasmania – Final Report,* Department of Primary Industries, Water and Environment, Tasmania.

ESRI, 2009; ArcGIS v. 9.2., Environmental Systems Research Institute, Redlands, CA.

Everitt, J.H., Yang, C., Sriharan, S., & Judd, F.W., 2009; Using high resolution satellite imagery to map black mangrove on the Texas Gulf Coast. *Journal of Coastal Research,* 24, 6, 1582 – 1586.

Ferguson R. L., & Korfmacher K., 1997; Remote sensing and GIS analysis of seagrass meadows in North Carolina, USA, Aquatic Botany, 58, 3, 241-258.

Ferwerda, J. G., Leeuw, J. D., Atzberger, C., & Vekerdy, Z., 2007 ;Satellite-based monitoring of tropical seagrass vegetation: current techniques and future developments, *Hydrobiologia*, 591, 59–71.

Fung, T., & LeDrew, E., 1987; Application on Principal Component Analysis to Change Detection, *Photogrammetric Engineering and Remote Sensing*, 53, 12, 1649 – 1658.

Geoscience Australia (GA), 2009; ALOS Satellite data, Geoscience Australia, Australian Government, Available at;
< http://www.ga.gov.au/remote-sensing/satellites-sensors/alos.jsp>, [Accessed 3rd Oct].

Gilmore, E. T., Frazier, P. D., & Chouikha, M. F., 2004; An Independent Component Analysis Based Image Classification Scheme, IEEE International Conference on Acoustics, Speech, and Signal Processing, Available at: <http://www.ece.umassd.edu/Faculty/acosta/ICASSP/Icassp_2004/pdfs/0300577.pdf>, [Accessed 5th Sep].

Global Land Cover Facility (GLCF) 2009, "Data Formats", GLCF, Earth Science Data Interface, University of Maryland, Available at: < http://glcfapp.umiacs.umd.edu:8080/esdi/index.jsp>, [Accessed 3rd Oct].

Gluck M., Rempel R. and Uhlig P.W.C. 1996. An evaluation of remote sensing for regional wetland mapping applications. For est Research Report No. 137. Ontario Forest Research Institute, Sault Ste Marie, Ontario, Canada, 33 pp, In Satellite remote sensing of wetlands, Ozesmi, S. L., & Bauer, M. E., 2002, *Wetlands Ecology and Management,* 10, 381 – 402.

Gullström, M., Lunde´n, B., Bodin, M., Kangwe, J., O¨ hman, M. C., Mtolera, M. S. P., & Bjo¨rk, M., 2006; Assessment of changes in the seagrass-dominated submerged vegetation of tropical Chwaka Bay (Zanzibar) using satellite remote sensing, *Estuarine, Coastal and Shelf Science*, 67, 399 – 408.

Hemminga, M., & Duarte, C.M., 2000; *Seagrass Ecology*, Cambridge, UK: Cambridge University Press.

Hill, L. L., 2006; *Georeferencing: The Geographic Associations of Information*, Massachusetts Institute of Technology, Cambridge, Massachusetts London, England.

Hoan, N. T., & Tateishi, R., 2008; Cloud Removal of Optical Image using SAR Data for ALOS Applications. Experimenting on Simulated ALOS Data, *The International Archives of the Photogrammetry, Remote Sensing and Spatial Information Sciences,* Vol. XXXVII. Part B4. Beijing.

Hong, G., & Zhang, Y., 2008; A comparative study on radiometric normalization using high resolution satellite images, *International Journal of Remote Sensing*, 29, 2, 425 – 438.

Hyvärinen, A., 1999; Survey on Independent Component Analysis, *Neural Computing Surveys,* 2, 94-128.

Hyvärinen, A., & Oja, E., 2000; Independent Component Analysis: Algorithms and Applications, *Neural Networks,* 13, (4-5), 411-430.

Janzen, D. T., Fredeen, A. L., & Wheate, R. D., 2006; Radiometric correction techniques and accuracy assessment for Landsat TM data in remote forested regions, Canadian Journal of Remote Sensing, 32, 5, 330 – 340.

Japan Aerospace Exploration Agency (JAXA), 2007; ALOS. Overview, Japan Aerospace Exploration Agency, Available at; <http://www.jaxa.jp/projects/sat/alos/index_e.html>, [Accessed 3rd Oct].

Jensen, J.R., Narumalani, S., Weatherbee, O., & Mackey, H.E. Jr, 1993; Measurement of seasonal and yearly cattail and waterlily changes using multidate SPOT panchromatic data, *Photogram metric Engineering and Remote Sensing,* 59, 519 – 525, In Satellite remote sensing of wetlands, Ozesmi, S. L., & Bauer, M. E., *Wetlands Ecology and Management,* 10, 381 – 402.

Jensen, J. R., 2005; *Introductory digital image processing: a remote sensing perspective (3rd ed),* Pearson Prentice Hall, the U.S.A.

Ju, C. L., Chen, C. F., Chang, L. Y., & Chang, H. Y., 2006; Multi-Temporal Satellite Image Classification Using Spectral Class Database, Asian Conference on Remote Sensing, Available at: < http://www.aars-acrs.org/acrs/proceeding/ACRS2006/Papers/P-3_P64.pdf>, [Accessed 15th Sep].

Kelly, N. M., Fonseca, M., & Whitefield, P., 2001; Predictive mapping for management and conservation of seagrass beds in North Carolina, *AQUATIC CONSERVATION: MARINE AND FRESHWATER ECOSYSTEMS*, 11, 437 – 451.

Kelly, E., (ed.), 2005; The role of kelp in the marine environment, *Irish Wildlife Manuals*, No. 17, National Parks and Wildlife Service, Department of Environment, Heritage and Local Government, Dublin, Ireland.

Kemp, W. M., 2000; Chapter 1: Seagrass Ecology and Management: An Introduction, In Bortone, S. A., (eds) 2000; *Seagrasses: Monitoring, Ecology, Physiology, and Management*, CRC Press LLC, USA.

Kendrick, G. A., Hegge, B. J., Wyllie, A., Davidson, A., & Lord, D. A., 2000; Changes in Seagrass Cover on Success and Parmelia Banks, Western Australia Between 1965 and 1995, *Estuarine, Coastal and Shelf Science,*50, 341 – 353.

Kenworthy, W. J., 2000; The role of sexual reproduction in maintaining populations of *Halophila decipiens:* Implications for the biodiversity and conservation of tropical seagrass ecosystems, *Pacific Conservation Biology,* 5, 260 – 268.

Kirkman, H., 1990; *Seagrass distribution and mapping*, In Phillips, R. C., & McRoy, C. P., (eds); *Seagrass research methods*, Unesco, Paris.

Kirkman, H., 1996; Baseline and Monitoring Methods for Seagrass Meadows, *Journal of Environmental Management,* 47, 191 – 201

.

Kirkman, H. 1997, *Seagrasses of Australia*, Australia: State of the Environment Technical Paper Series (Estuaries and the Sea), Department of the Environment, Canberra.

Klemas, V. V., 2001; Remote Sensing of Landscape-Level Coastal Environmental Indicators, *Environmental Management*, l. 27, 1, 47–57.

Larkum, A.W.D., & West, R.J., 1990; Long-term changes of seagrass meadows in Botany Bay, Australia, *Aquatic Botany*, 37, 55 – 70, In *Seagrasses of Australia*, Kirkman, H., Australia: State of the Environment Technical Paper Series (Estuaries and the Sea), Department of the Environment, Canberra.

Lathauwer, L. D., Moor, B. D., & Vandewalle, J., 2000; An introduction to independent component analysis, Journal of Chemometrics, 14: 123–149.

Li, X., & Yeh, A. G. O., 1998; Principal component analysis of stacked multi-temporal images for the monitoring of rapid urban expansion in the Pearl River Delta, *int. j. remote sensing*, 19, 8, 1501 – 1518.

Lillesand, T., M., & Kiefer, R., W., 2008; *Remote sensing and image interpretation (6th ed)*, John Wiley & Sons, Inc, U. S. A.

LIST, 2003; The Land Information System Tasmania (The LIST), Data version supplied 2003.

Longstaff, B. J., Dennison, W. C., 1999; Seagrass survival during pulsed turbidity events: The effects of light deprivation on the seagrasses *Halodule pinifolia* and *Halophila ovalis, Aquatic Botany*, 65, 105 – 121.

Lotsch, A., Friedl, M. A., & Pinzón, J., 2003; Spatio–Temporal Deconvolution of NDVI Image Sequences Using Independent Component Analysis, IEEE Transactions on Geoscience and Remote Sensing, 41, 12.

Lu, D., Mausel, P., Brondízio, E. & Moran, E., 2004; Change detection techniques, International Journal of Remote Sensing,25:12,2365 – 2401.

Lu, D., & Weng, Q., 2007; A survey of image classification methods and techniques for improving classification performance, *International Journal of Remote Sensing*, 28, 5, 823 - 870.

Lyzenga, D. R., 1978; Passive remote sensing techniques for mapping water depth and bottom features, *Applied Optics*, 17, 3, 379 – 383.

Lyzenga, D.R., 1981; Remote sensing of bottom reflectance and water attenuation parameters in shallow water using aircraft and Landsat data, *International Journal of Remote Sensing*, 10, 53 – 69.

Macleod, R. D., & Congalton, R. G., 1998; A Quantitative Comparison of Change-Detection Algorithms for Monitoring Eelgrass from Remotely Sensed Data, *Photogrammetric Engineering & Remote Sensing*, 64, 3, 207 – 216.

Mas, J. F., 1999; Monitoring land-cover change: a comparison of change detection Techniques, *International Journal of Remote Sensing*, 20, 139 – 152.

Matarrese, R., Acquaro, M., Morea, A., Tijani, K., Chiaradia, M. T., 2008; Applications of Remote Sensing Techniques for Mapping *Posidonia Oceanica* Meadows, IEEE, Dept. of Physics, University and Polytechnic of Bari.

Markham, B., L. Williams, D. L., & Irons, J. R., 2004; Landsat sensor performance: history and current status, *IEEE Transactions on Geoscience and Remote Sensing*, 42, 12, 2691 – 2694.

McKenzie, L. J., Finkbeiner, M. A., & Kirkman, H., 2001a; *Methods for mapping seagrass distribution*, In: *Global Research Methods*, ed. Short, F. T., & Coles, R. G., Elsevier Science B. V., Amsterdam.

McKenzie, L. J., Campbell, S. J., & Roder, C. A., 2001b; Seagrass-Watch: Manual for Mapping & Monitoring Seagrass Resources by Community (citizen) volunteers. (QFS, NFC, Cairns) 100pp.

Meehan, A. J., & West, R. J., 2000; Recovery times for a damaged *Posidonia australis* bed in south eastern Australia, *Aquatic Botany,* 67, 161 – 167.

Meehan, A. J., Williams, R. J., & Watford, F. A., 2005; Detecting Trends in Seagrass Abundance Using Aerial Photograph Interpretation: Problems Arising with the Evolution of Mapping Methods, *Estuaries*, 28, 3, 462 – 472.

Morisette, J. T., 1997; *Using Generalized Linear Models to Enhance Satellite Based Land Cover Change Detection*, the Graduated Faculty of North Carolina State University, U.S.A, Available at: <http://www.lib.ncsu.edu/theses/available/etd-19970411-115134/>, [Accessed 5th Sep].

Mount, R. E., 2007; Rapid Monitoring of Extent and Condition of Seagrass Habitats with Aerial Photography "Mega-Quadrats", Spatial Science, 52, 1, 105 – 120.

Mumby, P.J., CLARK, C. D., GREEN, E. P., & EDWARDS, A. J., 1998; Benefits of water column correction and contextual editing for mapping coral reefs, *Int. J. Remote Sensing*, 19, 1, 203 – 210.

Munyati, C., 2000; Wetland change detection on the Kafue Flats, Zambia, by classification of a multitemporal remote sensing image dataset, *Internationa l Journal of Remote Sensing,*21, 9, 1787–1806.

Munyati, C., 2004; Use of Principal Component Analysis (PCA) of Remote Sensing Images in Wetland Change Detection on the Kafue Flats, Zambia, *Geocarto International*, 19, 3, 11 - 22.

National Aeronautics and Space Administration (NASA), 2009; The Landsat program, National Aeronautics and Space Administration, Available at: <http://landsat.gsfc.nasa.gov/>, [Accessed 3rd Oct].

Navalgund, R. R., Jayaraman, V., & Roy, P. S., 2007; Remote sensing applications: An overview, Current Science, 93, 12, 25.

Oliveira, E. D., Populus, J., & Guillaumont, B., 2006; Predictive modelling of coastal habitats using remote sensing data and fuzzy logic: A case for seaweed in Brittany (France), *European Association of Remote Sensing Laboratories*, 5, 2, 208-223.

Orth, R. J., Carruthers, T. J.B., Dennison, W. C., Duarte, C. M., Fourqurean, J. W., Heck, K. L., Hughes, A. R., Kendrick, G. A., Kenworthy, W. J., Olyarnik, S., Short, F. T., Waycott, M., & Williams, S. L., 2006; A Global crisis for seagrass ecosystems, *BioScience*, 56, 12, 987 – 996.

Ozesmi, S. L., & Bauer, M. E., 2002; Satellite remote sensing of wetlands, *Wetlands Ecology and Management,* 10, 381 – 402.

Paine, D. P., & Kiser, J. D., 2003; *Aerial Photography and Image interpretation (2^{nd} ed),* John Wiley & Sons, Inc., New Jersey, Canada.

Pasqualini, V., Pergent-Martini, C., Pergent, G., Agreil, M., Skoufas, G., Sourbes, L., & Tsirika, A., 2005; Use of SPOT 5 for mapping seagrasses: An application to Posidonia oceanica, *Remote Sensing of Environment*, 94, 39 – 45.

Paolini, L., Grings, F., Sobrino, J. A., Muñoz, J. C. J., & Karszenbaum, H., 2006; Radiometric correction effects in Landsat multi-date/multi-sensor change detection studies, *International Journal of Remote Sensing*, 27, 4, 685 – 704.

Phinn, S.R., 1998; A framework for selecting appropriate remotely sensed data dimensions for environmental monitoring and management. International Journal of Remote Sensing, 19, 3457–3463.

Phinn, S., Hess, L., & Finlayson, C. M., 1999; An assessment of the usefulness of remote sensing for wetland inventory and monitoring in Australia, In *Techniques for enhanced wetland inventory and monitoring, Supervising Scientist Report 147*, ed., Finlayson, C. M., & Spiers, A. G., Supervising Scientist, Camberra.

Phinn, S., Roelfsema, C., Dekker, A., & Brando, V., 2006a; Remote Sensing Applications requiring research, The University of Queensland, Available at; < http://www.gpem.uq.edu.au/CRSSIS/tools/rstoolkit/pdf/research.pdf >, [Accessed 10^{th} Sep

Phinn, S. R., Roelfsema, C. M., Dekker, A. G., Brando, V. E., Anstee, J., & Daniel, P., 2006b; Remote sensing for coastal ecosystem indicators assessment and monitoring; Maps, techniques and error assessment for seagrass benthic habitat in Moreton Bay, Technical Report 76, Cooperative Research Centre for Coastal Zone, Estuary and Waterway Management, Australia.

Preen, A.R., Lee Long, W.J., Coles, R.G., 1995; Flood and cyclone related loss, and partial recovery, of more than 1000 km2, *Aquatic Botany*, 52, 3 – 17.

Rees, C.G., 1993; *Tasmanian Seagrass communities*, Masters Thesis (M.Env.St.), University of Tasmania.

Richards, J. A., & Jia. X., 2006; *Remote Sensing Digital Image analysis: An Introduction, Fourth Edition*, Springer Berlin Heidelberg.

Robila, S. A., Haaland, P., Achalakul, T., & Taylor, S., 2000; *Exploring Independent Component Analysis for remote sensing*, Proceedings of the Workshop on Multi/Hyperspectral Sensors, Measurements, Modeling and Simulation, Redstone Arsenal, Alabama, U.S. Army Aviation & Missile Command.

Rogan, J., & Chen, D. M., 2004; Remote sensing technology for mapping and monitoring land-cover and land-use change, *Progress in Planning*, 61, 301–325.

RSI, 2009; Environment for Visualizing Images, ENVI, v. 4.6., Research Systems Inc., Boulder, Colo.

Sabins, F. F., 1997; *REMOTE SENSING Principles and Interpretation*, 3rd edn, W. H. Freeman and Company, New York.

Shah, C. A., Anderson, I., Gou, Z., Hao, S., & Leason, A., 2007; *Towards the development of next generation remote sensing technology – ERDAS IMAGINE incorporates a higher order feature extraction technique based on ICA*, To be published in Proceedings of American Society of Photogrammetry and Remote Sensing, Tampa, FL, Available at: <http://web.ecs.syr.edu/~cashah/ASPRS07ICAFeatureExtraction.pdf>, [Accessed 5th Sep].

Shanmugam, P., Ahn, Y., & Sanjeevi, S., 2006; A comparison of the classification of wetland characteristics by linear spectral mixture modelling and traditional hard classifiers on multispectral remotely sensed imagery in southern India, Ecological modelling, 194, 379 – 394.

Shapiro, A. C., & Rohmann, R. O., 2006; Mapping Changes in Submerged Aquatic Vegetation using Landsat Imagery and Benthic Habitat Data: Coral Reef Ecosystem Monitoring in Vieques Sound Between 1985 and 2000, *Bulletin of Marine Science*, 79, 2, 375 – 388.

Short, F. T., & Wyllie-Echeverria, S., 1996; Natural and human-induced disturbance of seagrasses, *Environmental Conservation*, 23, 1, 17 – 27.

Short, F. T., Coles, R. G., & Pergent-Martini, C., 2001; *Global seagrass distribution*, In: *Global Research Methods*, ed. Short, F. T., & Coles, R. G., Elsevier Science B. V., Amsterdam.

Shlens, J., 2005; A Tutorial on Principal Component Analysis, Center for Neural Science, New York University, Available at: <http://www.snl.salk.edu/~shlens/notes.html>, [Accessed 5th Sep].

Silva, T. S. F., Costa, M. P. F., Melack, J. M., Novo, E. M. L. M., 2008; Remote sensing of aquatic vegetation: theory and applications, Environ Monit Assess, 140, 131–145.

Smith, L. I., 2002; A tutorial on Principal Components Analysis, Department of Computer Science, University of Otago, Available at: <http://www.cs.otago.ac.nz/cosc453/student_tutorials/principal_components.pdf>, [Accessed 5th Sep].

Song, D. J., Ke, W., Jun, L., & Hua, D. Y., 2009; Urban Land Use Change Detection Using Multisensor Satellite Images, *Pedosphere*, 19, 1, 96 – 103.

Sprod, D., Armstrong, d., & Ketelaar, A., 2003; Cradle Coast Natural Resource Management Strategy: Situation Paper, Natural Heritage Trust.

Spruzen, F. L., Richardson, A. M. M., & Woehler, E. J., 2008; Spatial variation of intertidal macroinvertebrates and environmental variables in Robbins Passage wetlands, NW Tasmania, *Hydrobiologia*, 598, 325–342.

Swain, P. H., & Davis, S. M., (eds.), 1978; *Remote Sensing: The Quantitative Approach*, McGraw – Hill, N. Y.

Trautman, D. A., & Borowitzka, M. A., 1999; Distribution of the epiphytic organisms on *Posidonia australis* and *P. sinuosa,* two seagrasses with differing leaf morphology, Marine Ecology Progress Series, 179, 215-229.

Thomas, J. P., 1995; Remote sensing and relating coastal development to living marine resources, Natural Areas Journal, 15, 1, 21 – 36.

Thorhaug, A., Richardson, A. D., & Berlyn, G. P., 2006; Spectral Reflectance of *THALASSIA TESTUDINUM* (HYDROCHARITACEAE) Seagrass: Low Salinity Effects, *American Journal of Botany*, 93, 1, 110 - 117.

U.S. Geological Survey (USGS), 2005; *Landsat: A Global Land Imaging Project; Geography – Land Remote Sensing*, U.S. Geological Survey, Available at: <http://landsat.usgs.gov/about_project_descriptions.php>, [Accessed 1st Aug].

Valta-Hulkkonen, K., Kanninen, A., & Pellikka, P., 2004; Remote sensing and GIS for detecting changes in the aquatic vegetation of a rehabilitated lake, *International Journal of Remote Sensing*, 25, 24, 5745 – 5758.

Verbyla, D. L., 1995; *SATELLITE REMOTE SENSING of NATURAL RESOURCES*, CRC Press, Inc, Florida.

Wabnitz, C. C., Andréfouët, S., Torres-Pulliza, D., Muller-Karger, F. E., & Kramer, P. A., 2008; Regional-scale seagrass habitat mapping in the Wider Caribbean region using Landsat sensors: Applications to conservation and ecology, *Remote Sensing of Environment*, doi:10.1016/j.rse.2008.01.020, 1 – 13.

Wang, Z., Yu, X., Zhang, L., 2008; A Remote Sensing Image Fusion Algorithm Based on Ordinal Fast Independent Component Analysis, *Proceedings of the International Workshop on Knowledge Discovery and Data Mining*, WKDD, Adelaide, Australia.

Xia, L., Ruan, R., Zhang, X., 2007; *Change Detection of Wetland in Hongze Lake using a Time Series of Remotely Sensed Imagery*, ISPRS Workshop on Updating Geo-spatial Databases with Imagery & The 5th ISPRS Workshop on DMGISs, Urumchi, China.

Zhong, J., & Wang, R., 2006; Multi-temporal remote sensing change detection based on independent component analysis, *International Journal of Remote Sensing*, 27, 10, 2055 — 2061.

Appendix 1 Change statistics between 1990 and 2000, whole Boullanger Bay

Pixel Counts	Saltmarsh [Green]	Sparse SAV [Sea Green]	Sand [Yellow]	Dense SAV [Cyan]	Row Total	Class Total
Unclassified	319	153	5504	3188	9164	84791
Saltmarsh [Green]	3071	158	12	0	3241	3241
Sparse SAV [Sea Green]	226	19172	5722	2022	27142	27148
Sand [Yellow]	415	7220	39673	4029	51337	52101
Dense SAV [Cyan]	3	851	3905	36965	41724	45156
Deep Water [Blue]	1	3	10277	11831	22112	67861
Cloud [White]	0	0	0	0	0	0
Masked Pixels	0	0	0	0	0	0
Class Total	4035	27557	65093	58035	0	0
Class Changes	964	8385	25420	21070	0	0
Image Difference	-794	-409	-12992	-12879	0	0

Percentages	Saltmarsh [Green]	Sparse SAV [Sea Green]	Sand [Yellow]	Dense SAV [Cyan]	Row Total	Class Total
Unclassified	7.906	0.555	8.456	5.493	10.808	100
Saltmarsh [Green]	76.109	0.573	0.018	0	100	100
Sparse SAV [Sea Green]	5.601	69.572	8.79	3.484	99.978	100
Sand [Yellow]	10.285	26.2	60.948	6.942	98.534	100
Dense SAV [Cyan]	0.074	3.088	5.999	63.694	92.4	100
Deep Water [Blue]	0.025	0.011	15.788	20.386	32.584	100
Cloud [White]	0	0	0	0	0	0
Masked Pixels	0	0	0	0	0	0
Class Total	100	100	100	100	0	0
Class Changes	23.891	30.428	39.052	36.306	0	0
Image Difference	-19.678	-1.484	-19.959	-22.192	0	0

Area (Square Meters)	Saltmarsh [Green]	Sparse SAV [Sea Green]	Sand [Yellow]	Dense SAV [Cyan]	Row Total	Class Total
Unclassified	199375	95625	3440000	1992500	5727500	52994375
Saltmarsh [Green]	1919375	98750	7500	0	2025625	2025625
Sparse SAV [Sea Green]	141250	11982500	3576250	1263750	16963750	16967500
Sand [Yellow]	259375	4512500	24795625	2518125	32085625	32563125
Dense SAV [Cyan]	1875	531875	2440625	23103125	26077500	28222500
Deep Water [Blue]	625	1875	6423125	7394375	13820000	42413125
Cloud [White]	0	0	0	0	0	0
Masked Pixels	0	0	0	0	0	0
Class Total	2521875	17223125	40683125	36271875	0	0
Class Changes	602500	5240625	15887500	13168750	0	0
Image Difference	-496250	-255625	-8120000	-8049375	0	0

Appendix 2 Change statistics between 2000 and 2004, whole Boullanger Bay

Pixel Counts	Saltmarsh [Green]	Sparse SAV [Sea Green]	Sand [Yellow]	Dense SAV [Cyan]	Row Total	Class Total
Unclassified	6	91	954	1927	2978	59370
Saltmarsh [Green]	2947	99	193	1	3240	3390
Sparse SAV [Sea Green]	170	18085	6332	961	25548	25641
Sand [Yellow]	117	7746	38563	1991	48417	51086
Dense SAV [Cyan]	1	1127	4245	29357	34730	43951
Deep Water [Blue]	0	0	1814	10919	12733	96860
Cloud [White]	0	0	0	0	0	0
Masked Pixels	0	0	0	0	0	0
Class Total	3241	27148	52101	45156	0	0
Class Changes	294	9063	13538	15799	0	0
Image Difference	149	-1507	-1015	-1205	0	0

Percentages	Saltmarsh [Green]	Sparse SAV [Sea Green]	Sand [Yellow]	Dense SAV [Cyan]	Row Total	Class Total
Unclassified	0.185	0.335	1.831	4.267	5.016	100
Saltmarsh [Green]	90.929	0.365	0.37	0.002	95.575	100
Sparse SAV [Sea Green]	5.245	66.616	12.153	2.128	99.637	100
Sand [Yellow]	3.61	28.532	74.016	4.409	94.775	100
Dense SAV [Cyan]	0.031	4.151	8.148	65.012	79.02	100
Deep Water [Blue]	0	0	3.482	24.181	13.146	100
Cloud [White]	0	0	0	0	0	0
Masked Pixels	0	0	0	0	0	0
Class Total	100	100	100	100	0	0
Class Changes	9.071	33.384	25.984	34.988	0	0
Image Difference	4.597	-5.551	-1.948	-2.669	0	0

Area (Square Meters)	Saltmarsh [Green]	Sparse SAV [Sea Green]	Sand [Yellow]	Dense SAV [Cyan]	Row Total	Class Total
Unclassified	3750	56875	596250	1204375	1861250	37106250
Saltmarsh [Green]	1841875	61875	120625	625	2025000	2118750
Sparse SAV [Sea Green]	106250	11303125	3957500	600625	15967500	16025625
Sand [Yellow]	73125	4841250	24101875	1244375	30260625	31928750
Dense SAV [Cyan]	625	704375	2653125	18348125	21706250	27469375
Deep Water [Blue]	0	0	1133750	6824375	7958125	60537500
Cloud [White]	0	0	0	0	0	0
Masked Pixels	0	0	0	0	0	0
Class Total	2025625	16967500	32563125	28222500	0	0
Class Changes	183750	5664375	8461250	9874375	0	0
Image Difference	93125	-941875	-634375	-753125	0	0

Appendix 3 Change statistics between 2004 and 2006, whole Boullanger Bay

Pixel Counts	Saltmarsh [Green]	Sparse SAV [Sea Green]	Sand [Yellow]	Dense SAV [Cyan]	Row Total	Class Total
Unclassified	656	5053	16853	15519	38081	109172
Saltmarsh [Green]	2008	469	43	1	2521	2523
Sparse SAV [Sea Green]	397	14636	5608	415	21056	21112
Sand [Yellow]	327	4318	24631	4508	33784	42443
Dense SAV [Cyan]	2	1162	2981	21111	25256	36026
Deep Water [Blue]	0	3	970	2397	3370	69022
Cloud [White]	0	0	0	0	0	0
Masked Pixels	0	0	0	0	0	0
Class Total	3390	25641	51086	43951	0	0
Class Changes	1382	11005	26455	22840	0	0
Image Difference	-867	-4529	-8643	-7925	0	0

Percentages	Saltmarsh [Green]	Sparse SAV [Sea Green]	Sand [Yellow]	Dense SAV [Cyan]	Row Total	Class Total
Unclassified	19.351	19.707	32.989	35.31	34.882	100
Saltmarsh [Green]	59.233	1.829	0.084	0.002	99.921	100
Sparse SAV [Sea Green]	11.711	57.08	10.978	0.944	99.735	100
Sand [Yellow]	9.646	16.84	48.215	10.257	79.599	100
Dense SAV [Cyan]	0.059	4.532	5.835	48.033	70.105	100
Deep Water [Blue]	0	0.012	1.899	5.454	4.883	100
Cloud [White]	0	0	0	0	0	0
Masked Pixels	0	0	0	0	0	0
Class Total	100	100	100	100	0	0
Class Changes	40.767	42.92	51.785	51.967	0	0
Image Difference	-25.575	-17.663	-16.919	-18.031	0	0

Area (Square Meters)	Saltmarsh [Green]	Sparse SAV [Sea Green]	Sand [Yellow]	Dense SAV [Cyan]	Row Total	Class Total
Unclassified	410000	3158125	10533125	9699375	23800625	68232500
Saltmarsh [Green]	1255000	293125	26875	625	1575625	1576875
Sparse SAV [Sea Green]	248125	9147500	3505000	259375	13160000	13195000
Sand [Yellow]	204375	2698750	15394375	2817500	21115000	26526875
Dense SAV [Cyan]	1250	726250	1863125	13194375	15785000	22516250
Deep Water [Blue]	0	1875	606250	1498125	2106250	43138750
Cloud [White]	0	0	0	0	0	0
Masked Pixels	0	0	0	0	0	0
Class Total	2118750	16025625	31928750	27469375	0	0
Class Changes	863750	6878125	16534375	14275000	0	0
Image Difference	-541875	-2830625	-5401875	-4953125	0	0

Appendix 4 Change statistics between 2006 and 2008, whole Boullanger Bay

Pixel Counts	Saltmarsh [Green]	Sparse SAV [Sea Green]	Sand [Yellow]	Dense SAV [Cyan]	Row Total	Class Total
Unclassified	1	3	1436	1128	2568	63336
Saltmarsh [Green]	2007	348	271	0	2626	3293
Sparse SAV [Sea Green]	415	14802	6770	780	22767	31834
Sand [Yellow]	100	5196	24356	4578	34230	49744
Dense SAV [Cyan]	0	761	5348	20432	26541	47964
Deep Water [Blue]	0	2	4262	9108	13372	84127
Cloud [White]	0	0	0	0	0	0
Masked Pixels	0	0	0	0	0	0
Class Total	2523	21112	42443	36026	0	0
Class Changes	516	6310	18087	15594	0	0
Image Difference	770	10722	7301	11938	0	0

Percentages	Saltmarsh [Green]	Sparse SAV [Sea Green]	Sand [Yellow]	Dense SAV [Cyan]	Row Total	Class Total
Unclassified	0.04	0.014	3.383	3.131	4.055	100
Saltmarsh [Green]	79.548	1.648	0.639	0	79.745	100
Sparse SAV [Sea Green]	16.449	70.112	15.951	2.165	71.518	100
Sand [Yellow]	3.964	24.612	57.385	12.707	68.812	100
Dense SAV [Cyan]	0	3.605	12.6	56.715	55.335	100
Deep Water [Blue]	0	0.009	10.042	25.282	15.895	100
Cloud [White]	0	0	0	0	0	0
Masked Pixels	0	0	0	0	0	0
Class Total	100	100	100	100	0	0
Class Changes	20.452	29.888	42.615	43.285	0	0
Image Difference	30.519	50.786	17.202	33.137	0	0

Area (Square Meters)	Saltmarsh [Green]	Sparse SAV [Sea Green]	Sand [Yellow]	Dense SAV [Cyan]	Row Total	Class Total
Unclassified	625	1875	897500	705000	1605000	39585000
Saltmarsh [Green]	1254375	217500	169375	0	1641250	2058125
Sparse SAV [Sea Green]	259375	9251250	4231250	487500	14229375	19896250
Sand [Yellow]	62500	3247500	15222500	2861250	21393750	31090000
Dense SAV [Cyan]	0	475625	3342500	12770000	16588125	29977500
Deep Water [Blue]	0	1250	2663750	5692500	8357500	52579375
Cloud [White]	0	0	0	0	0	0
Masked Pixels	0	0	0	0	0	0
Class Total	1576875	13195000	26526875	22516250	0	0
Class Changes	322500	3943750	11304375	9746250	0	0
Image Difference	481250	6701250	4563125	7461250	0	0

Appendix 5 Change statistics between 1990 and 2000, saltmarsh/ seagrass boundary

Pixel Counts	Masked Pixels	Saltmarsh [Green]	Sparse SAV [Sea Green]	Sand [Yellow]	Dense SAV [Cyan]	Deep Water [Blue]	Row Total	Class Total
Unclassified	0	0	0	0	0	0	0	1633
Saltmarsh [Green]	0	631	9	1	0	0	641	641
Sparse SAV [Sea Green]	0	1	102	31	0	0	134	134
Sand [Yellow]	0	3	65	24	0	0	92	92
Dense SAV [Cyan]	0	0	0	0	0	0	0	0
Deep Water [Blue]	0	0	0	0	0	0	0	0
Cloud [White]	0	0	0	0	0	0	0	0
Masked Pixels	0	0	0	0	0	0	0	0
Class Total	0	635	176	56	0	0	0	0
Class Changes	0	4	74	32	0	0	0	0
Image Difference	0	6	-42	36	0	0	0	0

Percentages	Masked Pixels	Saltmarsh [Green]	Sparse SAV [Sea Green]	Sand [Yellow]	Dense SAV [Cyan]	Deep Water [Blue]	Row Total	Class Total
Unclassified	0	0	0	0	0	0	0	100
Saltmarsh [Green]	0	99.37	5.114	1.786	0	0	100	100
Sparse SAV [Sea Green]	0	0.157	57.955	55.357	0	0	100	100
Sand [Yellow]	0	0.472	36.932	42.857	0	0	100	100
Dense SAV [Cyan]	0	0	0	0	0	0	0	0
Deep Water [Blue]	0	0	0	0	0	0	0	0
Cloud [White]	0	0	0	0	0	0	0	0
Masked Pixels	0	0	0	0	0	0	0	0
Class Total	0	100	100	100	0	0	0	0
Class Changes	0	0.63	42.045	57.143	0	0	0	0
Image Difference	0	0.945	-23.864	64.286	0	0	0	0

Area (Square Meters)	Masked Pixels	Saltmarsh [Green]	Sparse SAV [Sea Green]	Sand [Yellow]	Dense SAV [Cyan]	Deep Water [Blue]	Row Total	Class Total
Unclassified	0	0	0	0	0	0	0	1020625
Saltmarsh [Green]	0	394375	5625	625	0	0	400625	400625
Sparse SAV [Sea Green]	0	625	63750	19375	0	0	83750	83750
Sand [Yellow]	0	1875	40625	15000	0	0	57500	57500
Dense SAV [Cyan]	0	0	0	0	0	0	0	0
Deep Water [Blue]	0	0	0	0	0	0	0	0
Cloud [White]	0	0	0	0	0	0	0	0
Masked Pixels	0	0	0	0	0	0	0	0
Class Total	0	396875	110000	35000	0	0	0	0
Class Changes	0	2500	46250	20000	0	0	0	0
Image Difference	0	3750	-26250	22500	0	0	0	0

Appendix 6 Change statistics between 2000 and 2004, saltmarsh/ seagrass boundary

Pixel Counts	Sand [Yellow]	Masked Pixels	Saltmarsh [Green]	Sparse SAV [Sea Green]	Dense SAV [Cyan]	Deep Water [Blue]	Row Total	Class Total
Unclassified	0	0	0	0	0	0	0	1633
Saltmarsh [Green]	3	0	622	2	0	0	627	627
Sparse SAV [Sea Green]	36	0	5	103	0	0	144	144
Sand [Yellow]	53	0	14	25	0	0	92	92
Dense SAV [Cyan]	0	0	0	4	0	0	4	4
Deep Water [Blue]	0	0	0	0	0	0	0	0
Cloud [White]	0	0	0	0	0	0	0	0
Masked Pixels	0	0	0	0	0	0	0	0
Class Total	92	0	641	134	0	0	0	0
Class Changes	39	0	19	31	0	0	0	0
Image Difference	0	0	-14	10	4	0	0	0

Percentages	Sand [Yellow]	Masked Pixels	Saltmarsh [Green]	Sparse SAV [Sea Green]	Dense SAV [Cyan]	Deep Water [Blue]	Row Total	Class Total
Unclassified	0	0	0	0	0	0	0	100
Saltmarsh [Green]	3.261	0	97.036	1.493	0	0	100	100
Sparse SAV [Sea Green]	39.13	0	0.78	76.866	0	0	100	100
Sand [Yellow]	57.609	0	2.184	18.657	0	0	100	100
Dense SAV [Cyan]	0	0	0	2.985	0	0	100	100
Deep Water [Blue]	0	0	0	0	0	0	0	0
Cloud [White]	0	0	0	0	0	0	0	0
Masked Pixels	0	0	0	0	0	0	0	0
Class Total	100	0	100	100	0	0	0	0
Class Changes	42.391	0	2.964	23.134	0	0	0	0
Image Difference	0	0	-2.184	7.463	0	0	0	0

Area (Square Meters)	Sand [Yellow]	Masked Pixels	Saltmarsh [Green]	Sparse SAV [Sea Green]	Dense SAV [Cyan]	Deep Water [Blue]	Row Total	Class Total
Unclassified	0	0	0	0	0	0	0	1020625
Saltmarsh [Green]	1875	0	388750	1250	0	0	391875	391875
Sparse SAV [Sea Green]	22500	0	3125	64375	0	0	90000	90000
Sand [Yellow]	33125	0	8750	15625	0	0	57500	57500
Dense SAV [Cyan]	0	0	0	2500	0	0	2500	2500
Deep Water [Blue]	0	0	0	0	0	0	0	0
Cloud [White]	0	0	0	0	0	0	0	0
Masked Pixels	0	0	0	0	0	0	0	0
Class Total	57500	0	400625	83750	0	0	0	0
Class Changes	24375	0	11875	19375	0	0	0	0
Image Difference	0	0	-8750	6250	2500	0	0	0

Appendix 7 Change statistics between 2004 and 2006, saltmarsh/ seagrass boundary

Pixel Counts	Masked Pixels	Saltmarsh [Green]	Sparse SAV [Sea Green]	Sand [Yellow]	Dense SAV [Cyan]	Deep Water [Blue]	Row Total	Class Total
Unclassified	0	0	0	0	0	0	0	1633
Saltmarsh [Green]	0	589	20	3	0	0	612	612
Sparse SAV [Sea Green]	0	33	119	27	4	0	183	183
Sand [Yellow]	0	5	5	62	0	0	72	72
Dense SAV [Cyan]	0	0	0	0	0	0	0	0
Deep Water [Blue]	0	0	0	0	0	0	0	0
Cloud [White]	0	0	0	0	0	0	0	0
Masked Pixels	0	0	0	0	0	0	0	0
Class Total	0	627	144	92	4	0	0	0
Class Changes	0	38	25	30	4	0	0	0
Image Difference	0	-15	39	-20	-4	0	0	0

Percentages	Masked Pixels	Saltmarsh [Green]	Sparse SAV [Sea Green]	Sand [Yellow]	Dense SAV [Cyan]	Deep Water [Blue]	Row Total	Class Total
Unclassified	0	0	0	0	0	0	0	100
Saltmarsh [Green]	0	93.939	13.889	3.261	0	0	100	100
Sparse SAV [Sea Green]	0	5.263	82.639	29.348	100	0	100	100
Sand [Yellow]	0	0.797	3.472	67.391	0	0	100	100
Dense SAV [Cyan]	0	0	0	0	0	0	0	0
Deep Water [Blue]	0	0	0	0	0	0	0	0
Cloud [White]	0	0	0	0	0	0	0	0
Masked Pixels	0	0	0	0	0	0	0	0
Class Total	0	100	100	100	100	0	0	0
Class Changes	0	6.061	17.361	32.609	100	0	0	0
Image Difference	0	-2.392	27.083	-21.739	-100	0	0	0

Area (Square Meters)	Masked Pixels	Saltmarsh [Green]	Sparse SAV [Sea Green]	Sand [Yellow]	Dense SAV [Cyan]	Deep Water [Blue]	Row Total	Class Total
Unclassified	0	0	0	0	0	0	0	1020625
Saltmarsh [Green]	0	368125	12500	1875	0	0	382500	382500
Sparse SAV [Sea Green]	0	20625	74375	16875	2500	0	114375	114375
Sand [Yellow]	0	3125	3125	38750	0	0	45000	45000
Dense SAV [Cyan]	0	0	0	0	0	0	0	0
Deep Water [Blue]	0	0	0	0	0	0	0	0
Cloud [White]	0	0	0	0	0	0	0	0
Masked Pixels	0	0	0	0	0	0	0	0
Class Total	0	391875	90000	57500	2500	0	0	0
Class Changes	0	23750	15625	18750	2500	0	0	0
Image Difference	0	-9375	24375	-12500	-2500	0	0	0

Appendix 8 Change statistics between 2006 and 2008, saltmarsh/ seagrass boundary

Pixel Counts	Masked Pixels	Saltmarsh [Green]	Sparse SAV [Sea Green]	Sand [Yellow]	Dense SAV [Cyan]	Deep Water [Blue]	Row Total	Class Total
Unclassified	0	0	0	0	0	0	0	1633
Saltmarsh [Green]	0	584	34	4	0	0	622	622
Sparse SAV [Sea Green]	0	14	88	1	0	0	103	103
Sand [Yellow]	0	14	61	67	0	0	142	142
Dense SAV [Cyan]	0	0	0	0	0	0	0	0
Deep Water [Blue]	0	0	0	0	0	0	0	0
Cloud [White]	0	0	0	0	0	0	0	0
Masked Pixels	0	0	0	0	0	0	0	0
Class Total	0	612	183	72	0	0	0	0
Class Changes	0	28	95	5	0	0	0	0
Image Difference	0	10	-80	70	0	0	0	0

Percentages	Masked Pixels	Saltmarsh [Green]	Sparse SAV [Sea Green]	Sand [Yellow]	Dense SAV [Cyan]	Deep Water [Blue]	Row Total	Class Total
Unclassified	0	0	0	0	0	0	0	100
Saltmarsh [Green]	0	95.425	18.579	5.556	0	0	100	100
Sparse SAV [Sea Green]	0	2.288	48.087	1.389	0	0	100	100
Sand [Yellow]	0	2.288	33.333	93.056	0	0	100	100
Dense SAV [Cyan]	0	0	0	0	0	0	0	0
Deep Water [Blue]	0	0	0	0	0	0	0	0
Cloud [White]	0	0	0	0	0	0	0	0
Masked Pixels	0	0	0	0	0	0	0	0
Class Total	0	100	100	100	0	0	0	0
Class Changes	0	4.575	51.913	6.944	0	0	0	0
Image Difference	0	1.634	-43.716	97.222	0	0	0	0

Area (Square Meters)	Masked Pixels	Saltmarsh [Green]	Sparse SAV [Sea Green]	Sand [Yellow]	Dense SAV [Cyan]	Deep Water [Blue]	Row Total	Class Total
Unclassified	0	0	0	0	0	0	0	1020625
Saltmarsh [Green]	0	365000	21250	2500	0	0	388750	388750
Sparse SAV [Sea Green]	0	8750	55000	625	0	0	64375	64375
Sand [Yellow]	0	8750	38125	41875	0	0	88750	88750
Dense SAV [Cyan]	0	0	0	0	0	0	0	0
Deep Water [Blue]	0	0	0	0	0	0	0	0
Cloud [White]	0	0	0	0	0	0	0	0
Masked Pixels	0	0	0	0	0	0	0	0
Class Total	0	382500	114375	45000	0	0	0	0
Class Changes	0	17500	59375	3125	0	0	0	0
Image Difference	0	6250	-50000	43750	0	0	0	0

Appendix 9 Map of water depth in Boullanger Bay. Source; (© Hydrogeographic service, RAN)